

# SURFACE SCIENCE



*Roger Nix*  
Queen Mary, University of London

Queen Mary, University of London  
Surface Science

Roger Nix

This text is disseminated via the Open Education Resource (OER) LibreTexts Project (<https://LibreTexts.org>) and like the hundreds of other texts available within this powerful platform, it is freely available for reading, printing and "consuming." Most, but not all, pages in the library have licenses that may allow individuals to make changes, save, and print this book. Carefully consult the applicable license(s) before pursuing such effects.

Instructors can adopt existing LibreTexts texts or Remix them to quickly build course-specific resources to meet the needs of their students. Unlike traditional textbooks, LibreTexts' web based origins allow powerful integration of advanced features and new technologies to support learning.



The LibreTexts mission is to unite students, faculty and scholars in a cooperative effort to develop an easy-to-use online platform for the construction, customization, and dissemination of OER content to reduce the burdens of unreasonable textbook costs to our students and society. The LibreTexts project is a multi-institutional collaborative venture to develop the next generation of open-access texts to improve postsecondary education at all levels of higher learning by developing an Open Access Resource environment. The project currently consists of 14 independently operating and interconnected libraries that are constantly being optimized by students, faculty, and outside experts to supplant conventional paper-based books. These free textbook alternatives are organized within a central environment that is both vertically (from advance to basic level) and horizontally (across different fields) integrated.

The LibreTexts libraries are Powered by [NICE CXOne](#) and are supported by the Department of Education Open Textbook Pilot Project, the UC Davis Office of the Provost, the UC Davis Library, the California State University Affordable Learning Solutions Program, and Merlot. This material is based upon work supported by the National Science Foundation under Grant No. 1246120, 1525057, and 1413739.

Any opinions, findings, and conclusions or recommendations expressed in this material are those of the author(s) and do not necessarily reflect the views of the National Science Foundation nor the US Department of Education.

Have questions or comments? For information about adoptions or adaptations contact [info@LibreTexts.org](mailto:info@LibreTexts.org). More information on our activities can be found via Facebook (<https://facebook.com/Libretexts>), Twitter (<https://twitter.com/libretexts>), or our blog (<http://Blog.Libretexts.org>).

This text was compiled on 01/10/2024

# TABLE OF CONTENTS

## Licensing

### 1: Structure of Solid Surfaces

- o 1.1: Introduction
- o 1.2: Miller Indices (hkl)
- o 1.3: Surface Structures- fcc Metals
- o 1.4: Surface Structures- hcp Metals
- o 1.5: Surface Structures- bcc metals
- o 1.6: Energetics of Surfaces
- o 1.7: Relaxation and Reconstruction
- o 1.8: Particulate Metals
- o 1.9: Other Single Crystal Surfaces

### 2: Adsorption of Molecules on Surfaces

- o 2.1: Introduction to Molecular Adsorption
- o 2.3: Kinetics of Adsorption
- o 2.4: PE Curves and Energetics of Adsorption
- o 2.5: Adsorbate Geometries and Structures
- o 2.6: The Desorption Process

### 3: The Langmuir Isotherm

- o 3.1: Introduction
- o 3.2: Langmuir Isotherm - derivation from equilibrium considerations
- o 3.3: Langmuir Isotherm from a Kinetics Consideration
- o 3.4: Variation of Surface Coverage with Temperature and Pressure
- o 3.5: Applications - Kinetics of Catalytic Reactions

### 4: UHV and Effects of Gas Pressure

- o 4.E: UHV and Effects of Gas Pressure (Exercises)

### 5: Surface Analytical Techniques

- o 5.1: Surface Sensitivity and Surface Specificity
- o 5.2: Auger Electron Spectroscopy
- o 5.3: Photoelectron Spectroscopy
- o 5.4: Vibrational Spectroscopy
- o 5.5: Secondary Ion Mass Spectrometry
- o 5.6: Temperature-Programmed Techniques

### 6: Overlayer Structures and Surface Diffraction

- o 6.1: Classification of Overlayer Structures
- o 6.2: Low Energy Electron Diffraction (LEED)
- o 6.3: Reflection High Energy Electron Diffraction (RHEED)
- o 6.4: Examples - Surface Structures

## 7: Surface Imaging and Depth Profiling

- [7.1: Basic concepts in surface imaging and localized spectroscopy](#)
- [7.2: Electron Microscopy - SEM and SAM](#)
- [7.3: Imaging XPS](#)
- [7.4: SIMS - Imaging and Depth Profiling](#)
- [7.5: Auger Depth Profiling](#)
- [7.6: Scanning Probe Microscopy - STM and AFM](#)

[Index](#)

[Index](#)

[Detailed Licensing](#)

## Licensing

---

A detailed breakdown of this resource's licensing can be found in [Back Matter/Detailed Licensing](#).

## CHAPTER OVERVIEW

### 1: Structure of Solid Surfaces

In most technological applications, metals are used either in a finely divided form or in a massive, polycrystalline form. At the microscopic level, most materials, with the notable exception of a few truly amorphous specimens, can be considered as a collection or aggregate of single crystal crystallites. The surface chemistry of the material as a whole is therefore crucially dependent upon the nature and type of surfaces exposed on these crystallites.

#### Topic hierarchy

- [1.1: Introduction](#)
- [1.2: Miller Indices \(hkl\)](#)
- [1.3: Surface Structures- fcc Metals](#)
- [1.4: Surface Structures- hcp Metals](#)
- [1.5: Surface Structures- bcc metals](#)
- [1.6: Energetics of Surfaces](#)
- [1.7: Relaxation and Reconstruction](#)
- [1.8: Particulate Metals](#)
- [1.9: Other Single Crystal Surfaces](#)

---

This page titled [1: Structure of Solid Surfaces](#) is shared under a [CC BY-NC-SA 4.0](#) license and was authored, remixed, and/or curated by [Roger Nix](#).

## 1.1: Introduction

---

In most technological applications, metals are used either in a finely divided form (e.g. supported metal catalysts) or in a massive, polycrystalline form (e.g. electrodes, mechanical fabrications). At the microscopic level, most materials, with the notable exception of a few truly amorphous specimens, can be considered as a collection or aggregate of single crystal crystallites. The surface chemistry of the material as a whole is therefore crucially dependent upon the nature and type of surfaces exposed on these crystallites. *In principle*, therefore, we can understand the surface properties of any material if we

1. (This approach assumes that we can neglect the possible influence of crystal defects and solid state interfaces on the surface chemistry). It is therefore vitally important that we can independently study different, well-defined surfaces. The most commonly employed technique, is to prepare macroscopic (i.e. size  $\sim$  cm) single crystals of metals and then to deliberately cut them in a way which exposes a large area of the specific surface of interest.

Most metals only exist in one bulk structural form - the most common metallic crystal structures being:

- o For each of these crystal systems, there are in principle an infinite number of possible surfaces which can be exposed. In practice, however, only a limited number of planes (predominantly the so-called "low-index" surfaces) are found to exist in any significant amount and we can concentrate our attention on these surfaces. Furthermore, it is possible to predict the ideal atomic arrangement at a given surface of a particular metal by considering how the bulk structure is intersected by the surface. Firstly, however, we need to look in detail at the bulk crystal structures.

---

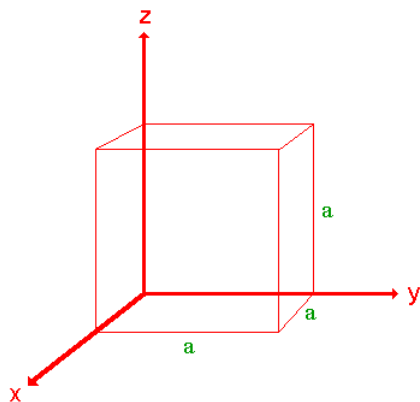
This page titled [1.1: Introduction](#) is shared under a [CC BY-NC-SA 4.0](#) license and was authored, remixed, and/or curated by [Roger Nix](#).



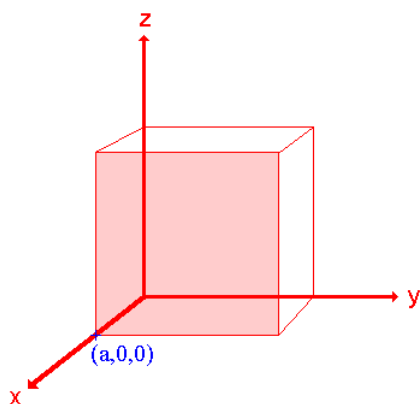
## 1.2: Miller Indices (hkl)

The orientation of a surface or a crystal plane may be defined by considering how the plane (or indeed any parallel plane) intersects the main crystallographic axes of the solid. The application of a set of rules leads to the assignment of the Miller Indices ( $hkl$ ), which are a set of numbers which quantify the intercepts and thus may be used to uniquely identify the plane or surface.

The following treatment of the procedure used to assign the Miller Indices is a simplified one (it may be best if you simply regard it as a "recipe") and only a **cubic** crystal system (one having a cubic unit cell with dimensions  $a \times a \times a$ ) will be considered.



The procedure is most easily illustrated using an example so we will first consider the following surface/plane:



**Step 1:** Identify the intercepts on the  $x$ -,  $y$ - and  $z$ - axes.

In this case the intercept on the  $x$ -axis is at  $x = a$  ( at the point  $(a,0,0)$  ), but the surface is parallel to the  $y$ - and  $z$ -axes - strictly therefore there is no intercept on these two axes but we shall consider the intercept to be at infinity ( $\infty$ ) for the special case where the plane is parallel to an axis. The intercepts on the  $x$ -,  $y$ - and  $z$ -axes are thus

Intercepts:  $a, \infty, \infty$

**Step 2:** Specify the intercepts in fractional co-ordinates

Co-ordinates are converted to fractional co-ordinates by dividing by the respective cell-dimension - for example, a point  $(x,y,z)$  in a unit cell of dimensions  $a \times b \times c$  has fractional co-ordinates of  $(x/a, y/b, z/c)$ . In the case of a cubic unit cell each co-ordinate will simply be divided by the cubic cell constant,  $a$ . This gives

Fractional Intercepts:  $a/a, \infty/a, \infty/a$  i.e.  $1, \infty, \infty$

**Step 3:** Take the reciprocals of the fractional intercepts

This final manipulation generates the Miller Indices which (by convention) should then be specified without being separated by any commas or other symbols. The Miller Indices are also enclosed within standard brackets (...) when one is specifying a unique

surface such as that being considered here.

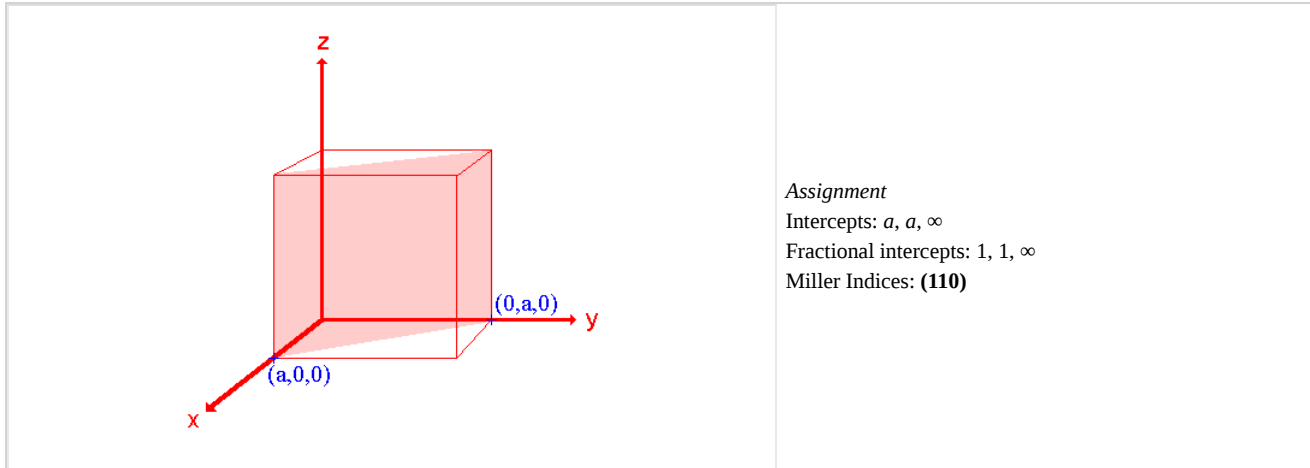
The reciprocals of 1 and  $\infty$  are 1 and 0 respectively, thus yielding

Miller Indices: **(100)**

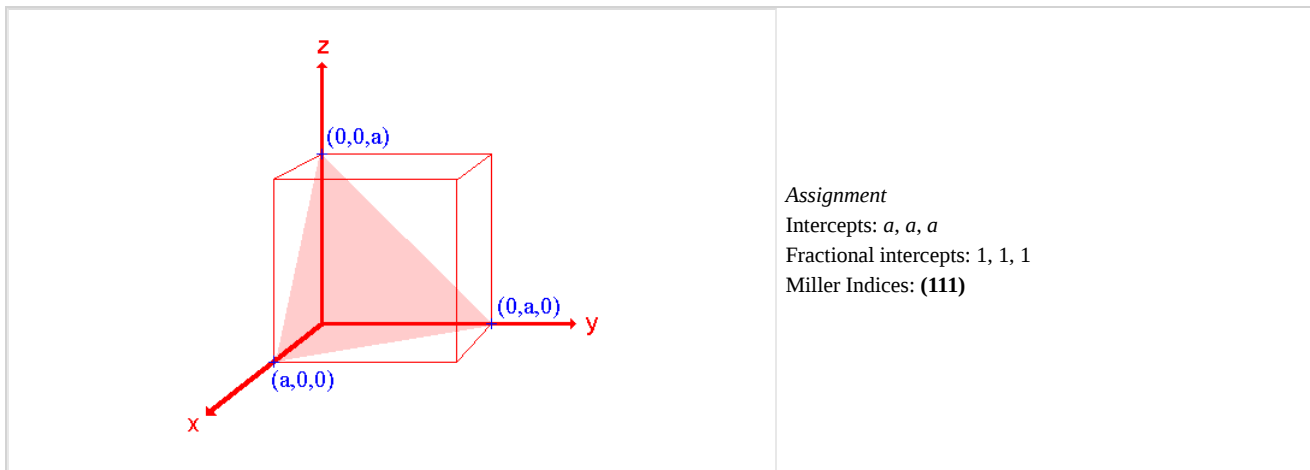
So the surface/plane illustrated is the (100) plane of the cubic crystal.

### Other Examples

#### 1. The (110) surface

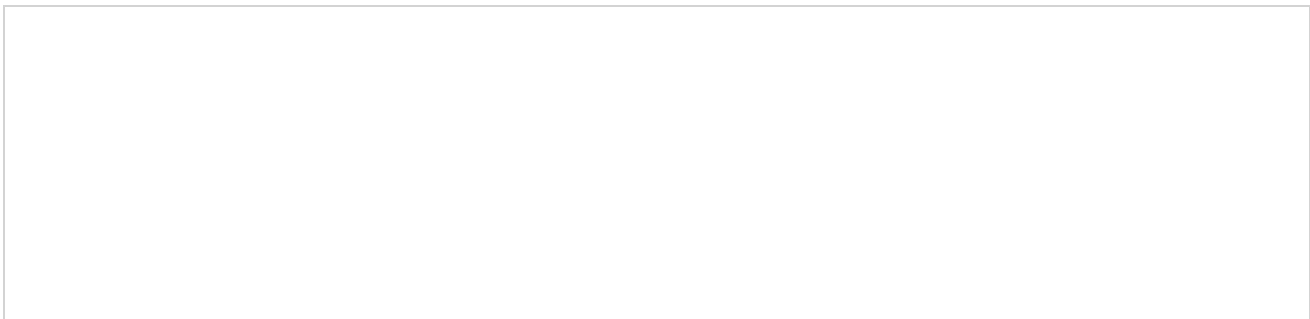


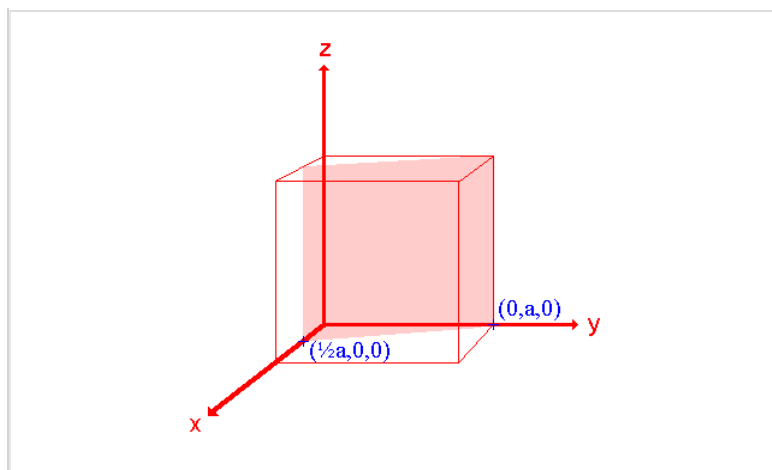
#### 2. The (111) surface



The (100), (110) and (111) surfaces considered above are the so-called **low index surfaces** of a cubic crystal system (the "low" refers to the Miller indices being small numbers - 0 or 1 in this case). These surfaces have a particular importance but there are an infinite number of other planes that may be defined using Miller index notation. We shall just look at one more ...

#### 3. The (210) surface






*Assignment*

Intercepts:  $\frac{1}{2} a, a, \infty$

Fractional intercepts:  $\frac{1}{2}, 1, \infty$

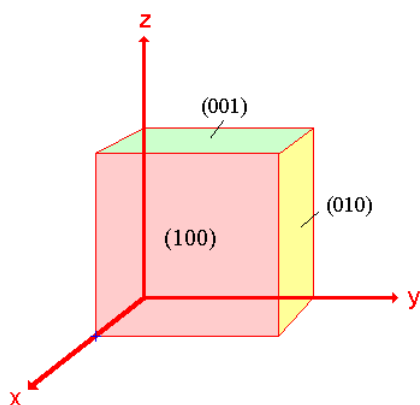
Miller Indices: **(210)**

Further notes:

- i. in some instances the Miller indices are best multiplied or divided through by a common number in order to simplify them by, for example, removing a common factor. This operation of multiplication simply generates a parallel plane which is at a different distance from the origin of the particular unit cell being considered. e.g. (200) is transformed to (100) by dividing through by 2.
- ii. if any of the intercepts are at negative values on the axes then the negative sign will carry through into the Miller indices; in such cases the negative sign is actually denoted by overstriking the relevant number. e.g. (00  $\bar{1}$ ) is instead denoted by 
- iii. in the *hcp* crystal system there are four principal axes; this leads to four Miller Indices e.g. you may see articles referring to an *hcp* (0001) surface. It is worth noting, however, that the intercepts on the first three axes are necessarily related and not completely independent; consequently the values of the first three Miller indices are also linked by a simple mathematical relationship.

### What are symmetry-equivalent surfaces ?

In the following diagram the three highlighted surfaces are related by the symmetry elements of the cubic crystal - they are entirely equivalent.



In fact there are a total of 6 faces related by the symmetry elements and equivalent to the (100) surface - any surface belonging to this set of symmetry related surfaces may be denoted by the more general notation  $\{100\}$  where the Miller indices of one of the surfaces is instead enclosed in curly-brackets.

*Final important note:* in the cubic system the  $(hkl)$  plane and the vector  $[hkl]$ , defined in the normal fashion with respect to the origin, are normal to one another **but** this characteristic is unique to the cubic crystal system and does **not** apply to crystal systems of lower symmetry.

This page titled [1.2: Miller Indices \(hkl\)](#) is shared under a [CC BY-NC-SA 4.0](#) license and was authored, remixed, and/or curated by [Roger Nix](#).

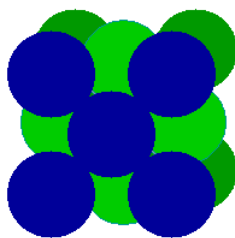
## 1.3: Surface Structures- fcc Metals

Many of the technologically most important metals possess the *fcc* structure, e.g., the catalytically important precious metals (Pt, Rh, Pd) all exhibit an *fcc* structure. The low index faces of this system are the most commonly studied of surfaces: as we shall see they exhibit a range of

- Surface symmetry
- Surface atom coordination
- Surface reactivity

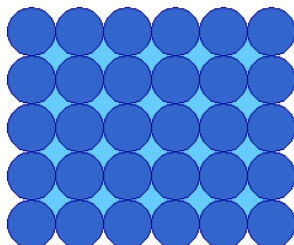
### The fcc (100) Surface

The (100) surface is that obtained by cutting the *fcc* metal parallel to the front surface of the *fcc* cubic unit cell - this exposes a surface (the atoms in blue) with an atomic arrangement of 4-fold symmetry



fcc unit cell (100) face

The diagram below shows the conventional birds-eye view of the (100) surface - this is obtained by rotating the preceding diagram through 45° to give a view which emphasizes the 4-fold (rotational) symmetry of the surface layer atoms.



The tops of the second layer atoms are just visible through the holes in the first layer, but would not be accessible to molecules arriving from the gas phase.

#### ? Exercise 1.3.1

What is the coordination number of the surface layer atoms on the fcc(100) surface ?

#### Answer

The coordination number of the surface layer atoms is 8

Rationale: Each surface atom has four nearest neighbors in the 1st layer, and another four in the layer immediately below ; a total of 8. This contrasts with the CN of metal atoms in the bulk of the solid which is 12 for a fcc metal.

There are several other points worthy of note:

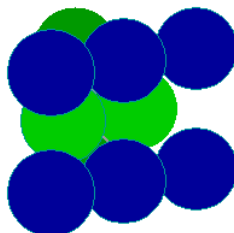
1. All the surface atoms are equivalent
2. The surface is relatively smooth at the atomic scale
3. The surface offers various adsorption sites for molecules which have different local symmetries and lead to different coordination geometries - specifically there are:
  - On-top sites (above a single metal atom)
  - Bridging sites, between two atoms

- o Hollow sites, between four atoms

Depending upon the site occupied, an adsorbate species (with a single point of attachments to the surface) is therefore likely to be bonded to either one, two or four metal atoms.

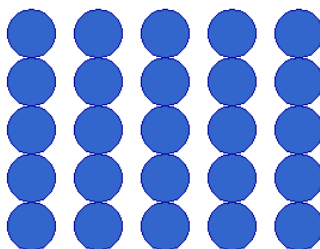
### The fcc(110) surface

The (110) surface is obtained by cutting the *fcc* unit cell in a manner that intersects the *x* and *y* axes but not the *z*-axis - this exposes a surface with an atomic arrangement of 2-fold symmetry.



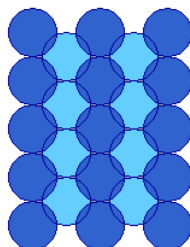
fcc unit cell (110) face

The diagram below shows the conventional birds-eye view of the (110) surface - emphasizing the rectangular symmetry of the surface layer atoms. The diagram has been rotated such that the rows of atoms in the first atomic layer now run vertically, rather than horizontally as in the previous diagram.



It is clear from this view that the atoms of the topmost layer are much less closely packed than on the (100) surface - in one direction (along the rows) the atoms are in contact i.e. the distance between atoms is equal to twice the metallic(atomic) radius, but in the orthogonal direction there is a substantial gap between the rows.

This means that the atoms in the underlying second layer are also, to some extent, exposed at the surface



(110) surface plane, e.g. Cu(110)

The preceding diagram illustrates some of those second layer atoms, exposed at the bottom of the troughs.

In this case, the determination of atomic coordination numbers requires a little more careful thought: one way to double-check your answer is to remember that the CN of atoms in the bulk of the *fcc* structure is 12, and then to subtract those which have been removed from above in forming the surface plane.

#### ? Exercise 1.3.2

What is the coordination number of the topmost layer atoms on the fcc(110) surface?

**Answer**

The coordination number of the topmost layer atoms is 7

Rationale: Each surface atom has two nearest neighbors in the 1st layer, and another four in the layer immediately below, and one directly below it in the third layer; this gives a total of 7.

To confirm this consider those that have been removed from the layers above - clearly there would have been 4 nearest neighbors in the layer immediately above the surface layer ( equivalent to the four in the layer immediately below). In addition, there would have been one nearest neighbor directly above each surface atom ( equivalent to the one directly below in the third layer). Hence, 7 (present) + 5 (removed) = 12 - which is correct !

If we compare this coordination number with that obtained for the (100) surface, it is worth noting that the surface atoms on a more open ("rougher") surface have a lower CN; this has important implications when it comes to the **chemical reactivity** of surfaces.

#### Question

Do the atoms in the second layer have the bulk coordination ?

**No** - the fact that they are clearly exposed (visible) at the surface implies that they have a lower CN than they would in the bulk.

#### Exercise 1.3.3

What is the coordination number of these second layer atoms on the fcc(110) surface ?

#### Answer

The coordination number of the second layer atoms is 11

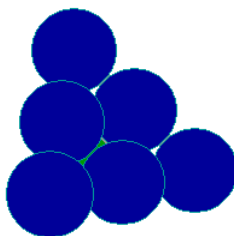
Rationale: The atoms in the second layer are only missing one atom from their complete coordination shell ( the atom that would have been directly above them) i.e. they have  $CN = (12-1) = 11$

In summary, we can note that

1. All first layer surface atoms are equivalent, but second layer atoms are also exposed
2. The surface is atomically rough, and highly anisotropic
3. The surface offers a wide variety of possible adsorption sites, including:
  - o On-top sites
  - o Short bridging sites between two atoms in a single row
  - o Long bridging sites between two atoms in adjacent rows
  - o Higher coordination sites ( in the troughs)

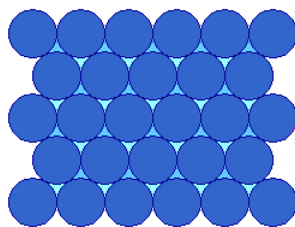
### The fcc (111) Surface

The (111) surface is obtained by cutting the *fcc* metal in such a way that the surface plane intersects the *x*-, *y*- and *z*- axes at the same value - this exposes a surface with an atomic arrangement of 3-fold ( apparently 6-fold, hexagonal) symmetry. This layer of surface atoms actually corresponds to one of the close-packed layers on which the *fcc* structure is based.



fcc unit cell (111) face

The diagram below shows the conventional birds-eye view of the (111) surface - emphasizing the hexagonal packing of the surface layer atoms. Since this is the most efficient way of packing atoms within a single layer, they are said to be "close-packed".



(111) surface plane, e.g. Pt(111)

### ? Exercise 1.3.4

What is the coordination number of the surface layer atoms on the fcc(111) surface?

#### Answer

The coordination number of the surface layer atoms is 9

Rationale: Each surface atom has six nearest neighbors in the 1st layer, and another three in the layer immediately below ; a total of 9.

The following features are worth noting ;

1. All surface atoms are equivalent and have a relatively high CN
2. The surface is almost smooth at the atomic scale
3. The surface offers the following adsorption sites:
  - o On-top sites
  - o Bridging sites, between two atoms
  - o Hollow sites, between three atoms

### How do these surfaces intersect in irregular-shaped samples

Flat surfaces of single crystal samples correspond to a single Miller Index plane and, as we have seen, each individual surface has a well-defined atomic structure. It is these flat surfaces that are used in most surface science investigations, but it is worth a brief aside to consider what type of surfaces exist for an irregular shaped sample (but one that is still based on a single crystal). Such samples can exhibit facets corresponding to a range of different Miller Index planes. This is best illustrated by looking at the diagrams below.

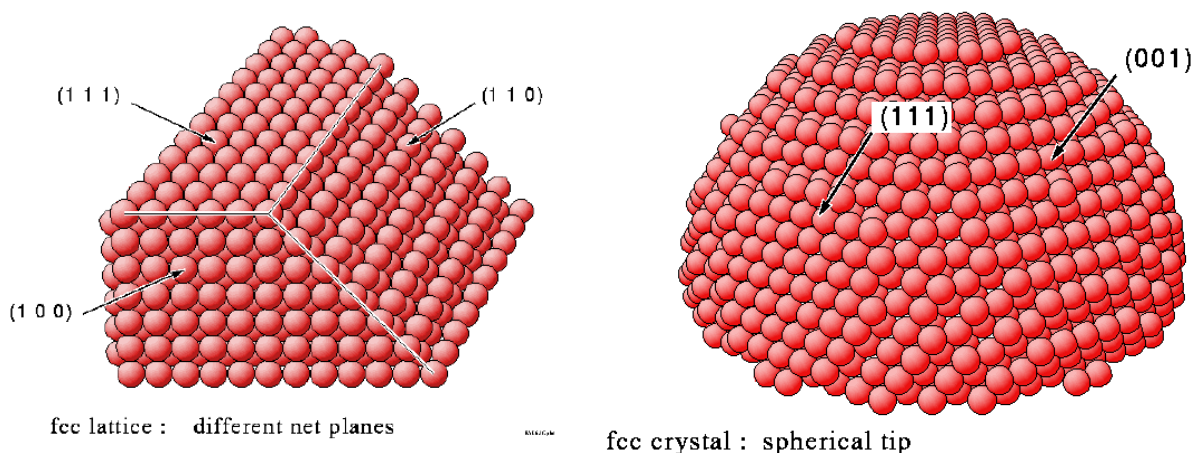


Figure: (left) an angled corner. (right) a spherical tip. From the [BALSAC](#) picture gallery of Prof. K. Hermann, Fritz-Haber-Institut, Berlin

## Summary

Depending upon how an *fcc* single crystal is cleaved or cut, flat surfaces of macroscopic dimensions which exhibit a wide range of structural characteristics may be produced. The single crystal surfaces discussed here ( (100), (110) & (111)) represent only the most frequently studied surface planes of the *fcc* system - however, they are also the most commonly occurring surfaces on such metals and the knowledge gained from studies on this limited selection of surfaces goes a long way in propagating the development of our understanding of the surface chemistry of these metals. For further information on other *fcc* metal surfaces you should take a look at [Section 1.8](#) which includes a brief description of high index *fcc* surfaces with illustrative examples.

---

This page titled [1.3: Surface Structures- \*fcc\* Metals](#) is shared under a [CC BY-NC-SA 4.0](#) license and was authored, remixed, and/or curated by [Roger Nix](#).



## 1.4: Surface Structures- hcp Metals

---

This important class of metallic structures includes metals such as Co, Zn, Ti & Ru.

The Miller Index notation used to describe the orientation of surface planes for all crystallographic systems is slightly more complex in this case since the crystal structure does not lend itself to description using a standard cartesian set of axes- instead the notation is based upon three axes at 120 degrees in the close-packed plane, and one axis (the *c*-axis) perpendicular to these planes. This leads to a four-digit index structure ; however, since the third of these is redundant it is sometimes left out !

### I. The hcp (0001) surface

This is the most straightforward of the *hcp* surfaces since it corresponds to a surface plane which intersects only the *c*-axis, being coplanar with the other 3 axes i.e. it corresponds to the close packed planes of hexagonally arranged atoms that form the basis of the structure. It is also sometimes referred to as the (001) surface.

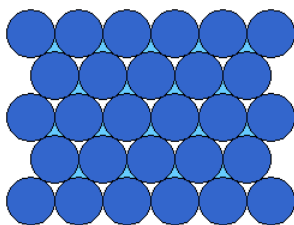


Figure (0001) surface plane, e.g. Ru(0001)

This conventional plan view of the (0001) surface shows the hexagonal packing of the surface layer atoms.

- Which fcc surface does it resemble ?

### Summary

We can summarize the characteristics of this surface by noting that:

1. All the surface atoms are equivalent and have CN=9
2. The surface is almost smooth at the atomic scale
3. The surface offers the following adsorption sites:
  - On-top sites
  - Bridging sites, between two atoms
  - Hollow sites, between three atoms

---

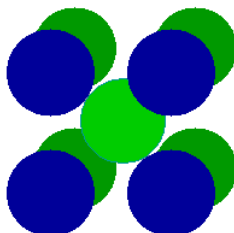
This page titled [1.4: Surface Structures- hcp Metals](#) is shared under a [CC BY-NC-SA 4.0](#) license and was authored, remixed, and/or curated by [Roger Nix](#).

## 1.5: Surface Structures- bcc metals

A number of important metals ( e.g. Fe, W, Mo ) have the bcc structure. As a result of the low packing density of the bulk structure, the surfaces also tend to be of a rather open nature with surface atoms often exhibiting rather low coordination numbers.

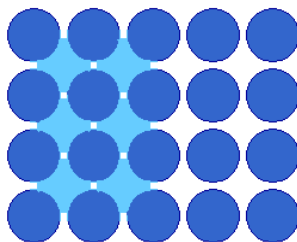
### I. The bcc (100) surface

The (100) surface is obtained by cutting the metal parallel to the front surface of the bcc cubic unit cell - this exposes a relatively open surface with an atomic arrangement of 4-fold symmetry.



bcc unit cell (100) face

The diagram below shows a plan view of this (100) surface - the atoms of the second layer (shown on left) are clearly visible, although probably inaccessible to any gas phase molecules.

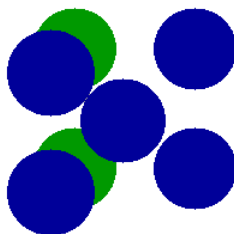


bcc (100) surface plane, e.g. Fe(100)

- What is the coordination number of the surface layer atoms on the bcc(100) surface?
- Is the coordination of the second layer atoms the same as that of bulk atoms ?

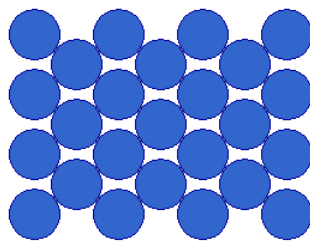
### II. The bcc (110) surface

The (110) surface is obtained by cutting the metal in a manner that intersects the x and y axes but creates a surface parallel to the z-axis - this exposes a surface which has a higher atom density than the (100) surface.



bcc unit cell (110) face

The following diagram shows a plan view of the (110) surface - the atoms in the surface layer strictly form an array of rectangular symmetry, but the surface layer coordination of an individual atom is quite close to hexagonal.

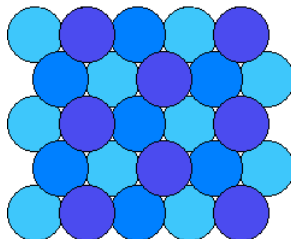


bcc(110) surface plane, e.g. Fe(110)

- What is the coordination number of the surface layer atoms on the bcc(110) surface?

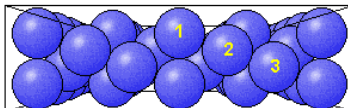
### III. The bcc (111) surface

The (111) surface of bcc metals is similar to the (111) face of fcc metals only in that it exhibits a surface atomic arrangement exhibiting 3-fold symmetry - in other respects it is very different.



Top View: bcc(111) surface plane e.g. Fe(111)

In particular it is a very much more open surface with atoms in both the second and third layers clearly visible when the surface is viewed from above. This open structure is also clearly evident when the surface is viewed in cross-section as shown in the diagram below in which atoms of the various layers have been annotated.



Side View: bcc(111) surface plane, e.g. Fe(111)

---

This page titled [1.5: Surface Structures- bcc metals](#) is shared under a [CC BY-NC-SA 4.0](#) license and was authored, remixed, and/or curated by [Roger Nix](#).

## 1.6: Energetics of Surfaces

---

All surfaces are energetically unfavorable in that they have a positive free energy of formation. A simple rationalization for why this must be the case comes from considering the formation of new surfaces by cleavage of a solid and recognizing that bonds have to be broken between atoms on either side of the cleavage plane in order to split the solid and create the surfaces. Breaking bonds requires work to be done on the system, so the surface free energy (surface tension) contribution to the total free energy of a system must therefore be positive.

The unfavorable contribution to the total free energy may, however, be minimized in several ways:

1. By reducing the amount of surface area exposed
2. By predominantly exposing surface planes which have a low surface free energy
3. By altering the local surface atomic geometry in a way which reduces the surface free energy

The first and last points are considered elsewhere (1.7 Particulate Metals, & 1.6 Relaxation and Reconstruction, respectively) - only the second point will be considered further here.

Of course, systems already possessing a high surface energy (as a result of the preparation method) will not always readily interconvert to a lower energy state at low temperatures due to the kinetic barriers associated with the restructuring - such systems (e.g. highly dispersed materials such as those in colloidal suspensions or supported metal catalysts) are thus "metastable".

---

This page titled [1.6: Energetics of Surfaces](#) is shared under a [CC BY-NC-SA 4.0](#) license and was authored, remixed, and/or curated by [Roger Nix](#).

## 1.7: Relaxation and Reconstruction

The phenomena of relaxation and reconstruction involve rearrangements of surface ( and near surface ) atoms, this process being driven by the energetics of the system i.e. the desire to reduce the surface free energy (see [Energetics of Surfaces](#)). As with all processes, there may be kinetic limitations which prevent or hinder these rearrangements at low temperatures. Both processes may occur with clean surfaces in ultrahigh vacuum, but it must be remembered that adsorption of species onto the surface may enhance, alter or even reverse the process !

### I. Relaxation

Relaxation is a small and subtle rearrangement of the surface layers which may nevertheless be significant energetically, and seems to be commonplace for metal surfaces. It involves adjustments in the layer spacings perpendicular to the surface, there is **no** change either in the periodicity parallel to the surface or to the symmetry of the surface.

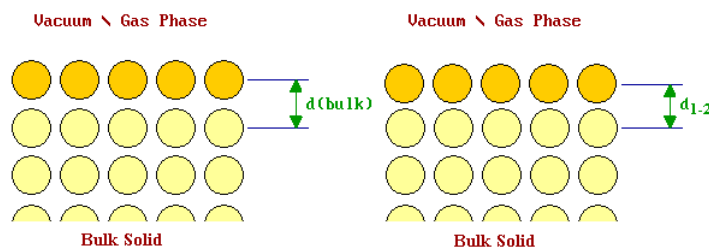
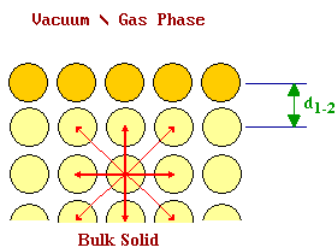
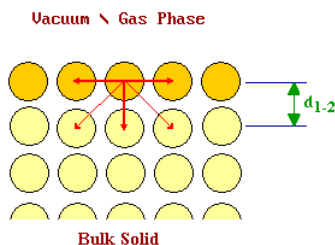


**Figure** (left) Unrelaxed Surface and (right) Relaxed Surface with  $d_{1-2} < d_{\text{bulk}}$ .

The right picture shows the relaxed surface: the first layer of atoms is typically drawn in slightly towards the second layer (i.e.  $d_{1-2} < d_{text{bulk}}$ ). We can consider what might be the driving force for this process at the atomic level. If we use a localized model for the bonding in the solid then it is clear that an atom in the bulk is acted upon by a balanced, symmetrical set of forces.



On the other hand, an atom at the unrelaxed surface suffers from an imbalance of forces and the surface layer of atoms may therefore be pulled in towards the second layer.



(Whether this is a reasonable model for bonding in a metal is open to question !)

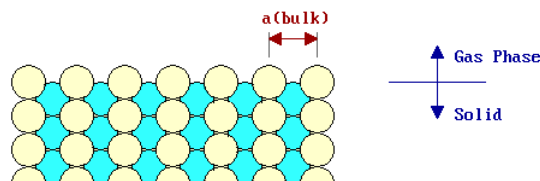
The magnitude of the contraction in the first layer spacing is generally small ( < 10 % )- compensating adjustments to other layer spacings may extend several layers into the solid.

### II. Reconstruction

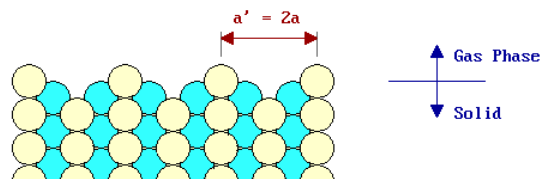
The reconstruction of surfaces is a much more readily observable effect, involving larger (yet still atomic scale) displacements of the surface atoms. It occurs with many of the less stable metal surfaces (e.g. it is frequently observed on fcc(110) surfaces), but is

much more prevalent on semiconductor surfaces.

Unlike relaxation, the phenomenon of reconstruction involves a change in the periodicity of the surface structure - the diagram below shows a surface, viewed from the side, which corresponds to an unreconstructed termination of the bulk structure.



This may be contrasted with the following picture which shows a schematic of a reconstructed surface - this particular example is similar to the "missing row model" proposed for the structure of a number of reconstructed (110) fcc metal surfaces.



Since reconstruction involves a change in the periodicity of the surface and in some cases also a change in surface symmetry, it is readily detected using surface diffraction techniques (e.g. LEED & RHEED).

The overall driving force for reconstruction is once again the minimization of the surface free energy - at the atomic level, however, it is not always clear why the reconstruction should reduce the surface free energy. For some metallic surfaces, it may be that the change in periodicity of the surface induces a splitting in surface-localized bands of energy levels and that this can lead to a lowering of the total electronic energy when the band is initially only partly full.

In the case of many semiconductors, the simple reconstructions can often be explained in terms of a "surface healing" process in which the co-ordinative unsaturation of the surface atoms is reduced by bond formation between adjacent atoms. For example, the formation of a Si(100) surface requires that the bonds between the Si atoms that form the new surface layer and those that were in the layer immediately above in the solid are broken - this leaves two "dangling bonds" per surface Si atom.

A relatively small co-ordinated movement of the atoms in the topmost layer can reduce this unsatisfied co-ordination - pairs of Si atoms come together to form surface "Si dimers", leaving only one dangling bond per Si atom. This process leads to a change in the surface periodicity: the period of the surface structure is doubled in one direction giving rise to the so-called (2x1) reconstruction observed on all clean Si(100) surfaces [ [Si\(100\)-\(2x1\)](#) ].

More examples:	
Si(111)-(7x7)	From the web-pages of the Omicron NanoTechnology GmbH (showing data courtesy of Prof. Hongiun Gao's group, Institute of Physics, CAS, Beijing, China).

In this section, attention has been concentrated on the reconstruction of clean surfaces. It is, however, worth noting that reconstruction of the substrate surface is frequently induced by the adsorption of molecular or atomic species onto the surface - this phenomenon is known as *adsorbate-induced reconstruction* (see Section 2.5 for some examples).

## Summary

The minimization of surface energy means that even single crystal surfaces will not exhibit the ideal geometry of atoms to be expected by truncating the bulk structure of the solid parallel to a particular plane. The differences between the real structure of the clean surface and the ideal structure may be imperceptibly small (e.g. a very slight *surface relaxation*) or much more marked and involving a change in the surface periodicity in one or more of the main symmetry directions (*surface reconstruction*).

This page titled [1.7: Relaxation and Reconstruction](#) is shared under a [CC BY-NC-SA 4.0](#) license and was authored, remixed, and/or curated by [Roger Nix](#).

## 1.8: Particulate Metals

As mentioned in the Introduction, macroscopic single crystals of metals are not generally employed in technological applications.

Massive metallic structures (electrodes etc.) are polycrystalline in nature - the size of individual crystallites being determined by the mechanical treatment and thermal history of the metal concerned. Nevertheless, the nature and properties of the exposed polycrystalline, metal surface is still principally determined by the characteristics of the individual crystal surfaces present. Furthermore, the proportions in which the different crystal surfaces occur is controlled by their relative thermodynamic stabilities. Thus, a macroscopic piece of an fcc metal will generally expose predominantly (111)-type surface planes.

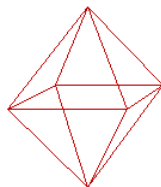
A more interesting case for consideration is that of metals in a highly dispersed system - the classic example of which is a supported metal catalyst (such as those employed in the petrochemical industries and automotive catalytic converters). In such catalysts the average metal particle size is invariably sub-micron and may be as small as 1 nm . These metal particles are often tiny single crystals or simple twinned crystals.

The shape of these small crystals is principally determined by the surface free energy contribution to the total energy. There are two ways in which the surface energy can be reduced for a crystal of fixed mass / volume:

1. By minimizing the surface area of the crystallite
2. By ensuring that only surfaces of low surface free energy are exposed.

If matter is regarded as continuous then the optimum shape for minimizing the surface free energy is a sphere (since this has the lowest surface area/volume ratio of any 3D object) - this is why liquid droplets in free space are basically spherical.

Unfortunately, we cannot ignore the discrete, atomic nature of matter and the detailed atomic structure of surfaces when considering particles of the size found in catalysts. If, for example, we consider an fcc metal (eg. Pt) and ensure that only the most stable (111)-type surfaces are exposed, then we end up with a crystal which is an octahedron.

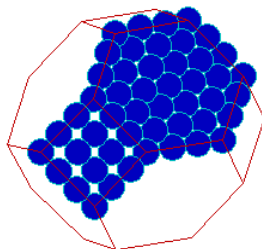


Octahedron exposing, 8 symmetry-related, fcc(111)-type faces

### Note

There are 8 different, but crystallographically-equivalent, surface planes which have the (111) surface structure - the {111} faces. They are related by the symmetry elements of the cubic fcc system.

A compromise between exposing only the lowest energy surface planes and minimizing the surface area is obtained by truncating the vertices of the octahedron - this generates a cubo-octahedral particle as shown below, with 8 (111)-type surfaces and 6 smaller, (100)-type surfaces and gives a lower (surface area / volume) ratio.



Crystals of this general form are often used as conceptual models for the metal particles in supported catalysts.

The atoms in the middle of the {111} faces show the expected CN=9 characteristic of the (111) surface. Similarly, those atoms in the centre of the {100} surfaces have the characteristic CN=8 of the (100) surface. However, there are also many atoms at the

corners and intersection of surface planes on the particle which show lower coordination numbers.

What is the lowest coordination number exhibited by a surface atom on this crystallite ?

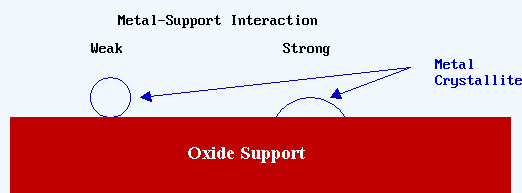
This model for the structure of catalytic metal crystallites is not always appropriate: it is only reasonable to use it when there is a relatively weak interaction between the metal and the support phase (e.g. many silica supported catalysts).

A stronger metal-support interaction is likely to lead to increased "wetting" of the support by the metal, giving rise to:

- a greater metal-support contact area
- a significantly different metal particle morphology

#### ✓ Example 1.8.1

In the case of a strong metal-support interaction the metal/oxide interfacial free energy is low and it is inappropriate to consider the surface free energy of the metal crystallite in isolation from that of the support.



Our knowledge of the structure of very small particles comes largely from high resolution electron microscopy (HREM) studies - with the best modern microscopes it is possible to directly observe such particles and resolve atomic structure.

This page titled [1.8: Particulate Metals](#) is shared under a [CC BY-NC-SA 4.0](#) license and was authored, remixed, and/or curated by [Roger Nix](#).



## 1.9: Other Single Crystal Surfaces

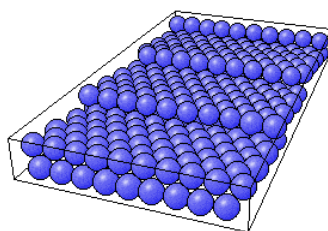
Although some of the more common metallic surface structures have been discussed in previous sections (1.2-1.4), there are many other types of single crystal surface which may be prepared and studied. These include

- high index surfaces of metals
- single crystal surfaces of compounds

These will not be covered in any depth, but a few illustrative examples are given below to give you a flavor of the additional complexity involved when considering such surfaces.

### High Index Surfaces of Metals

High index surfaces are those for which one or more of the **Miller Indices** are relatively large numbers. The most commonly studied surfaces of this type are **vicinal surfaces** which are cut at a relatively small angle to one of the low index surfaces. The ideal surfaces can then be considered to consist of terraces which have an atomic arrangement identical with the corresponding low index surface, separated by monatomic steps (steps which are a single atom high).



*Perspective view of the fcc(775) surface*

As seen above, the ideal fcc(775) surface has a regular array of such steps and these steps are both straight and parallel to one another.

#### ? Exercise 1.9.1

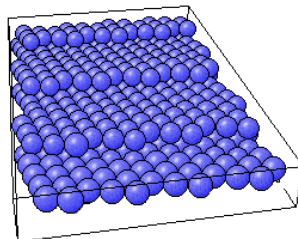
What is the coordination number of a step atom on this surface ?

#### Answer

The coordination number of the atoms at the steps is 7

Rationale: Each step atom has four nearest neighbors in the surface layer of terrace atoms which terminates at the step, and another three in the layer immediately below ; a total of 7. This contrasts with the CN of surface atoms on the terraces which is 9.

By contrast a surface for which all the Miller indices differ must not only exhibit steps but must also contain kinks in the steps. An example of such a surface is the fcc(10.8.7) surface - the ideal geometry of which is shown below.



*Perspective view of the fcc(10.8.7) surface*

### ? Exercise 1.9.2

What is the lowest coordination number exhibited by any of the atoms on this surface?

#### Answer

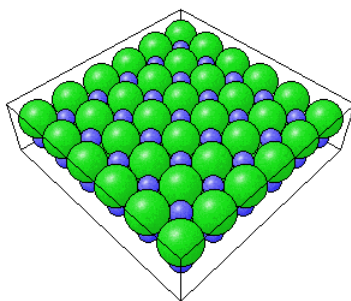
The lowest coordination number is 6 which is that exhibited by atoms at the kinks in the steps.

Rationale: The lowest coordination number is exhibited by atoms "on the outside" of the kinks in the steps. Such atoms have only three nearest neighbors in the surface layer of terrace atoms which terminates at the step, and another three in the layer immediately below ; a total of 6. This contrasts with the surface atoms on the terraces which have a coordination number of 9 and the normal step atoms which have a coordination number of 7.

Real vicinal surfaces do not, of course, exhibit the completely regular array of steps and kinks illustrated for the ideal surface structures, but they do exhibit this type of step and terrace morphology. The special adsorption sites available adjacent to the steps are widely recognized to have markedly different characteristics to those available on the terraces and may thus have an important role in certain types of catalytic reaction.

## Single Crystal Surfaces of Compounds

The ideal surface structures of the low index planes of compound materials can be easily deduced from the bulk structures in exactly the same way as can be done for the basic metal structures. For example, the NaCl(100) surface that would be expected from the bulk structure is shown below:



*Perspective view of the NaCl(100) surface*

In addition to the relaxation and reconstruction exhibited by elemental surfaces, the surfaces of compounds may also show deviations from the bulk stoichiometry due to surface localised reactions (e.g. surface reduction) and/or surface segregation of one or more components of the material.

---

This page titled [1.9: Other Single Crystal Surfaces](#) is shared under a [CC BY-NC-SA 4.0](#) license and was authored, remixed, and/or curated by [Roger Nix](#).

## CHAPTER OVERVIEW

### 2: Adsorption of Molecules on Surfaces

- [2.1: Introduction to Molecular Adsorption](#)
- [2.2: How do Molecules Bond to Surfaces?](#)
- [2.3: Kinetics of Adsorption](#)
- [2.4: PE Curves and Energetics of Adsorption](#)
- [2.5: Adsorbate Geometries and Structures](#)
- [2.6: The Desorption Process](#)

---

This page titled [2: Adsorption of Molecules on Surfaces](#) is shared under a [CC BY-NC-SA 4.0](#) license and was authored, remixed, and/or curated by [Roger Nix](#).

## 2.1: Introduction to Molecular Adsorption

The adsorption of molecules on to a surface is a necessary prerequisite to any surface mediated chemical process. For example, in the case of a surface catalyzed reaction it is possible to break down the whole continuously-cycling process into the following five basic steps:

1. Diffusion of reactants to the active surface
2. Adsorption of one or more reactants onto the surface
3. Surface reaction
4. Desorption of products from the surface
5. Diffusion of products away from the surface

The above scheme not only emphasizes the importance of the adsorption process but also its reverse - namely desorption. It is these two processes which are considered in this chapter.

### Notes on Terminology

- **Substrate** - frequently used to describe the solid surface onto which adsorption can occur; the substrate is also occasionally (although not here) referred to as the adsorbent.
- **Adsorbate** - the general term for the atomic or molecular species which are adsorbed (or are capable of being adsorbed) onto the substrate.
- **Adsorption** - the process in which a molecule becomes adsorbed onto a surface of another phase (note - to be distinguished from absorption which is used when describing uptake into the bulk of a solid or liquid phase)
- **Coverage** - a measure of the extent of adsorption of a species onto a surface (unfortunately this is defined in more than one way !). It is usually denoted by the lower case Greek "theta",  $\theta$
- **Exposure** - a measure of the amount of gas which a surface has seen; more specifically, it is the product of the pressure and time of exposure (normal unit is the Langmuir, where  $1 \text{ L} = 10^{-6} \text{ Torr s}$ ).

This page titled [2.1: Introduction to Molecular Adsorption](#) is shared under a [CC BY-NC-SA 4.0](#) license and was authored, remixed, and/or curated by [Roger Nix](#).

## 2.2: How do Molecules Bond to Surfaces?

There are two principal modes of adsorption of molecules on surfaces: Physical Adsorption (physisorption) and Chemical Adsorption (chemisorption). The basis of distinction is the nature of the bonding between the molecule and the surface with:

- **Physical Adsorption:** the only bonding is by weak Van der Waals - type forces. There is no significant redistribution of electron density in either the molecule or at the substrate surface.
- **Chemisorption:** a chemical bond, involving substantial rearrangement of electron density, is formed between the adsorbate and substrate. The nature of this bond may lie anywhere between the extremes of virtually complete ionic or complete covalent character.

Typical Characteristics of Adsorption Processes

	Chemisorption	Physisorption
Material Specificity (variation between substrates of different chemical composition)	Substantial variation between materials	Slight dependence upon substrate composition
Crystallographic Specificity (variation between different surface planes of the same crystal)	Marked variation between crystal planes	Virtually independent of surface atomic geometry
Temperature Range (over which adsorption occurs)	Virtually unlimited (but a given molecule may effectively adsorb only over a small range)	Near or below the condensation point of the gas (e.g. Xe < 100 K, CO <sub>2</sub> < 200 K)
Adsorption Enthalpy	Wide range (related to the chemical bond strength) - typically 40 - 800 kJ mol <sup>-1</sup>	Related to factors like molecular mass and polarity - typically 5-40 kJ mol <sup>-1</sup> (similar to heat of liquefaction)
Nature of Adsorption	Often dissociative May be irreversible	Non-dissociative Reversible
Saturation Uptake	Limited to one monolayer	Multilayer uptake possible
Kinetics of Adsorption	Very variable - often an activated process	Fast - since it is a non-activated process

The most definitive method for establishing the formation of a chemical bond between the adsorbing molecule and the substrate (i.e. chemisorption) is to use an appropriate spectroscopic technique, for example

- IR (Section 5.4) to observe the vibrational frequency of the substrate/adsorbate bond
- UPS (Section 5.3) to monitor intensity & energy shifts in the valence orbitals of the adsorbate and substrate

This page titled [2.2: How do Molecules Bond to Surfaces?](#) is shared under a [CC BY-NC-SA 4.0](#) license and was authored, remixed, and/or curated by [Roger Nix](#).

## 2.3: Kinetics of Adsorption

The rate of adsorption,  $R_{ads}$ , of a molecule onto a surface can be expressed in the same manner as any kinetic process. For example, when it is expressed in terms of the partial pressure of the molecule in the gas phase above the surface:

$$R_{ads} = k' P^x \quad (2.3.1)$$

where:

- $x$  - kinetic order
- $k'$  - rate constant
- $P$  - partial pressure

If the rate constant is then expressed in an [Arrhenius form](#), then we obtain a kinetic equation of the form:

$$R_{ads} = A e^{-E_a/RT} P^x \quad (2.3.2)$$

where  $E_a$  is the [activation energy](#) for adsorption and  $A$  the [pre-exponential \(frequency\)](#) factor. It is much more informative, however, to consider the factors controlling this process at the molecular level. The rate of adsorption is governed by (1) the rate of arrival of molecules at the surface and (2) the proportion of incident molecules which undergo adsorption. Hence, we can express the rate of adsorption (per unit area of surface, i.e., molecules  $\text{m}^{-2} \text{s}^{-1}$ ) as a product of the incident molecular flux,  $F$ , and a sticking probability,  $S$ .

$$R_{ads} = S F \quad (2.3.3)$$

The sticking probability varies from 0 (never sticking) to 1 (always sticking). The flux (in molecules  $\text{m}^{-2} \text{s}^{-1}$ ) of incident molecules is given by the **Hertz-Knudsen equation**

$$F = \frac{P}{\sqrt{2\pi m k T}} \quad (2.3.4)$$

where

- $P$  - gas pressure [  $\text{N m}^{-2}$  ]
- $m$  - mass of one molecule [  $\text{kg}$  ]
- $T$  - temperature [  $\text{K}$  ]

The sticking probability is clearly a property of the adsorbate / substrate system under consideration but must lie in the range  $0 < S < 1$ ; it may depend upon various factors - foremost amongst these being the existing coverage of adsorbed species ( $\theta$ ) and the presence of any activation barrier to adsorption. In general, therefore

$$S = f(\theta) e^{-E_a/RT} \quad (2.3.5)$$

where, once again,  $E_a$  is the activation energy for adsorption and  $f(\theta)$  is some, as yet undetermined, function of the existing surface coverage of adsorbed species. Combining the equations for  $S$  and  $F$  yields the following expression for the rate of adsorption:

$$R = \frac{f(\theta) P}{\sqrt{2\pi m k T}} e^{-E_a/RT} \quad (2.3.6)$$

1. Equation [2.3.6](#) indicates that the rate of adsorption is expected to be first order with regard to the partial pressure of the molecule in the gas phase above the surface.
2. It should be recognized that the activation energy for adsorption may itself be dependent upon the surface coverage, i.e.  $E_a = E(\theta)$ .
3. If it is further assumed that the sticking probability is directly proportional to the concentration of vacant surface sites (which would be a reasonable first approximation for non-dissociative adsorption) then  $f(\theta)$  is proportional to  $(1 - \theta)$ , where, in this instance,  $\theta$  is the fraction of sites which are occupied (i.e. the Langmuir definition of surface coverage).

For a discussion of some of the factors which determine the magnitude of the activation energy of adsorption you should see [Section 2.4](#) which looks at the typical PE curve associated with various types of adsorption process.

## Estimating Surface Coverages arising as a result of Gas Exposure

If a surface is initially clean and it is then exposed to a gas pressure under conditions where the rate of desorption is very slow, then the coverage of adsorbed molecules may initially be estimated simply by consideration of the kinetics of adsorption. As noted above, the rate of adsorption is given by Equation 2.3.3, which can be written in term of a derivative

$$\frac{dN_{ads}}{dt} = SF \quad (2.3.7)$$

where  $N_{ads}$  is the number of adsorbed species per unit area of surface.

Equation 2.3.7 must be integrated to obtain an expression for  $N_{ads}$ , since the sticking probability is coverage (and hence also time) dependent. However, if it is assumed that the sticking probability is essentially constant (which may be a reasonable approximation for relatively low coverages), then this integration simply yields:

$$N_{ads} = SFt \quad (2.3.8)$$

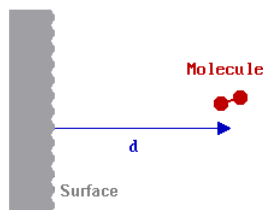
---

This page titled [2.3: Kinetics of Adsorption](#) is shared under a [CC BY-NC-SA 4.0](#) license and was authored, remixed, and/or curated by [Roger Nix](#).

## 2.4: PE Curves and Energetics of Adsorption

In this section, we will consider both the energetics of adsorption and factors which influence the kinetics of adsorption by looking at the "potential energy diagram/curve" for the adsorption process. The potential energy curve for the adsorption process is a representation of the variation of the energy (PE or  $E$ ) of the system as a function of the distance ( $d$ ) of an adsorbate from a surface.

Within this simple one-dimensional (1D) model, the only variable is the distance ( $d$ ) of the adsorbing molecule from the substrate surface.



Thus, the energy of the system is a function only of this variable i.e.

$$E = E(d) \quad (2.4.1)$$

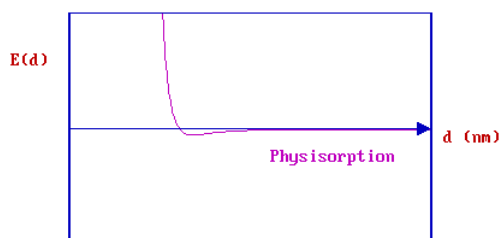
It should be remembered that this is a very simplistic model which neglects many other parameters which influence the energy of the system (a single molecule approaching a clean surface), including for example

- the angular orientation of the molecule
- changes in the internal bond angles and bond lengths of the molecule
- the position of the molecule parallel to the surface plane

The interaction of a molecule with a given surface will also clearly be dependent upon the presence of any existing adsorbed species, whether these be surface impurities or simply pre-adsorbed molecules of the same type (in the latter case we are starting to consider the effect of surface coverage on the adsorption characteristics). Nevertheless, it is useful to first consider the interaction of an isolated molecule with a clean surface using the simple 1D model. For the purposes of this Module, we will also not be overly concerned whether the "energy" being referred to should strictly be the internal energy, the enthalpy or free energy of the system.

### CASE I - Physisorption

In the case of pure physisorption, e.g., Ar/metals, the only attraction between the adsorbing species and the surface arises from weak, **van der Waals forces**. As illustrated below, these forces give rise to a shallow minimum in the PE curve at a relatively large distance from the surface (typically  $d > 0.3 \text{ nm}$ ) before the strong repulsive forces arising from electron density overlap cause a rapid increase in the total energy.

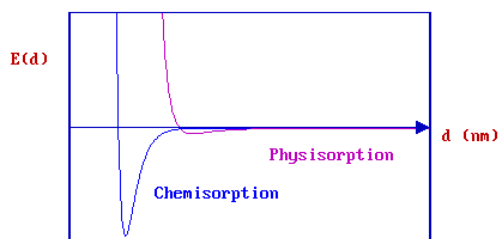


There is no barrier to prevent the atom or molecule which is approaching the surface from entering this physisorption well, i.e. the process is not activated and the kinetics of physisorption are invariably fast.

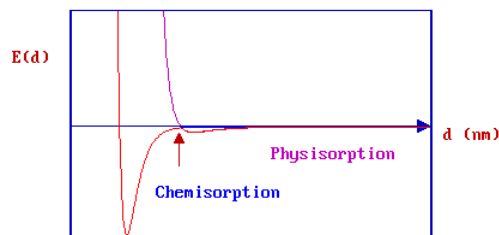
### CASE II - Physisorption + Molecular Chemisorption

The weak physical adsorption forces and associated long-range attraction will be present to varying degrees in all adsorbate / substrate systems. However, in cases where chemical bond formation between the adsorbate and substrate can also occur, the PE curve is dominated by a much deeper chemisorption minimum at shorter values of  $d$ .



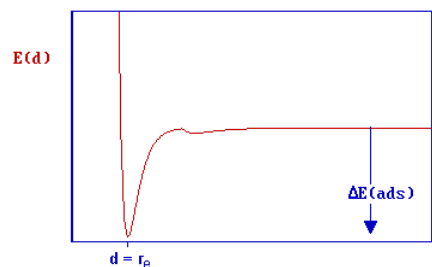


The graph above shows the PE curves due to physisorption and chemisorption separately - in practice, the PE curve for any real molecule capable of undergoing chemisorption is best described by a combination of the two curves, with a curve crossing at the point at which chemisorption forces begin to dominate over those arising from physisorption alone.



The minimum energy pathway obtained by combining the two PE curves is now highlighted in red. Any perturbation of the combined PE curve from the original, separate curves is most likely to be evident close to the highlighted crossing point.

For clarity, we will now consider only the overall PE curve:

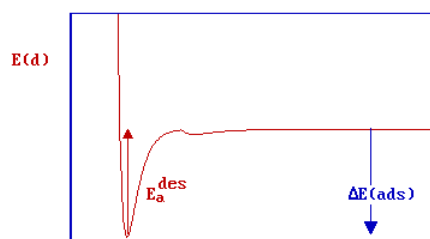


The depth of the chemisorption well is a measure of the strength of binding to the surface - in fact it is a direct representation of the energy of adsorption, whilst the location of the global minimum on the horizontal axis corresponds to the equilibrium bond distance ( $r_e$ ) for the adsorbed molecule on this surface.

The energy of adsorption is *negative*, and since it corresponds to the energy *change* upon adsorption it is better represented as  $\Delta E(\text{ads})$  or  $\Delta E_{\text{ads}}$ . However, you will also often find the depth of this well associated with the enthalpy of adsorption,  $\Delta H(\text{ads})$ .

The "heat of adsorption",  $Q$ , is taken to be a positive quantity equal in magnitude to the enthalpy of adsorption ; i.e.  $Q = -\Delta H(\text{ads})$

In this particular case, there is clearly no barrier to be overcome in the adsorption process and there is no activation energy of adsorption (i.e.  $E_a^{\text{ads}} = 0$ , but do remember the previously mentioned limitations of this simple 1D model). There is of course a significant barrier to the reverse, desorption process - the red arrow in the diagram below represents the activation energy for desorption.



Clearly in this particular case, the magnitudes of the energy of adsorption and the activation energy for desorption can also be equated i.e.

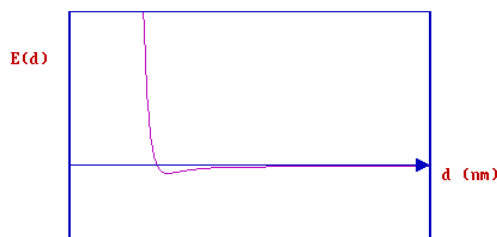
$$E_a^{des} = \Delta E(ads) \quad (2.4.2)$$

or

$$E_a^{des} \approx -\Delta H(ads) \quad (2.4.3)$$

### CASE III - Physisorption + Dissociative Chemisorption

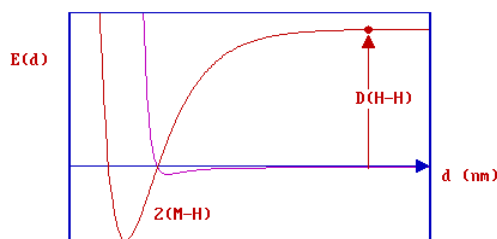
In this case the main differences arise from the substantial changes in the PE curve for the chemisorption process. Again, we start off with the basic PE curve for the physisorption process which represents how the molecule can weakly interact with the surface:



If we now consider a specific molecule such as  $H_2$  and initially treat it as being completely **isolated** from the surface ( i.e. when the distance,  $d$ , is very large ) then a substantial amount of energy has to be put into the system in order to cause dissociation of the molecule.



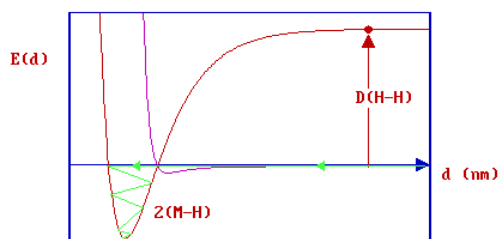
- this is the bond dissociation energy [  $D(H-H)$  ], some  $435 \text{ kJ mol}^{-1}$  or  $4.5 \text{ eV}$ .



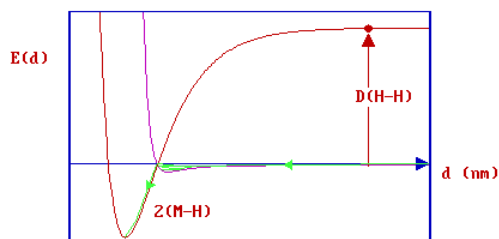
The red dot in the diagram above thus represents two hydrogen atoms, equidistant (and a long distance) from the surface and also now well separated from each other. If these atoms are then allowed to approach the surface they may ultimately both form strong chemical bonds to the substrate .... this corresponds to the minimum in the red curve which represents the chemisorption PE curve for the two H atoms.

In reality, of course, such a mechanism for dissociative hydrogen chemisorption is not practical - the energy downpayment associated with breaking the H-H bond is far too severe.

Instead, a hydrogen molecule will initially approach the surface along the physisorption curve. If it has sufficient energy it may pass straight into the chemisorption well ( "direct chemisorption" ) ....



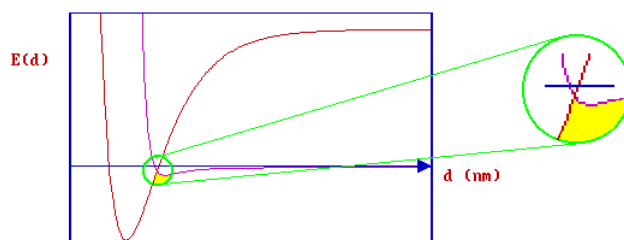
or, alternatively, it may first undergo transient physisorption - a state from which it can then either desorb back as a molecule into the gas phase or cross over the barrier into the dissociated, chemisorptive state (as illustrated *schematically* below).



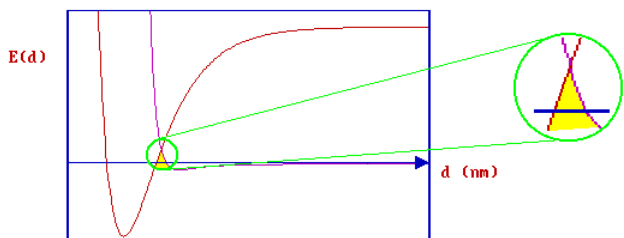
In this latter case, the molecule can be said to have undergone "precursor-mediated" chemisorption.

The characteristics of this type of dissociative adsorption process are clearly going to be strongly influenced by the position of the crossing point of the two curves (molecular physisorption v's dissociative chemisorption) - relatively small shifts in the position of either of the two curves can significantly alter the size of any barrier to chemisorption.

In the example immediately below there is no direct activation barrier to dissociative adsorption - the curve crossing is below the initial "zero energy" of the system.



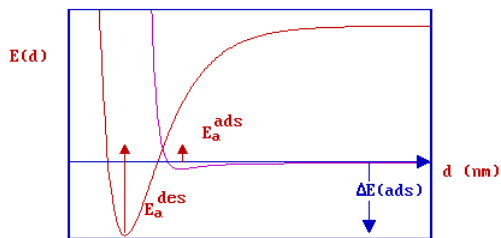
whilst, in this next case ....



there is a substantial barrier to chemisorption. Such a barrier has a major influence on the **kinetics** of adsorption.

*The depth of the physisorption well for the hydrogen molecule is actually very small (in some cases negligible), but this is not the case for other molecules and does not alter the basic conclusions regarding dissociative adsorption that result from this model; namely that the process may be either activated or non-activated depending on the exact location of the curve crossing.*

At this point it is useful to return to consider the effect of such a barrier on the relationship between the activation energies for adsorption and desorption, and the energy (or enthalpy) of adsorption.



Clearly, from the diagram

$$E_a^{des} - E_a^{ads} = -\Delta E_{ads} \quad (2.4.5)$$

but, since the activation energy for adsorption is nearly always very much smaller than that for desorption, and the difference between the energy and enthalpy of adsorption is also very small, it is still quite common to see the relationship

$$E_a^{des} \approx -\Delta H_{ads} \quad (2.4.6)$$

For a slightly more detailed treatment of the adsorption process, you are referred to the following examples of [More Complex PE Curves & Multi-Dimensional PE Surfaces](#).

---

This page titled [2.4: PE Curves and Energetics of Adsorption](#) is shared under a [CC BY-NC-SA 4.0](#) license and was authored, remixed, and/or curated by [Roger Nix](#).

## 2.5: Adsorbate Geometries and Structures

We can address the question of what happens when a molecule becomes adsorbed onto a surface at two levels; specifically we can aim to identify

1. the nature of the adsorbed species and its local adsorption geometry (i.e., its chemical structure and co-ordination to adjacent substrate atoms)
2. the overall structure of the extended adsorbate/substrate interface (i.e., the long range ordering of the surface)

The latter topic is covered in detail in [Section 6.1](#), while this section will consider only the local adsorption geometry and adsorbate structure.

Chemisorption, by definition, involves the formation of new chemical bonds between the adsorbed species and the surface atoms of the substrate - basically the same type of bonds that are present in any molecular complex. In considering what type of species may be formed on a metal surface, therefore, it is important not to abandon chemical common sense and, if in doubt, to look for inspiration at the structures of known metal-organic complexes.

### Chemisorption of Hydrogen and Halogens

#### Hydrogen (H<sub>2</sub>)

In the H<sub>2</sub> molecule, the valence electrons are all involved in the H-H  $\sigma$ -bond and there are no additional electrons which may interact with the substrate atoms. Consequently, chemisorption of hydrogen on metals is almost invariably a dissociative process in which the H-H bond is broken, thereby permitting the hydrogen atoms to independently interact with the substrate (see [Section 2.4](#) for a description of the energetics of this process). The adsorbed species in this instance therefore are hydrogen atoms.

The exact nature of the adsorbed hydrogen atom complex is generally difficult to determine experimentally, and the very small size of the hydrogen atom does mean that migration of hydrogen from the interface into sub-surface layers of the substrate can occur with relative ease on some metals (e.g. Pd, rare earth metals).

The possibility of molecular H<sub>2</sub> chemisorption at low temperatures cannot be entirely excluded, however, as demonstrated by the discovery of molecular hydrogen transition metal compounds, such as  $W(\eta^2-H_2)(CO)_3(P^iPr_3)_2$ , in which both atoms of the hydrogen molecule are coordinated to a single metal centre.

#### Halogens (F<sub>2</sub>, Cl<sub>2</sub>, Br<sub>2</sub> etc.)

Halogens also chemisorb in a dissociative fashion to give adsorbed halogen atoms. The reasons for this are fairly clear - in principle a halogen molecule could act as a Lewis base and bind to the surface without breakage of the X-X bond, in practice the lone pairs are strongly held by the highly electronegative halogen atom so any such interaction would be very weak and the thermodynamics lie very heavily in favour of dissociative adsorption [ i.e.  $D(X-X) + D(M-X_2) \ll 2 D(M-X)$  ]. Clearly the kinetic barrier to dissociation must also be low or non-existent for the dissociative adsorption to occur readily.

Another way of looking at the interaction of a halogen molecule with a metal surface is as follows: the significant difference in electronegativity between a typical metal and halogen is such that substantial electron transfer from the metal to halogen is favoured. If a halogen molecule is interacting with a metal surface then this transferred electron density will enter the  $\sigma^*$  antibonding orbital of the molecule, thereby weakening the X-X bond. At the same time the build-up of negative charge on the halogen atoms enhances the strength of the metal-halogen interaction. The net result of these two effects when taken to their limit is that the halogen molecule dissociates and the halogen atoms interact with the metal with a strong ionic contribution to the bonding.

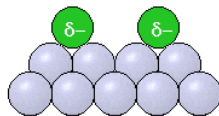
Halogen atoms tend to occupy high co-ordination sites on the surface - for example, the 3-fold hollow site on *fcc* (111) surfaces (**A**) and the 4-fold hollow site on *fcc*(100) surfaces (**B**).



(A) Plan View (B)

This behavior is typical of atomic adsorbates which almost invariably endeavor to maximize their co-ordination and hence prefer to occupy the highest-available co-ordination site on the surface. As a result of the electron transfer from the metal substrate to the

halogen atoms, each adsorbed atom is associated with a significant **surface dipole**.



### Cross-section

One consequence of this is that there are repulsive (dipole-dipole) interactions between the adsorbed atoms, which are especially evident at higher surface coverages and which can lead to a substantial reduction in the enthalpy of adsorption at specific coverages (if these coverages mark a watershed, above which the atoms are forced to occupy sites which are much closer together).

Another feature of the halogen adsorption chemistry of some metals is the transition from an adsorbed surface layer to surface compound formation at high gas exposures.

## Chemisorption of Nitrogen and Oxygen

### Oxygen

Oxygen is an example of a molecule which usually adsorb dissociatively, but are also found to adsorb molecularly on some metals (e.g. Ag, Pt). In those cases where both types of adsorption are observed it is the dissociative process that corresponds to the higher adsorption enthalpy.

As noted above, in the molecular adsorption state the interaction between the molecule and the surface is relatively weak. Molecules aligned such that the internuclear axis is parallel to the surface plane may bond to a single metal atom of the surface via both

1.  $\sigma$ -donor interaction, in which the charge transfer is from the occupied molecular  $\pi$ -bonding molecular orbital of the molecule into vacant orbitals of  $\sigma$ -symmetry on the metal (i.e.  $M \leftarrow O_2$ ), and
2.  $\pi$ -acceptor interaction, in which an occupied metal  $d$ -orbital of the correct symmetry overlaps with empty  $\pi^*$  orbitals of the molecule and the charge transfer is from the surface to the molecule (i.e.  $M \rightarrow O_2$ ).

Although the interaction of the molecule with the surface is generally weak, one might expect that there might be a substantial barrier to dissociation due to the high strength (and high dissociation enthalpy) of the O=O bond. Nevertheless on most metal surfaces, dissociation of oxygen is observed to be facile which is related to the manner in which the interaction with the surface can mitigate the high intrinsic bond energy (see [Section 2.4](#)) and thereby facilitate dissociation.

Once formed, oxygen atoms are strongly bound to the surface and, as noted previously, will tend to occupy the highest available co-ordination site. The strength of the interaction between adsorbate and substrate is such that the adjacent metal atoms are often seen to undergo significant displacements from the equilibrium positions that they occupy on the clean metal surface. This displacement may simply lead to a distortion of the substrate surface in the immediate vicinity of the adsorbed atom (so that, for example, the adjacent metal atoms are drawn in towards the oxygen and the metal-oxygen bond distance is reduced) or to a more extended surface reconstruction (see [Section 1.6](#))

Dissociative oxygen adsorption is frequently irreversible - rather than simply leading to desorption, heating of an adsorbed oxygen overlayer often results in either the gradual removal of oxygen from the surface by diffusion into the bulk of the substrate (e.g. Si(111) or Cu(111)) or to the formation of a surface oxide compound. Even at ambient temperatures, extended oxygen exposure often leads to the nucleation of a surface oxide. Depending on the reactivity of the metal concerned, further exposure at low temperatures may result either in a progressive conversion of the bulk material to oxide or the oxidation process may effectively stop after the formation of a passivating surface oxide film of a specific thickness (e.g. Al).

### Nitrogen

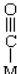
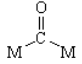
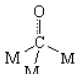
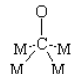
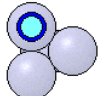
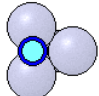
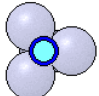
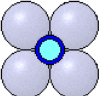
The interaction of nitrogen with metal surfaces shows many of the same characteristics as those described above for oxygen. However, in general  $N_2$  is less susceptible to dissociation as a result of the lower M-N bond strength and the substantial kinetic barrier associated with breaking the N=N triple bond.

## Chemisorption of Carbon Monoxide

Depending upon the metal surface, carbon monoxide may adsorb either in a molecular form or in a dissociative fashion - in some cases both states coexist on particular surface planes and over specific ranges of temperature.

1. On the reactive surfaces of metals from the left-hand side of the periodic table (e.g. Na, Ca, Ti, rare earth metals) the adsorption is almost invariably dissociative, leading to the formation of adsorbed carbon and oxygen atoms (and thereafter to the formation of surface oxide and oxy-carbide compounds).
2. By contrast, on surfaces of the metals from the right hand side of the *d*-block (e.g. Cu, Ag) the interaction is predominantly molecular; the strength of interaction between the CO molecule and the metal is also much weaker, so the M-CO bond may be readily broken and the CO desorbed from the surface by raising the surface temperature without inducing any dissociation of the molecule.
3. For the majority of the transition metals, however, the nature of the adsorption (dissociative v.s molecular) is very sensitive to the surface temperature and surface structure (e.g. the Miller index plane, and the presence of any lower co-ordination sites such as step sites and defects).

Molecularly chemisorbed CO has been found to bond in various ways to single crystal metal surfaces - analogous to its behaviour in isolated metal carbonyl complexes.

			
Terminal ("Linear") (all surfaces)	Bridging ( 2f site ) (all surfaces)	Bridging / 3f hollow ( <i>fcc</i> (111) )	Bridging / 4f hollow (rare- <i>fcc</i> (100) ?)
			

Whilst the above structural diagrams amply demonstrate the inadequacies of a simple valence bond description of the bonding of molecules to surface, they do to an extent also illustrate one of its features and strengths - namely that a given element, in this case carbon, tends to have a specific valence. Consequently, as the number of metal atoms to which the carbon is co-ordinated increases, so there is a corresponding reduction in the C-O bond order.

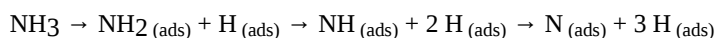
However, it must be emphasised that a molecule such as CO does not necessarily prefer to bind at the highest available co-ordination site. So, for example, the fact that there are 3-fold hollow sites on an *fcc*(111) surface does not mean that CO will necessarily adopt this site - the preferred site may still be a terminal or 2-fold bridging site, and the site or site(s) which is(are) occupied may change with either surface coverage or temperature. The energy difference between the various adsorption sites available for molecular CO chemisorption appears therefore to be very small. A description of the nature of the bonding in a terminal CO-metal complex, in terms of a simple molecular orbital model, is given in [Section 5.4](#).

## Chemisorption of Ammonia and other Group V/VI Hydrides

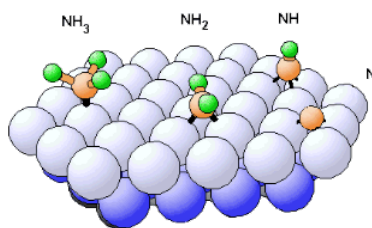
Ammonia has lone pairs available for bonding on the central nitrogen atom and may bond without dissociation to a single metal atom of a surface, acting as a Lewis base, to give a pseudo-tetrahedral co-ordination for the nitrogen atom.



Alternatively, progressive dehydrogenation may occur to give surface  $\text{NH}_x$  ( $x = 2, 1, 0$ ) species and adsorbed hydrogen atoms, i.e.



As the number of hydrogens bonded to the nitrogen atom is reduced, the adsorbed species will tend to move into a higher co-ordination site on the surface (thereby tending to maintain the valence of nitrogen).



Decomposition fragments of ammonia on an fcc(111) surface. (Picture adapted from the [BALSAC Picture Gallery](#) by K. Hermann, Fritz-Haber-Institut, Berlin)

Other Group V and Group VI hydrides (e.g.  $\text{PH}_3$ ,  $\text{H}_2\text{O}$ ,  $\text{H}_2\text{S}$ ) exhibit similar adsorption characteristics to ammonia.

## Chemisorption of Unsaturated Hydrocarbons

Unsaturated hydrocarbons (alkenes, alkynes, aromatic molecules etc.) all tend to interact fairly strongly with metal atom surfaces. At low temperatures (and on less reactive metal surfaces) the adsorption may be molecular, albeit perhaps with some distortion of bond angles around the carbon atom.

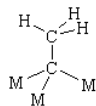
Ethene, for example, may bond to give both a  $\pi$ -complex (**A**) or a di- $\sigma$  adsorption complex (**B**):



(**A**) Chemisorbed (**B**) Ethene

[ Further examples: [models of chemisorbed ethene and ethyne on Cu\(111\)](#) ]

As the temperature is raised, or even at low temperatures on more reactive surfaces (in particular those that bind hydrogen strongly), a stepwise dehydrogenation may occur. One particularly stable surface intermediate found in the dehydrogenation of ethene is the *ethylidyne* complex, whose formation also involves H-atom transfer between the carbon atoms.



*Ethylidyne: this adsorbate preferentially occupies a 3-fold hollow site to give pseudo-tetrahedral co-ordination for the carbon atom.*

The ultimate product of complete dehydrogenation, and the loss of molecular hydrogen by desorption, is usually either carbidic or graphitic surface carbon.

This page titled [2.5: Adsorbate Geometries and Structures](#) is shared under a [CC BY-NC-SA 4.0](#) license and was authored, remixed, and/or curated by [Roger Nix](#).



## 2.6: The Desorption Process

An adsorbed species present on a surface at low temperatures may remain almost indefinitely in that state. As the temperature of the substrate is increased, however, there will come a point at which the thermal energy of the adsorbed species is such that one of several things may occur:

1. a molecular species may decompose to yield either gas phase products or other surface species.
2. an atomic adsorbate may react with the substrate to yield a specific surface compound, or diffuse into the bulk of the underlying solid.
3. the species may desorb from the surface and return into the gas phase.

The last of these options is the desorption process. In the absence of decomposition the desorbing species will generally be the same as that originally adsorbed but this is not necessarily always the case.

(An example where it is not is found in the adsorption of some alkali metals on metallic substrates exhibiting a high work function where, at low coverages, the desorbing species is the alkali metal ion as opposed to the neutral atom. Other examples would include certain isomerization reactions.)

### Desorption Kinetics

The rate of desorption,  $R_{des}$ , of an adsorbate from a surface can be expressed in the general form:

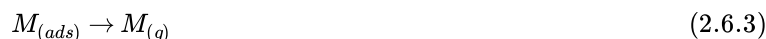
$$R_{des} = kN^x \quad (2.6.1)$$

with

- $x$  - kinetic order of desorption
- $k$  - rate constant for the desorption process
- $N$  - surface concentration of adsorbed species

The order of desorption can usually be predicted because we are concerned with an [elementary step](#) of a "reaction": specifically,

#### I. Atomic or Simple Molecular Desorption



- will usually be a first order process (i.e.  $x = 1$ ). Examples include ...

- The desorption of copper atoms from a tungsten surface



- the desorption of CO molecules from a copper surface



#### II. Recombinative Molecular Desorption



- will usually be a second order process (i.e.  $x = 2$ ). Examples include:

- desorption of O atoms as  $O_2$  from a Pt surface



- desorption of H atoms as  $H_2$  from a Ni surface



The rate constant for the desorption process may be expressed in an [Arrhenius form](#),

$$k_{des} = A \exp(-E_a^{des}/RT) \quad (2.6.9)$$

with

- $E_a^{des}$  is the activation energy for desorption, and
- $A$  is the pre-exponential factor; this can also be considered to be the "attempt frequency",  $\nu$ , at overcoming the barrier to desorption.

This then gives the following general expression for the rate of desorption

$$R_{des} = -\frac{dN}{dt} = \nu N^x \exp(-E_a^{des}/RT) \quad (2.6.10)$$

In the particular case of simple molecular adsorption, the pre-exponential/frequency factor ( $\nu$ ) may also be equated with the frequency of vibration of the bond between the molecule and substrate; this is because every time this bond is stretched during the course of a vibrational cycle can be considered an attempt to break the bond and hence an attempt at desorption.

## Surface Residence Times

One property of an adsorbed molecule that is intimately related to the desorption kinetics is the *surface residence time* - this is the average time that a molecule will spend on the surface under a given set of conditions (in particular, for a specified surface temperature) before it desorbs into the gas phase.

For a first order process such as the desorption step of a molecularly adsorbed species:



the average time ( $\tau$ ) prior to the process occurring is given by:

$$\tau = \frac{1}{k_1} \quad (2.6.12)$$

where  $k_1$  is the first order rate constant (no proof of this will be given here).

From equation 3 with  $x = 1$ , we know that

$$k_1 = \nu \exp(-E_a^{des}/RT) \quad (2.6.13)$$

and if we also substitute for  $E_a^{des}$  using the approximate relation  $E_a^{des} \approx -\Delta H_{ads}$  discussed in [Section 2.4](#), then we get the following expression for the surface residence time

$$\tau = \tau_o \exp(-\Delta H_{ads}/RT) \quad (2.6.14)$$

with

- $\tau_o$  corresponds to the period of vibration  $\approx 1/\nu$  of the bond between the adsorbed molecule and substrate and is frequently taken to be about  $10^{-13}$  s .

---

This page titled [2.6: The Desorption Process](#) is shared under a [CC BY-NC-SA 4.0](#) license and was authored, remixed, and/or curated by [Roger Nix](#).

## CHAPTER OVERVIEW

### 3: The Langmuir Isotherm

A continuous monolayer of adsorbate molecules surrounding a homogeneous solid surface is the conceptual basis for this adsorption model. The Langmuir isotherm is formally equivalent to the [Hill equation](#) in biochemistry.

[3.1: Introduction](#)

[3.2: Langmuir Isotherm - derivation from equilibrium considerations](#)

[3.3: Langmuir Isotherm from a Kinetics Consideration](#)

[3.4: Variation of Surface Coverage with Temperature and Pressure](#)

[3.5: Applications - Kinetics of Catalytic Reactions](#)

---

This page titled [3: The Langmuir Isotherm](#) is shared under a [CC BY-NC-SA 4.0](#) license and was authored, remixed, and/or curated by [Roger Nix](#).

### 3.1: Introduction

---

Whenever a gas is in contact with a solid there will be an equilibrium established between the molecules in the gas phase and the corresponding adsorbed species (molecules or atoms) which are bound to the surface of the solid.

As with all chemical equilibria, the position of equilibrium will depend upon a number of factors:

1. The relative stabilities of the adsorbed and gas phase species involved
2. The temperature of the system (both the gas and surface, although these are normally the same)
3. The pressure of the gas above the surface

In general, factors (2) and (3) exert opposite effects on the concentration of adsorbed species - that is to say that the surface coverage may be increased by raising the gas pressure but will be reduced if the surface temperature is raised.

The Langmuir isotherm was developed by Irving Langmuir in 1916 to describe the dependence of the surface coverage of an adsorbed gas on the pressure of the gas above the surface at a fixed temperature. There are many other types of isotherm (Temkin, Freundlich ...) which differ in one or more of the assumptions made in deriving the expression for the surface coverage; in particular, on how they treat the surface coverage dependence of the enthalpy of adsorption. Whilst the Langmuir isotherm is one of the simplest, it still provides a useful insight into the pressure dependence of the extent of surface adsorption.

#### Note: Surface Coverage & the Langmuir Isotherm

When considering adsorption isotherms it is conventional to adopt a definition of surface coverage ( $\theta$ ) which defines the maximum (saturation) surface coverage of a particular adsorbate on a given surface always to be unity, i.e.  $\theta_{max} = 1$ . This way of defining the surface coverage differs from that usually adopted in surface science where the more common practice is to equate  $\theta$  with the ratio of adsorbate species to surface substrate atoms (which leads to saturation coverages which are almost invariably less than unity).

---

This page titled [3.1: Introduction](#) is shared under a [CC BY-NC-SA 4.0](#) license and was authored, remixed, and/or curated by [Roger Nix](#).

## 3.2: Langmuir Isotherm - derivation from equilibrium considerations

We may derive the Langmuir isotherm by treating the adsorption process as we would any other equilibrium process - except in this case the equilibrium is between the gas phase molecules ( $M$ ), together with vacant surface sites, and the species adsorbed on the surface. Thus, for a non-dissociative (molecular) adsorption process, we consider the adsorption to be represented by the following chemical equation:



where:

- $S - *$  represents a vacant surface site

### Assumption 1

In writing Equation 3.2.1 we are making an inherent assumption that there are a fixed number of localized surface sites present on the surface. This is the first major assumption of the Langmuir isotherm.

We may now define an equilibrium constant ( $K$ ) in terms of the concentrations of "reactants" and "products"

$$K = \frac{[S - M]}{[S - *][M]} \quad (3.2.2)$$

We may also note that:

- $[S - M]$  is proportional to the surface coverage of adsorbed molecules, i.e. proportional to  $\theta$
- $[S - *]$  is proportional to the number of vacant sites, i.e. proportional to  $(1-\theta)$
- $[M]$  is proportional to the pressure of gas,  $P$

Hence, it is also possible to define another equilibrium constant,  $b$ , as given below:

$$b = \frac{\theta}{(1-\theta)P} \quad (3.2.3)$$

Rearrangement then gives the following expression for the surface coverage

$$\theta = \frac{bP}{1 + bP} \quad (3.2.4)$$

which is the usual form of expressing the Langmuir Isotherm. As with all chemical reactions, the equilibrium constant,  $b$ , is both temperature-dependent and related to the Gibbs free energy and hence to the enthalpy change for the process.

### Assumption 2

$b$  is only a constant (independent of  $\theta$ ) if the enthalpy of adsorption is independent of coverage. This is the second major assumption of the Langmuir Isotherm.

This page titled [3.2: Langmuir Isotherm - derivation from equilibrium considerations](#) is shared under a [CC BY-NC-SA 4.0](#) license and was authored, remixed, and/or curated by [Roger Nix](#).

### 3.3: Langmuir Isotherm from a Kinetics Consideration

The equilibrium that may exist between gas adsorbed on a surface and molecules in the gas phase is a dynamic state, i.e. **the equilibrium represents a state in which the rate of adsorption of molecules onto the surface is exactly counterbalanced by the rate of desorption of molecules back into the gas phase.** It should therefore be possible to derive an isotherm for the adsorption process simply by considering and equating the rates for these two processes.

Expressions for the rate of adsorption and rate of desorption have been derived in Sections 2.3 & 2.6 respectively: specifically,

$$R_{ads} = \frac{f(\theta)P}{\sqrt{2\pi mkT}} \exp(-E_a^{ads}/RT) \quad (3.3.1)$$

$$R_{des} = v f'(\theta) \exp(-E_a^{ads}/RT) \quad (3.3.2)$$

Equating these two rates yields an equation of the form:

$$\frac{P f(\theta)}{f'(\theta)} = C(T) \quad (3.3.3)$$

where  $\theta$  is the fraction of sites occupied at equilibrium and the terms  $f(\theta)$  and  $f'(\theta)$  contain the pre-exponential surface coverage dependence of the rates of adsorption and desorption respectively and all other factors have been taken over to the right hand side to give a temperature-dependent "constant" characteristic of this particular adsorption process,  $C(T)$ . We now need to make certain simplifying assumptions. The first is one of the key assumptions of the Langmuir isotherm.

#### Note: Assumption 1

Adsorption takes place only at specific localized sites on the surface and the saturation coverage corresponds to complete occupancy of these sites.

Let us initially further restrict our consideration to a simple case of **reversible molecular adsorption**, i.e.



where

- $S_{-}$  represents a vacant surface site and
- $S-M$  the adsorption complex.

Under these circumstances it is reasonable to assume coverage dependencies for rates of the two processes of the form:

- **Adsorption** (forward reaction in Equation 3.3.4):

$$f(\theta) = c(1 - \theta) \quad (3.3.5)$$

i.e. proportional to the fraction of sites that are unoccupied.

- **Desorption** (reverse reaction in Equation 3.3.4):

$$f'(\theta) = c'\theta \quad (3.3.6)$$

i.e. proportional to the fraction of sites which are occupied by adsorbed molecules.

#### Note

These coverage dependencies in Equations 3.3.5 and 3.3.6 are exactly what would be predicted by noting that the forward and reverse processes are elementary reaction steps, in which case it follows from standard chemical kinetic theory that

- The forward adsorption process will exhibit kinetics having a first order dependence on the concentration of vacant surface sites and first order dependence on the concentration of gas particles (proportional to pressure).
- The reverse desorption process will exhibit kinetics having a first order dependence on the concentration of adsorbed molecules.

Substitution of Equations 3.3.5 and 3.3.6 into Equation 3.3.3 yields:

$$\frac{P(1-\theta)}{\theta} = B(T) \quad (3.3.7)$$

where

$$B(T) = \left(\frac{c'}{c}\right) C(T). \quad (3.3.8)$$

After rearrangement this gives the *Langmuir Isotherm* expression for the surface coverage

$$\theta = \frac{bP}{1+bP} \quad (3.3.9)$$

where  $b = 1/B(T)$  is a function of temperature and contains an exponential term of the form

$$b \propto \exp[(E_a^{des} - E_a^{ads})/RT] = \exp[-\Delta H_{ads}/RT] \quad (3.3.10)$$

with

$$\Delta H_{ads} = E_a^{des} - E_a^{ads}. \quad (3.3.11)$$

#### Note: Assumption 2

$b$  can be regarded as a **constant** with respect to coverage only if the enthalpy of adsorption is itself **independent** of coverage; this is the second major assumption of the Langmuir Isotherm.

---

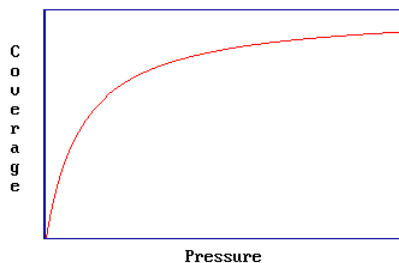
This page titled [3.3: Langmuir Isotherm from a Kinetics Consideration](#) is shared under a [CC BY-NC-SA 4.0](#) license and was authored, remixed, and/or curated by [Roger Nix](#).

### 3.4: Variation of Surface Coverage with Temperature and Pressure

Application of the assumptions of the Langmuir Isotherm leads to readily derivable expressions for the pressure dependence of the surface coverage (see Sections 3.2 and 3.3) - in the case of a simple, reversible molecular adsorption process the expression is

$$\theta = \frac{bP}{1 + bP} \quad (3.4.1)$$

where  $b = b(T)$ . This is illustrated in the graph below which shows the characteristic Langmuir variation of coverage with pressure for molecular adsorption.



Note two extremes in Equation 3.4.1:

- At low pressures

$$\lim_{P \rightarrow 0} \theta = bP \quad (3.4.2)$$

- At high pressures

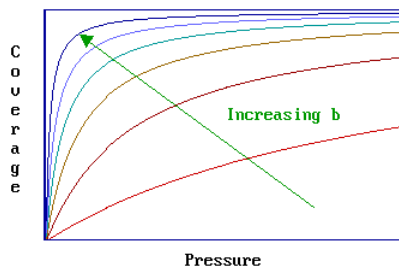
$$\lim_{P \rightarrow \infty} \theta = 1 \quad (3.4.3)$$

At a given pressure the extent of adsorption is determined by the value of  $b$ , which is dependent upon both the temperature ( $T$ ) and the enthalpy (heat) of adsorption. Remember that the magnitude of the adsorption enthalpy (a negative quantity itself) reflects the strength of binding of the adsorbate to the substrate.

The value of  $b$  is increased by

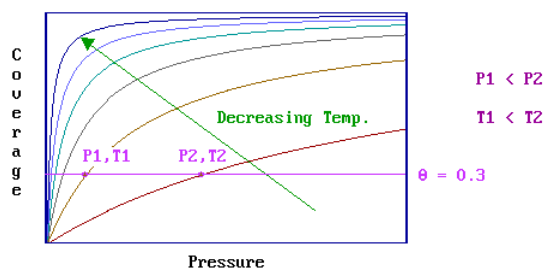
1. a reduction in the system temperature
2. an increase in the strength of adsorption

Therefore the set of curves shown below illustrates the effect of either (i) increasing the magnitude of the adsorption enthalpy at a fixed temperature, or (ii) decreasing the temperature for a given adsorption system.



A given equilibrium surface coverage may be attainable at various combinations of pressure and temperature as highlighted below ... note that as the temperature is lowered the pressure required to achieve a particular equilibrium surface coverage decreases.





- this is often used as justification for one of the main ideologies of surface chemistry ; specifically, that it is possible to study technologically-important (high pressure / high temperature) surface processes within the low pressure environment of typical surface analysis systems by working at low temperatures. It must be recognized however that, at such low temperatures, kinetic restrictions that are not present at higher temperatures may become important.

If you wish to see how the various factors relating to the adsorption and desorption of molecules influence the surface coverage then try out the Interactive Demonstration of the Langmuir Isotherm (note - this is based on the derivation discuss previously ).

### Determination of Enthalpies of Adsorption

It has been shown in previous sections how the value of  $b$  is dependent upon the enthalpy of adsorption. It has also just been demonstrated how the value of  $b$  influences the pressure/temperature (P-T) dependence of the surface coverage. The implication of this is that it must be possible to determine the enthalpy of adsorption for a particular adsorbate/substrate system by studying the P-T dependence of the surface coverage. Various methods based upon this idea have been developed for the determination of adsorption enthalpies - one method is outlined below:

Step 1: Involves determination of a number of adsorption isotherms, where a single isotherm is a coverage / pressure curve at a fixed temperature (Figure 3.4.1).

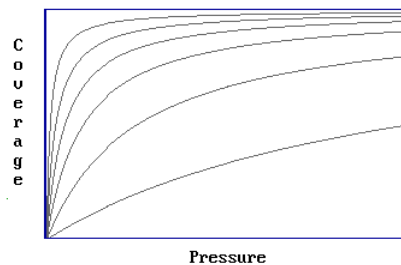


**Figure 3.4.1**

Step 2: It is then possible to read off a number of pairs of values of pressure and temperature which yield the same surface coverage (Figure 3.4.2)

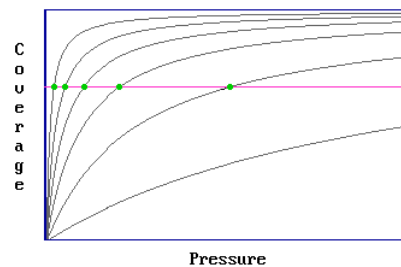


**Figure 3.4.2:**

Step 3: The Clausius-Clapeyron equation

$$\left( \frac{\partial \ln P}{\partial \frac{1}{T}} \right)_{\theta} = \frac{\Delta H_{abs}}{R} \quad (3.4.4)$$

may then be applied to this set of (P-T) data and a plot of  $(\ln P)$  v's  $(1/T)$  should give a straight line, the slope of which yields the adsorption enthalpy (Figure .

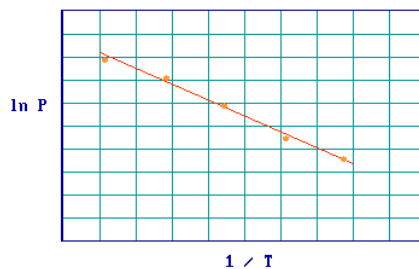


**Figure 3.4.3:**

The value obtained for the adsorption enthalpy is that pertaining at the surface coverage for which the P-T data was obtained, but steps 2 & 3 may be repeated for different surface coverages enabling the adsorption enthalpy to be determined over the whole range of coverages. This method is applicable only when the adsorption process is thermodynamically **reversible**.

---

This page titled [3.4: Variation of Surface Coverage with Temperature and Pressure](#) is shared under a [CC BY-NC-SA 4.0](#) license and was authored, remixed, and/or curated by [Roger Nix](#).

## 3.5: Applications - Kinetics of Catalytic Reactions

It is possible to predict how the kinetics of certain heterogeneously-catalyzed reactions might vary with the partial pressures of the reactant gases above the catalyst surface by using the Langmuir isotherm expression for equilibrium surface coverages.

### Unimolecular Decomposition

Consider the surface decomposition of a molecule A, i.e. the process



Let us assume that:

1. The decomposition reaction occurs uniformly across the surface sites at which molecule A may be adsorbed and is not restricted to a limited number of special sites.
2. The products are very weakly bound to the surface and, once formed, are rapidly desorbed.
3. The rate determining step (rds) is the surface decomposition step.

Under these circumstances, the molecules of A adsorbed on the surface are in equilibrium with those in the gas phase and we may predict the surface concentration of A from the Langmuir isotherm, i.e.

$$\theta = \frac{bP}{1 + bP} \quad (3.5.2)$$

The rate of the surface decomposition (and hence of the reaction) is given by an expression of the form

$$rate = k\theta \quad (3.5.3)$$

This is assuming that the decomposition of A(ads) occurs in a simple unimolecular elementary reaction step and that the kinetics are first order with respect to the surface concentration of this adsorbed intermediate). Substituting for the coverage,  $\theta$ , gives us the required expression for the rate in terms of the pressure of gas above the surface

$$rate = \frac{kbP}{1 + bP} \quad (3.5.4)$$

It is useful to consider two extremes:

#### Low Pressure/Binding Limit

This is the low pressure (or weak binding, i.e., small  $b$ ) limit: under these conditions the steady state surface coverage,  $\theta$ , of the reactant molecule is very small.

$$bP \ll 1 \quad (3.5.5)$$

then

$$1 + bP \approx 1 \quad (3.5.6)$$

and Equation 3.5.4 can be simplified to

$$rate \approx kbP \quad (3.5.7)$$

Under this limiting case, the kinetics follow a first order reaction (with respect to the partial pressure of A) with an apparent first order rate constant  $k' = kb$ .

#### High Pressure/Binding Limit

This is the high pressure (or strong binding, i.e., large  $b$ ) limit: under these conditions the steady state surface coverage,  $\theta$ , of the reactant molecule is almost unity and

$$bP \gg 1 \quad (3.5.8)$$

then

$$1 + bP \approx bP \quad (3.5.9)$$

and Equation 3.5.4 can be simplified to

$$rate \approx k \quad (3.5.10)$$

under this limiting case, the kinetics follow a zero order reaction (with respect to the partial pressure of  $A$ ). The rate shows the same pressure variation as does the surface coverage, but this hardly surprising since it is directly proportional to  $\theta$ .

These two limiting cases can be identified in the general kinetics from Equation 3.5.4 in Figure 3.5.1.

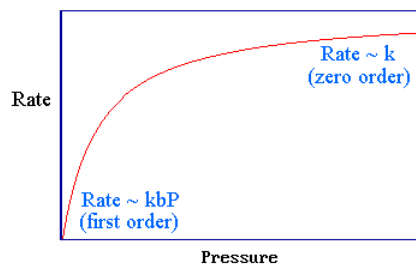
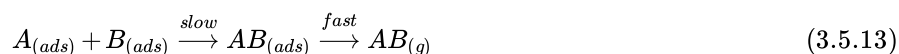


**Figure 3.5.1:**

### Bimolecular Reaction (between molecular adsorbates)

Consider a Langmuir-Hinshelwood reaction of the following type:



We will further assume, as noted in the above scheme, that the surface reaction between the two adsorbed species (left side of Equation 3.5.13) is the rate determining step.

If the two adsorbed molecules are mobile on the surface and freely intermix then the rate of the reaction will be given by the following rate expression for the **bimolecular** surface combination step

$$Rate = k\theta_A\theta_B \quad (3.5.14)$$

For a single molecular adsorbate the surface coverage (as given by the standard Langmuir isotherm) is

$$\theta = \frac{bP}{1 + bP} \quad (3.5.15)$$

Where two molecules ( $A$  &  $B$ ) are competing for the same adsorption sites then the relevant expressions are (see derivation):

$$\theta_A = \frac{b_A P_A}{1 + b_A P_A + b_B P_B} \quad (3.5.16)$$

and

$$\theta_B = \frac{b_B P_B}{1 + b_A P_A + b_B P_B} \quad (3.5.17)$$

Substituting these into the rate expression gives:

$$Rate = k\theta_A\theta_B = \frac{k b_A P_A b_B P_B}{(1 + b_A P_A + b_B P_B)^2} \quad (3.5.18)$$

Once again, it is interesting to look at several extreme limits

#### Low Pressure/Binding Limit

$$b_A P_A \ll 1 \quad (3.5.19)$$

and

$$b_B P_B \ll 1 \quad (3.5.20)$$

In this limit that  $\theta_A$  &  $\theta_B$  are both very low, and

$$rate \rightarrow kb_A P_A b_B P_B = k' P_A P_B \quad (3.5.21)$$

i.e. *first order* in both reactants

#### Mixed Pressure/Binding Limit

$$b_A P_A \ll 1 \ll b_B P_B \quad (3.5.22)$$

In this limit  $\theta_A \rightarrow 0$ ,  $\theta_B \rightarrow 1$ , and

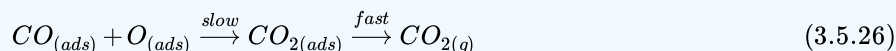
$$Rate \rightarrow \frac{kb_A P_A}{b_B P_B} = \frac{k' P_A}{P_B} \quad (3.5.23)$$

i.e. *first order* in  $A$ , but *negative first order* in  $B$

Clearly, depending upon the partial pressure and binding strength of the reactants, a given model for the reaction scheme can give rise to a variety of apparent kinetics: this highlights the dangers inherent in the reverse process - namely trying to use kinetic data to obtain information about the reaction mechanism.

#### ✓ Example 3.5.1: CO Oxidation Reaction

On precious metal surfaces (e.g. Pt), the  $CO$  oxidation reaction is generally believed to be a *Langmuir-Hinshelwood mechanism* of the following type:



As  $CO_2$  is comparatively weakly-bound to the surface, the desorption of this product molecule is relatively fast and in many circumstances it is the surface reaction between the two adsorbed species that is the rate determining step.

If the two adsorbed molecules are assumed to be mobile on the surface and freely intermix then the rate of the reaction will be given by the following rate expression for the bimolecular surface combination step

$$Rate = k \theta_{CO} \theta_O \quad (3.5.27)$$

Where two such species (one of which is molecularly adsorbed, and the other dissociatively adsorbed) are competing for the same adsorption sites then the relevant expressions are (see derivation):

$$\theta_{CO} = \frac{b_{CO} P_{CO}}{1 + \sqrt{b_O P_{O_2}} + b_{CO} P_{CO}} \quad (3.5.28)$$

and

$$\theta_O = \frac{\sqrt{b_O P_{O_2}}}{1 + \sqrt{b_O P_{O_2}} + b_{CO} P_{CO}} \quad (3.5.29)$$

Substituting these into the rate expression gives:

$$rate = k \theta_{CO} \theta_O = \frac{kb_{CO} P_{CO} \sqrt{b_O P_{O_2}}}{(1 + \sqrt{b_O P_{O_2}} + b_{CO} P_{CO})^2} \quad (3.5.30)$$

Once again, it is interesting to look at certain limits. If the  $CO$  is much more strongly bound to the surface such that

$$b_{CO} P_{CO} \gg 1 + \sqrt{b_O P_{O_2}} \quad (3.5.31)$$

then

$$1 + \sqrt{b_O P_{O_2}} + b_{CO} P_{CO} \approx b_{CO} P_{CO} \quad (3.5.32)$$

and the Equation 3.5.30 simplifies to give

$$rate \approx \frac{k \sqrt{b_O P_{O_2}}}{b_{CO} P_{CO}} = k' \frac{P_{O_2}^{1/2}}{P_{CO}} \quad (3.5.33)$$

In this limit the kinetics are half-order with respect to the gas phase pressure of molecular oxygen, but negative order with respect to the  $CO$  partial pressure, i.e.  $CO$  acts as a poison (despite being a reactant) and increasing its pressure slows down the reaction. This is because the  $CO$  is so strongly bound to the surface that it blocks oxygen adsorbing, and without sufficient oxygen atoms on the surface the rate of reaction is reduced.

This page titled [3.5: Applications - Kinetics of Catalytic Reactions](#) is shared under a [CC BY-NC-SA 4.0](#) license and was authored, remixed, and/or curated by [Roger Nix](#).

## CHAPTER OVERVIEW

### 4: UHV and Effects of Gas Pressure

4.1: What is UltraHigh Vacuum?

4.2: Why is UHV required for surface studies ?

4.E: UHV and Effects of Gas Pressure (Exercises)

---

This page titled [4: UHV and Effects of Gas Pressure](#) is shared under a [CC BY-NC-SA 4.0](#) license and was authored, remixed, and/or curated by Roger Nix.

## 4.1: What is UltraHigh Vacuum?

---

Vacuum technology has advanced considerably over the last 25 years and very low pressures are now routinely obtainable. Firstly, we need to remind ourselves of the units of pressure:

- The SI unit of pressure is the Pascal (  $1 \text{ Pa} = 1 \text{ N m}^{-2}$  )
- Normal atmospheric pressure (  $1 \text{ atm.}$  ) is 101325 Pa or 1013 mbar (  $1 \text{ bar} = 10^5 \text{ Pa}$  ).
- An older unit of pressure is the Torr (  $1 \text{ Torr} = 1 \text{ mmHg}$  ). One atmosphere is ca. 760 Torr ( i.e.  $1 \text{ Torr} = 133.3 \text{ Pa}$  ).

While the mbar is often used as a unit of pressure for describing the level of vacuum, the most commonly employed unit is still the Torr (the *SI unit*, the Pa, is almost never used). Classification of the degree of vacuum is hardly an exact science - it much depends upon who you are talking to - but as a rough guideline:

Rough (low) vacuum:	$1 - 10^{-3} \text{ Torr}$
Medium vacuum:	$10^{-3} - 10^{-5} \text{ Torr}$
High vacuum (HV):	$10^{-6} - 10^{-8} \text{ Torr}$
Ultrahigh vacuum (UHV):	$< 10^{-9} \text{ Torr}$

Virtually all surface studies are carried out under UHV conditions - the question is **why** ? This is the question that we will address in [Section 4.2](#).

---

This page titled [4.1: What is UltraHigh Vacuum?](#) is shared under a [CC BY-NC-SA 4.0](#) license and was authored, remixed, and/or curated by [Roger Nix](#).



## 4.2: Why is UHV required for surface studies ?

Ultra high vacuum is required for most surface science experiments for two principal reasons:

1. To enable atomically clean surfaces to be prepared for study, and such surfaces to be maintained in a contamination-free state for the duration of the experiment.
2. To permit the use of low energy electron and ion-based experimental techniques without undue interference from gas phase scattering.

To put these points in context we shall now look at the variation of various parameters with pressure

### Gas Density

The gas density  $\rho$  is easily estimated from the [ideal gas law](#):

$$\rho = \frac{N}{V} = \frac{P}{kT} \quad (4.2.1)$$

with

- $\rho$  is the gas density [ molecules/ m<sup>-3</sup> ]
- $P$  is the pressure [ N m<sup>-2</sup> ]
- $k$  is Boltzmann constant, which is  $\frac{R}{N_A} = 1.38 \times 10^{-23} \text{ J K}^{-1}$  )
- $T$  is absolute temperature [ K ]

### Mean Free Path of Particles in the Gas Phase

The average distance that a particle (atom, electron, molecule ..) travels in the gas phase between collisions can be determined from a simple hard-sphere collision model - this quantity is known as the *mean free path* of the particle, here denoted by  $\lambda$ , and for neutral molecules is given by the equation:

$$\lambda = \frac{kT}{\sqrt{2}P\sigma} \quad (4.2.2)$$

with

- $\lambda$  is the mean free path [m]
- $P$  - pressure [ N m<sup>-2</sup> ]
- $k$  - Boltzmann constant ( = 1.38 x 10<sup>-23</sup> J K<sup>-1</sup> )
- $T$  - temperature [ K ]
- $\sigma$  - collision cross section [ m<sup>2</sup> ]

### Incident Molecular Flux on Surfaces

One of the crucial factors in determining how long a surface can be maintained clean (or, alternatively, how long it takes to build-up a certain surface concentration of adsorbed species) is the number of gas molecules impacting on the surface from the gas phase. The incident *flux* is the number of incident molecules per unit time per unit area of surface.

The flux takes no account of the angle of incidence, it is merely a summation of all the arriving molecules over all possible incident angles

For a given set of conditions ( $P, T$  etc.) the flux is readily calculated using a combination of the ideas of statistical physics, the ideal gas equation and the [Maxwell-Boltzmann gas velocity distribution](#).

*Step 1:*

It can be readily shown that the incident flux,  $F$ , is related to the gas density above the surface by

$$F = \frac{1}{2}n\bar{c} \quad (4.2.3)$$

with

- $n$  is the molecular gas density [ molecules  $m^{-3}$  ]
- $F$  is the flux [ molecules  $m^{-2} s^{-1}$  ]
- $\bar{c}$  is the average molecular speed [  $m s^{-1}$  ]

Step 2: the molecular gas density is given by the ideal gas equation, namely

$$n = \frac{N}{V} = \frac{P}{kT} \quad (\text{molecules } m^{-3}) \quad (4.2.4)$$

Step 3: the mean molecular speed is obtained from the Maxwell-Boltzmann distribution of gas velocities by integration, yielding

$$\bar{c} = \sqrt{\frac{8kT}{m\pi}} \quad (m s^{-1}) \quad (4.2.5)$$

where

- $m$  - molecular mass [ kg ]
- $k$  - Boltzmann constant ( =  $1.38 \times 10^{-23} \text{ J K}^{-1}$  )
- $T$  - temperature [ K ]
- $\pi = 3.1416$

Step 4: combining the equations from the first three steps gives the Hertz-Knudsen formula for the incident flux

$$F = \frac{P}{\sqrt{2\pi mkT}} \quad [\text{molecules } m^{-2} s^{-1}] \quad (4.2.6)$$

Note

1. all quantities in the above equation need to be expressed in SI units
2. the molecular flux is directly proportional to the pressure

### Gas Exposure: The "Langmuir"

The *gas exposure* is measure of the amount of gas which a surface has been subjected to. It is numerically quantified by taking the product of the pressure of the gas above the surface and the time of exposure (if the pressure is constant, or more generally by calculating the integral of pressure over the period of time of concern).

Although the exposure may be given in the SI units of Pa s (Pascal seconds), the normal and far more convenient unit for exposure is the *Langmuir*, where  $1 \text{ L} = 10^{-6} \text{ Torr s}$  . i.e.

$$(\text{Exposure}/L) = 10^6 \times (\text{Pressure}/\text{Torr}) \times (\text{Time}/s) \quad (4.2.7)$$

### Sticking Coefficient & Surface Coverage

The *sticking coefficient*,  $S$ , is a measure of the fraction of incident molecules which adsorb upon the surface i.e. it is a probability and lies in the range 0 - 1, where the limits correspond to no adsorption and complete adsorption of all incident molecules respectively. In general,  $S$  depends upon many variables i.e.

$$S = f(\text{surface coverage, temperature, crystal face} \dots) \quad (4.2.8)$$

The *surface coverage* of an adsorbed species may itself, however, be specified in a number of ways:

1. as the number of adsorbed species per unit area of surface (e.g. in molecules  $cm^{-2}$ ).
2. as a fraction of the maximum attainable surface coverage i.e.

$$\theta = \frac{\text{actual surface coverage}}{\text{saturation surface coverage}} \quad (4.2.9)$$

3. - in which case  $\theta$  lies in the range 0 - 1 .
4. relative to the atom density in the topmost atomic layer of the substrate i.e.

$$\theta = \frac{\text{No. of adsorbed species per unit area of surface}}{\text{No. of surface substrate atoms per unit area}} \quad (4.2.10)$$

where  $\theta_{max}$  is usually less than one, but can for an adsorbate such as H occasionally exceed one.

Note:

1. whichever definition is used, the surface coverage is normally denoted by the Greek  $\theta$
2. the second means of specifying the surface coverage is only usually employed for adsorption isotherms (e.g. the Langmuir isotherm). The third method is the most generally accepted way of defining the surface coverage.
3. a *monolayer* (1 ML) of adsorbate is taken to correspond to the maximum attainable surface concentration of adsorbed species bound to the substrate.

#### ✓ Example 4.2.1:

How long will it take for a clean surface to become covered with a complete monolayer of adsorbate?

#### Solution

This is dependent upon the flux of gas phase molecules incident upon the surface, the actual coverage corresponding to the monolayer and the coverage-dependent sticking probability and other aspect. however, it is possible to get a minimum estimate of the time required by assuming a unit sticking probability (i.e.  $S = 1$ ) and noting that monolayer coverages are generally of the order of  $10^{15}$  per  $\text{cm}^2$  or  $10^{19}$  per  $\text{m}^2$ . Then

$$\text{Time / ML} \sim ( 10^{19} / F ) [ \text{s} ]$$

### Variation of Parameters with Pressure

All values given below are approximate and are generally dependent on factors such as temperature and molecular mass.

Degree of Vacuum	Pressure (Torr)	Gas Density (molecules $\text{m}^{-3}$ )	Mean Free Path (m)	Time / ML (s)
Atmospheric	760	$2 \times 10^{25}$	$7 \times 10^{-8}$	$10^{-9}$
Low	1	$3 \times 10^{22}$	$5 \times 10^{-5}$	$10^{-6}$
Medium	$10^{-3}$	$3 \times 10^{19}$	$5 \times 10^{-2}$	$10^{-3}$
High	$10^{-6}$	$3 \times 10^{16}$	50	1
UltraHigh	$10^{-10}$	$3 \times 10^{12}$	$5 \times 10^5$	$10^4$

We can therefore conclude that the following requirements exist for:

Collision Free Conditions	⇒	$P < 10^{-4}$ Torr
Maintenance of a Clean Surface	⇒	$P < 10^{-9}$ Torr

### Summary

For most surface science experiments there are a number of factors necessitating a high vacuum environment:

1. For surface spectroscopy, the mean free path of probe and detected particles (ions, atoms, electrons) in the vacuum environment must be significantly greater than the dimensions of the apparatus in order that these particles may travel to the surface and from the surface to detector without undergoing any interaction with residual gas phase molecules. This requires pressures better than  $10^{-4}$  Torr. There are, however, some techniques, such as IR spectroscopy, which are "photon-in/photon-out" techniques and do not suffer from this requirement.  
(On a practical level, it is also the case that the lifetime of channeltron and multiplier detectors used to detect charged particles is substantially reduced by operation at pressures above  $10^{-6}$  Torr).
2. Most spectroscopic techniques are also capable of detecting molecules in the gas phase; in these cases it is preferable that the number of species present on the surface substantially exceeds those present in the gas phase immediately above the surface - to achieve a surface/gas phase discrimination of better than 10:1 when analysing ca. 1% of a monolayer on a flat surface this requires that the gas phase concentration is less than ca.  $10^{12}$  molecules  $\text{cm}^{-3}$  ( $= 10^{18}$  molecules  $\text{m}^{-3}$ ), i.e. that the (partial) pressure is of the order of  $10^{-4}$  Torr or lower.

To begin experiments with a reproducibly clean surface, and to ensure that significant contamination by background gases does

not occur during an experiment, the background pressure must be such that the time required for contaminant build-up is substantially greater than that required to conduct the experiment i.e. of the order of hours. The implication with regard to the required pressure depends upon the nature of the surface, but for the more reactive surfaces this necessitates the use of UHV (i.e.  $< 1 \times 10^{-9}$  Torr).

It is clear therefore that it is the last factor that usually determines the need for a very good vacuum in order to carry out reliable surface science experiments.

---

This page titled [4.2: Why is UHV required for surface studies ?](#) is shared under a [CC BY-NC-SA 4.0](#) license and was authored, remixed, and/or curated by [Roger Nix](#).

## 4.E: UHV and Effects of Gas Pressure (Exercises)

This section provides a limited number of examples of the application of the formulae given in the previous section to determine the:

- Density of Molecules in the Gas Phase
- Mean Free Path of Molecules in the Gas Phase
- Flux of Molecules incident upon a Surface
- Rate of Adsorption of Molecules and Surface Coverages

If you have not already been through [Section 4.2](#) then I would suggest that you stop now and return to this page only after you have done so !

*Within any one of the following sub-sections, it will be assumed that you have already done the previous questions and may make use of the answers from these questions - you are therefore advised to work through the questions in the order they are presented.*

### A. Molecular Gas Densities

Calculate the molecular gas density for an ideal gas at 300 K, under the following conditions (giving your answer in molecules  $\text{m}^{-3}$ ):

<input type="text"/>	At a pressure of $10^{-6}$ Torr
<input type="text"/>	At a pressure of $10^{-9}$ Torr

### B. Mean Free Path of Molecules in the Gas Phase

Calculate the mean free path of CO molecules in a vessel at the indicated pressure and temperature, using a value for the collision cross section of CO of  $0.42 \text{ nm}^2$ .

<input type="text"/>	$P = 10^{-4}$ Torr, at 300 K
<input type="text"/>	$P = 10^{-9}$ Torr, at 300 K

### C. Fluxes of Molecules Incident upon a Surface

Calculate the flux of molecules incident upon a solid surface under the following conditions:

[Note -  $1 \text{ u} = 1.66 \times 10^{-27} \text{ kg}$ ; atomic masses ;  $m(\text{O}) = 16.0 \text{ u}$ ,  $m(\text{H}) = 1.0 \text{ u}$ ]

<input type="text"/>	Oxygen gas ( $P = 1 \text{ Torr}$ ) at 300 K
<input type="text"/>	Oxygen gas ( $P = 10^{-6} \text{ Torr}$ ) at 300 K
<input type="text"/>	Hydrogen gas ( $P = 10^{-6} \text{ Torr}$ ) at 300 K
<input type="text"/>	Hydrogen gas ( $P = 10^{-6} \text{ Torr}$ ) at 1000 K

### D. The Kinetically Limited Uptake of Molecules onto a Surface

The rate of adsorption of molecules onto a surface can be determined from the flux of molecules incident on the surface and the sticking probability pertaining at that instant in time (note that in general the sticking probability itself will be dependent upon a number of factors including the existing coverage of adsorbed species).

In the following examples we will assume that the surface is initially clean (i.e. the initial coverage is zero), and that there is no desorption of the molecules once they have adsorbed. You should determine coverages as the ratio of the adsorbate concentration to the density of surface substrate atoms (which you may assume to be  $10^{19} \text{ m}^{-2}$ ). In the first two questions we will assume that the sticking probability is constant over the coverage range concerned.

<input type="text"/>	Calculate the surface coverage obtained after exposure to a pressure of $10^{-8} \text{ Torr}$ of CO for 20 s at 300 K - you may take the sticking probability of CO on this surface to have a constant value of 0.9 up to the coverage concerned.
----------------------	--

— Calculate the surface coverage of atomic nitrogen obtained by dissociative adsorption after exposure to a pressure of  $10^{-9}$  Torr of nitrogen gas for 20 s at 300 K - you may take the dissociative sticking probability of molecular nitrogen on this surface to be constant and equal to 0.1

In general, the sticking probability varies with coverage - most obviously, the sticking probability must tend to zero as the coverage approaches its saturation value. These calculations are not quite so easy !

— Calculate the surface coverage obtained after exposure to a pressure of  $10^{-9}$  Torr of CO for 200 s at 300 K - the sticking probability of CO in this case should be taken to vary linearly with coverage between a value of unity at zero coverage and a value of zero at saturation coverage (which you should take to be  $6.5 \times 10^{18}$  molecules  $\text{m}^{-2}$ ).

This page titled [4.E: UHV and Effects of Gas Pressure \(Exercises\)](#) is shared under a [CC BY-NC-SA 4.0](#) license and was authored, remixed, and/or curated by [Roger Nix](#).

## CHAPTER OVERVIEW

### 5: Surface Analytical Techniques

- 5.1: Surface Sensitivity and Surface Specificity
- 5.2: Auger Electron Spectroscopy
- 5.3: Photoelectron Spectroscopy
- 5.4: Vibrational Spectroscopy
- 5.5: Secondary Ion Mass Spectrometry
- 5.6: Temperature-Programmed Techniques

---

This page titled [5: Surface Analytical Techniques](#) is shared under a [CC BY-NC-SA 4.0](#) license and was authored, remixed, and/or curated by Roger Nix.

## 5.1: Surface Sensitivity and Surface Specificity

### General Sensitivity Problems

The problems of sensitivity and detection limits are common to all forms of spectroscopy; some techniques are simply better than others in this respect! In its simplest form, the question of sensitivity boils down to whether it is possible to detect the desired signal above the noise level.

In virtually all surface studies (especially those on single crystal substrates) sensitivity is a major problem. Consider the case of a sample with a surface of size  $1 \text{ cm}^2$  - this will have ca.  $10^{15}$  atoms in the surface layer. In order to detect the presence of impurity atoms present at the 1 % level, a technique must be sensitive to ca.  $10^{13}$  atoms. Contrast this with a spectroscopic technique used to analyze a  $1 \text{ cm}^3$  bulk liquid sample i.e. a sample of ca.  $10^{22}$  molecules. The detection of  $10^{13}$  molecules in this sample would require 1 ppb (one *part-per-billion*) sensitivity - very few techniques can provide anything like this level of sensitivity! This is one reason why common spectroscopic techniques such as NMR (detection limit ca.  $10^{19}$  molecules) cannot be used for surface studies, except on samples with very high surface areas.

### Surface Sensitivity & Specificity

Assuming that a technique of sufficient sensitivity can be found, another major problem that needs to be addressed in surface spectroscopy is distinguishing between signals from the surface and the bulk of the sample. In principle, there are two ways around this problem:

1. To ensure that the surface signal is distinguishable (shifted) from the comparable bulk signal, and that the detection system has sufficient dynamic range to detect very small signals in the presence of neighboring large signals.
2. To ensure that the bulk signal is small compared to the surface signal i.e. that the vast majority of detected signal comes from the surface region of the sample.

It is the latter approach which is used by the majority of surface spectroscopic techniques - such techniques can then be said to be *surface sensitive*. To illustrate this, we shall look at one way in which surface sensitivity can be achieved - this makes use of the special properties of **Low Energy Electrons**. It is an approach employed in common surface spectroscopic techniques such as [Auger Electron Spectroscopy \(AES\)](#) and [X-ray Photoelectron Spectroscopy \(XPS\)](#).

We shall illustrate this approach by considering the latter technique (XPS) but you should remember that the ideas that we develop are more widely applicable.

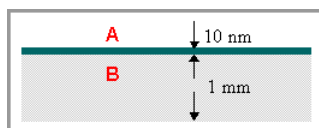
### XPS - A surface sensitive technique?

In answering this important question, we will actually address the topics listed below - you are strongly advised to work through them in the order in which they are given.

1. What do we really mean by surface sensitivity / specificity ?
2. How can we demonstrate that XPS is surface sensitive ?
3. Why is the XPS technique surface sensitive ?
4. How can we use knowledge of the IMFP to calculate the thickness of surface films ?
5. How can we change the degree of surface sensitivity ?

### What do we really mean by surface sensitivity / specificity?

Most analytical techniques used in chemistry are "bulk" techniques in the sense that they measure all the atoms within a typical sample (be it a solid, liquid, solution or gas phase sample) - so if, for example, we were to analyse a sample consisting of a 10 nm thick layer of one material (A) deposited on a 1 mm thick substrate of another material (B) ....

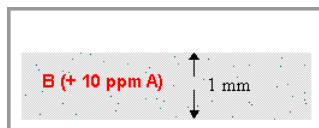


... and to ask the question ....



What would be the concentration of A in parts per million (ppm) which you would expect to be revealed by a bulk analysis of such a sample ?

... we would get the same result (10 ppm) as if we were looking at a sample in which component A was uniformly distributed throughout the bulk of B such as to give the same overall concentration in the sample as a whole.



By contrast, a *surface sensitive* technique is more sensitive to those atoms which are located near the surface than it is to atoms in the bulk which are well away from the surface (i.e. the main part of the signal comes from the surface region) - in the case of the first sample therefore a surface sensitive technique would produce a spectrum with enhanced signals due to component A, i.e.

$$\frac{I_A}{I_B} \gg 10^{-5} \quad (5.1.1)$$

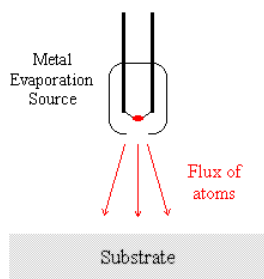
where  $I_A$  is the signal due to component A etc.

A truly *surface specific* technique should **only** give signals due to atoms in the surface region - but that, of course, rather depends how the "surface region" is defined!

Electron spectroscopic techniques such as XPS are **not** completely surface specific (although you will occasionally find this expression being used) in that whilst most of the signal comes from within a few atomic layers of the surface, a small part of the signal comes from much deeper into the solid - they are best described as being **surface sensitive** techniques. However, we should also note that there are a few techniques (e.g. low energy ion scattering [ISS/LEIS]) which are indeed virtually specific to the topmost layer of atoms.

### How can we demonstrate that XPS is surface sensitive ?

Consider again the first of the two samples considered in the previous section - such samples are often readily prepared by depositing material A by evaporation onto a substrate of material B.



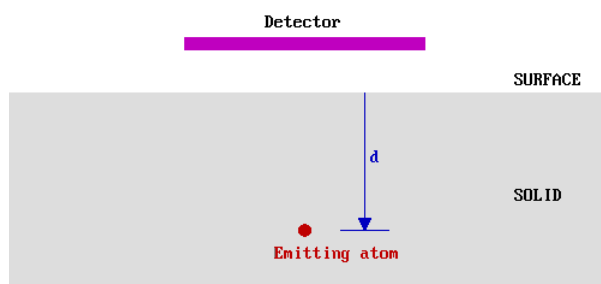
It is experimentally observed that in such a situation the XPS signals due to the substrate (material B) are rapidly attenuated, whilst those due to the condensed evaporant (material A) simultaneously increase to a limiting value.

#### Note

It is possible to measure deposition rates using equipment such as quartz crystal oscillators and thus obtain independent verification of the deposited film thickness. A detailed analysis of the variation of the signals due to A and B is also capable of yielding information about the mechanism of film growth.

### Why is the XPS technique surface sensitive ?

The soft X-rays employed in XPS penetrate a substantial distance into the sample ( $\sim \mu\text{m}$ ). Thus this method of excitation imparts no surface sensitivity at the required atomic scale. The surface sensitivity must therefore arise from the emission and detection of the photoemitted electrons. Consider, therefore, a hypothetical experiment in which electrons of a given energy,  $E_0$ , are emitted from atoms in a solid at various depths,  $d$ , below a flat surface.



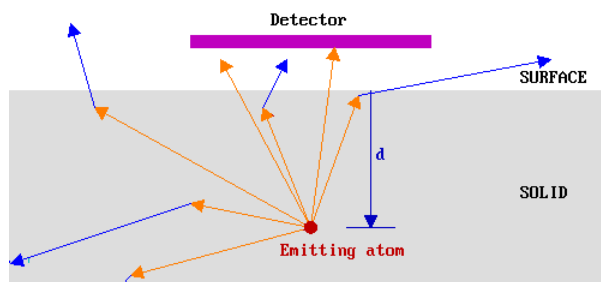
We shall assume that only those electrons which reach the surface and, at the time of leaving the solid, still have their initial energy ( $E_0$ ) are detected in this experiment. This is **not** literally true in an XPS experiment, but in XPS experiments it is only those photoelectrons possessing characteristic emission energies and contributing to the peaks and that we consider in the subsequent analysis; we do not consider photoelectrons which have lost some energy and contribute to the background of the spectrum rather than a specific peak.

There are two things which would therefore prevent an emitted electron from being detected:

1. If it were "captured" before reaching the surface, or emitted in the wrong direction and never reached the surface !
2. If it lost energy before reaching the surface, i.e. if it escaped from the solid and reached the detector, but with  $E < E_0$

The process by which an electron can lose energy as it travels through the solid is known as "inelastic scattering". Each inelastic scattering event leads to: (i) a reduction in the electron energy (ii) a change in the direction of travel.

In the diagram below arrows are used to represent possible trajectories of emitted electrons from a particular source atom. The orange arrows represent electrons travelling with their initial energy,  $E_0$ , whilst the blue arrows represent electron trajectories subsequent to an inelastic scattering event. Only the orange traces which extend out of the solid therefore correspond to electrons which would be detected in our hypothetical experiment.

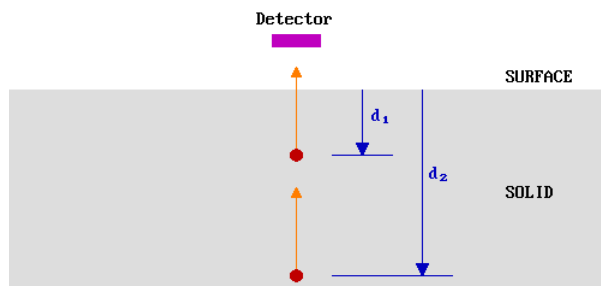


In this case, therefore, only a small fraction of the emitted electrons would have been detected. Clearly if the source atom had been closer to the surface, then a greater fraction of the emitted electrons would have been detected since:

1. The detector would subtend a greater (solid) angle at the emitting atom (this is actually not a significant factor in real experiments).
2. For an electron emitted towards the surface, there would be less chance of inelastic scattering before it escaped from the solid.

**So how does the probability of detection depend upon the distance of the emitting atom below the surface ?**

Let us first simplify the problem by only considering those electrons emitted directly towards (normal to) the surface - in our hypothetical experiment we can represent this by a smaller detector located directly above the emitting atoms.



The probability of escape from a given depth,  $P(d)$ , is determined by the likelihood of the electron **not** being inelastically scattered during its journey to the surface.

Clearly,  $P(d_2) < P(d_1)$  but, in order to quantify this we need to know more about the inelastic scattering process - this brings us to the subject of the ..

**Inelastic Mean Free Path (IMFP)** of electrons.

The IMFP is a measure of the average distance travelled by an electron through a solid before it is inelastically scattered; it is dependent upon

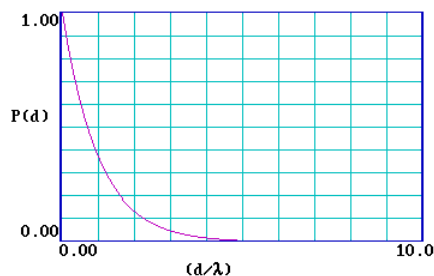
- The initial kinetic energy of the electron.
- The nature of the solid ( **but** most elements show very similar IMFP v's energy relationships).

The IMFP is actually defined by the following equation which gives the probability of the electron travelling a distance,  $d$ , through the solid without undergoing scattering

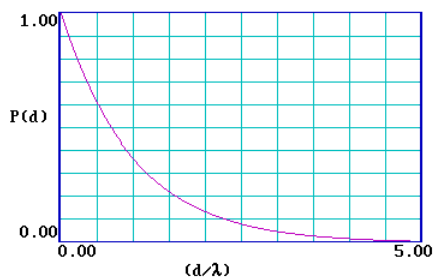
$$P(d) = \exp\left(\frac{-d}{\lambda}\right) \quad (5.1.2)$$

where  $\lambda$  is the IMFP for the electrons of energy  $E$ . (Note:  $\lambda = f(E)$ , and this inelastic mean free path, which relates to the movement of electrons in the solid, is completely unrelated to the mean free path in the gas phase once they escape from the solid).

The graph below illustrates this functional form of  $P(d)$  ...



... and it is clear that the probability of escape decays very rapidly and is essentially zero for a distance  $d > 5\lambda$  . It is therefore useful to re-plot the function for a range of  $(d/\lambda)$  from 0-5 .



⇒	What is the probability of escape when ... $d = 1\lambda$ ?
⇒	What is the probability of escape when ... $d = 2\lambda$ ?
⇒	What is the probability of escape when ... $d = 3\lambda$ ?

It is also interesting to look at this same problem from a different point of view. Let us assume that there are many sources of electrons uniformly distributed at all distances from the surface of the solid (which is in effect the situation pertaining in all XPS experiments) and again arrange to only detect those unscattered electrons which emerge normal to the surface - then we can ask ...

*What is the distribution of the depths of origin of those electrons that we do detect ?*

This new function, let's call it  $P'(d)$ , actually has the same exponential form as  $P(d)$  - i.e. the frequency of detection of electrons from different depths in the solid is directly proportional to the probability of electron escape from each depth.

### ? Exercise 5.1.1

So if we allow our detector to collect 100 electrons, we can ask how many electrons (on average) will have come from within a distance of one IMFP from the surface (i.e. how many originate from a distance,  $d$ , such that  $0 < (d/\lambda) < 1$ )?

This is a relatively simple problem in integration - try it !

#### Answer

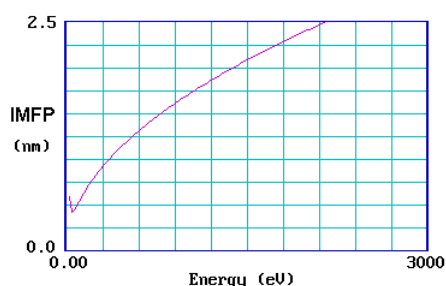
In summary, we can conclude from the answer to this question that the majority of electrons detected come from within one "imfp" of the surface. Virtually all ( $> 95\%$ ) of the electrons detected come from within 3 IMFPs of the surface.

#### Caution

Beware of terms such as "*sampling depth*" and "*electron escape depth*". It is not always clear whether these refer to 1, 3 or 5 IMFPs (or something else completely).

### So how big is the IMFP of typical electrons within a solid such as a metal ?

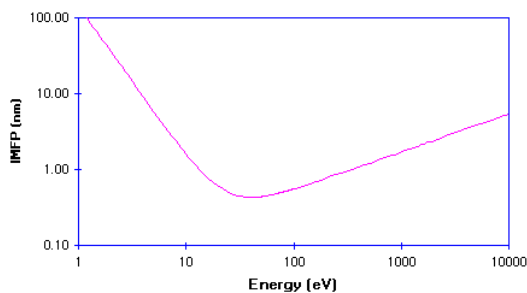
The graph below shows the so-called "universal curve" for the variation of the IMFP with initial electron energy (in eV).



It is reasonably accurate for most metals, although experimental measurements on different metals do show a substantial scatter about the general curve.

Other classes of solids also exhibit qualitatively similar universal curves, although the absolute values of the IMFP of electrons in materials such as inorganic solids and polymers do differ quite significantly from those in metals.

This IMFP data is more usually displayed on a *log-log* plot, since this more clearly shows how the IMFP varies at low kinetic energies - the graph below shows the general curve for metals re-plotted in this new format.



The IMFP exhibits a minimum for electrons with a kinetic energy of around 50 -100 eV ; at lower energies the probability of inelastic scattering decreases since the electron has insufficient energy to cause plasmon excitation (the main scattering mechanism in metals), and consequently the distance between inelastic collisions and the IMFP increases.

### Summary

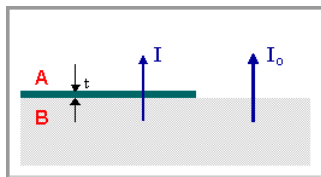
The Inelastic Mean Free Path (IMFP) in metals is typically less than:

- 10 Angstroms ( 1 nm ) for electron energies in the range  $15 < E/\text{eV} < 350$
- 20 Angstroms ( 2 nm ) for electron energies in the range  $10 < E/\text{eV} < 1400$

i.e. the IMFP of low energy electrons corresponds to only a few atomic layers. This means that any experimental technique such as XPS which involves the generation and detection of electrons of such energies will be surface sensitive.

### How can we use knowledge of the IMFP to calculate the thickness of surface films ?

We can now consider a situation where a substrate (or thick film) of one material, B, is covered by a thin film of a different material, A. The XPS signal from the underlying substrate will be attenuated (i.e. reduced in intensity) due to inelastic scattering of some of the photoelectrons as they traverse through the layer of material A.



For any single photoelectron, the probability of the electron passing through this overlayer without being subject to a scattering event is given by:

$$P = \exp\left(\frac{-t}{\lambda}\right) \quad (5.1.3)$$

where  $t$  is the thickness of the layer of material A.

It follows that the overall intensity of the XPS signal arising from B is reduced by this same factor, i.e. if the intensity of this signal in the absence of any covering layer is  $I_0$  then the intensity  $I$  in the presence of the overlayer is given by:

$$I = I_0 \exp\left(\frac{-t}{\lambda}\right) \quad (5.1.4)$$

It also follows that it is possible to estimate the thickness of a deposited layer (using the above equation), provided the reduction in the substrate signal is known (i.e. if spectra are acquired before and after deposition of the covering film).

### How can we change the degree of surface sensitivity?

For a given technique such as XPS which relies on inelastic electron scattering to provide the surface sensitivity, we can consider how it might be possible to increase the surface sensitivity when analysing a particular substrate.

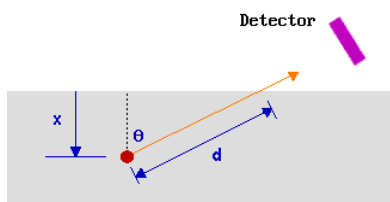
One approach would be to try and ensure that the electrons being detected have kinetic energies corresponding to the minimum in the universal curve for the IMFP. The problem with this approach is that

1. it requires us to be able to vary the X-ray radiation so that we can adjust the photon energy,  $h\nu$ , to give us the desired kinetic energy for the photoemitted electrons ; this is **not** generally possible with conventional laboratory x-ray sources (although tunable x-ray radiation is available at large synchrotron sources)
2. whilst it may be possible to adjust the kinetic energy of some particular photoelectrons to correspond to the minimum in the universal curve, this effect may not hold for all the other photoelectron peaks associated with the sample.

A much more generally useful approach is to collect photoelectrons at a more grazing emission angle.

The key point to recognise here is that it is actually the distance that the electrons have to travel through the solid (rather than the distance of the emitting atom below the surface) that is crucial in determining their probability of escape without inelastic scattering - only in the special case considered previously of normal emission are these two quantities the same.

Consider, for example, emission at some angle  $\theta$  to the surface normal.



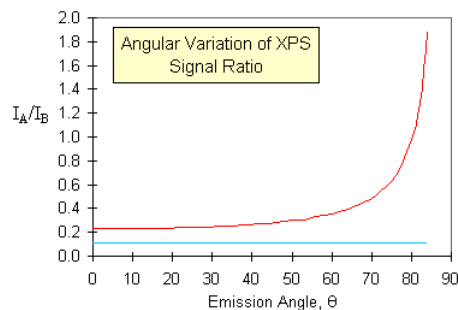
Once again 63% of the electrons will originate from atoms located such that the electrons have to travel a distance,  $d$ , which is less than  $1\lambda$  through the solid (see above). Under these measurement conditions, however, all these atoms are located within a smaller distance,  $x$ , from the surface where

$$x = d \cos \theta \quad (5.1.5)$$

So as the emission angle ( $\theta$ ) is increased,  $\cos \theta$  decreases, the analysed region becomes more surface localised and the surface sensitivity is increased.

One example of how this effect can be put to good use is in the study (and diagnosis) of *surface segregation*. The graph below shows simulated data for the variation of the XPS signal intensities with emission angle for

- a random alloy of 10% of element A in element B, with no segregation (lower blue curve)
- the same random alloy, but with surface segregation of A to give a surface monolayer of pure element A (upper red curve)



This page titled [5.1: Surface Sensitivity and Surface Specificity](#) is shared under a [CC BY-NC-SA 4.0](#) license and was authored, remixed, and/or curated by [Roger Nix](#).

## 5.2: Auger Electron Spectroscopy

Auger Electron Spectroscopy (*Auger spectroscopy* or AES) was developed in the late 1960's, deriving its name from the effect first observed by Pierre Auger, a French Physicist, in the mid-1920's. It is a surface specific technique utilizing the emission of low energy electrons in the *Auger process* and is one of the most commonly employed surface analytical techniques for determining the composition of the surface layers of a sample.

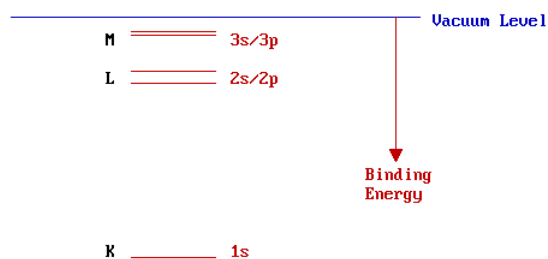
Auger spectroscopy can be considered as involving three basic steps:

1. Atomic ionization (by removal of a core electron)
2. Electron emission (the Auger process)
3. Analysis of the emitted Auger electrons

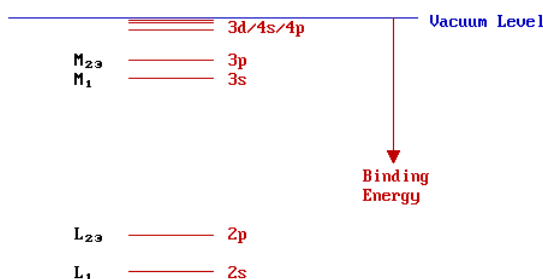
The last stage is simply a technical problem of detecting charged particles with high sensitivity, with the additional requirement that the kinetic energies of the emitted electrons must be determined. We will therefore concern ourselves only with the first two processes - before starting, however, it is useful to briefly review the electronic structure of atoms and solids, and associated nomenclature.

### Electronic Structure - Isolated Atoms

The diagram below schematically illustrates the energies of the various electron energy levels in an isolated, multi-electron atom, with the conventional chemical nomenclature for these orbitals given on the right hand side.



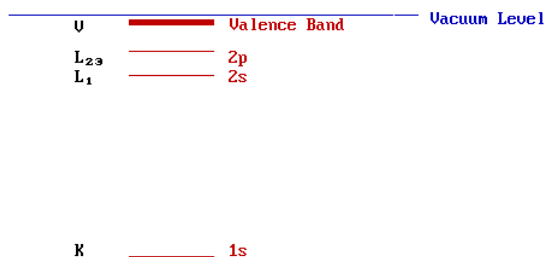
However, scientists working with x-rays tend to use the alternative nomenclature on the left and it is this nomenclature that is used in Auger spectroscopy. The designation of levels to the K,L,M,... shells is based on their having principal quantum numbers of 1,2,3,... respectively. It is convenient to expand the part of the energy scale close to the vacuum level in order to more clearly distinguish between the higher levels ....



The numerical component of the KLM.. style of nomenclature is usually written as a subscript immediately following the main shell designation. Levels with a non-zero value of the orbital angular momentum quantum number ( $l > 0$ ), i.e. p,d,f,.. levels, show spin-orbit splitting. The magnitude of this splitting, however, is too small to be evident on this diagram - hence, the double subscript for these levels (i.e. L<sub>2,3</sub> represents both the L<sub>2</sub> and L<sub>3</sub> levels).

### Electronic Structure - Solid State

In the solid state the core levels of atoms are little perturbed and essentially remain as discrete, localized (i.e. atomic-like) levels. The valence orbitals, however, overlap significantly with those of neighboring atoms generating bands of spatially-delocalised energy levels. The energy level diagram for the solid is therefore closely resemblance of that of the corresponding isolated atom, except for the levels closest to the vacuum level. The diagram below shows the electronic structure of Na metal:

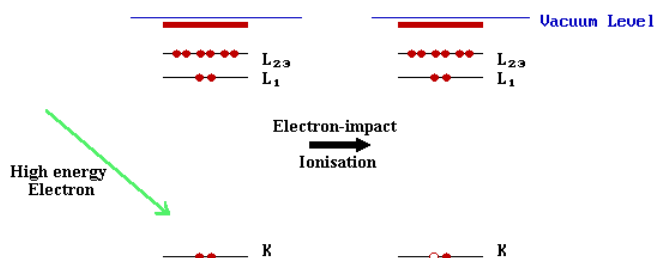


## The Auger Process & Auger Spectroscopy

Now let us return to the subject of Auger spectroscopy - in the following discussion, the Auger process is illustrated using the K, L<sub>1</sub> & L<sub>2,3</sub> levels. These could be the inner core levels of an atom in either a molecular or solid-state environment.

### Step I: Ionization

The Auger process is initiated by creation of a core hole - this is typically carried out by exposing the sample to a beam of high energy electrons (typically having a primary energy in the range 2 - 10 keV). Such electrons have sufficient energy to ionise all levels of the lighter elements, and higher core levels of the heavier elements.

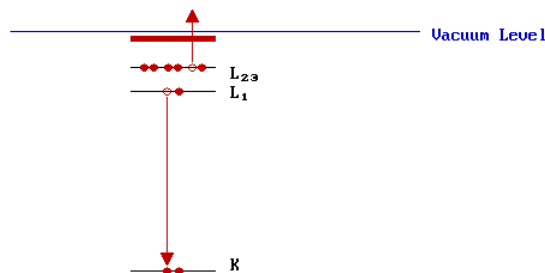


In the diagram above, ionisation is shown to occur by removal of a K-shell electron, but in practice such a crude method of ionisation will lead to ions with holes in a variety of inner shell levels.

In some studies, the initial ionisation process is instead carried out using soft x-rays ( $h\nu = 1000 - 2000 \text{ eV}$ ). In this case, the acronym XAES is sometimes used. As we shall see, however, this change in the method of ionisation has no significant effect on the final Auger spectrum.

### Step II: Relaxation & Auger Emission

The ionized atom that remains after the removal of the core hole electron is, of course, in a highly excited state and will rapidly relax back to a lower energy state by one of two routes: **X-ray fluorescence** or **Auger emission**. We will only consider the latter mechanism, an example of which is illustrated schematically below ....



In this example, one electron falls from a higher level to fill an initial core hole in the K-shell and the energy liberated in this process is simultaneously transferred to a second electron ; a fraction of this energy is required to overcome the binding energy of this second electron, the remainder is retained by this emitted **Auger electron** as kinetic energy. In the Auger process illustrated, the final state is a doubly-ionized atom with core holes in the L<sub>1</sub> and L<sub>2,3</sub> shells.



We can make a rough estimate of the KE of the Auger electron from the binding energies of the various levels involved. In this particular example,

$$KE = (E_K - E_{L1}) - E_{L23} \quad (5.2.1)$$

[ Why is this answer not likely to be very accurate ?]

#### Note

The KE of the Auger electron is independent of the mechanism of initial core hole formation.

Equation 5.2.1 can also be re-written in the form:

$$KE = E_K - (E_{L1} + E_{L23}) \quad (5.2.2)$$

It should be clear from this expression that the latter two energy terms could be interchanged without any effect - i.e. it is actually impossible to say which electron fills the initial core hole and which is ejected as an Auger electron; they are indistinguishable.

An Auger transition is therefore characterized primarily by:

1. the location of the initial hole
2. the location of the final two holes

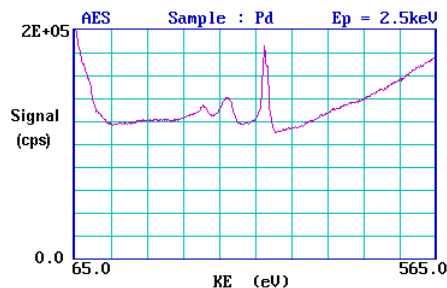
although the existence of different electronic states (terms) of the final doubly-ionized atom may lead to fine structure in high resolution spectra.

### Step III: Analysis and Interpretation

When describing the transition, the initial hole location is given first, followed by the locations of the final two holes in order of decreasing binding energy, i.e. the transition illustrated is a  $KL_1L_{2,3}$  transition. If we just consider these three electronic levels there are clearly several possible Auger transitions: specifically,

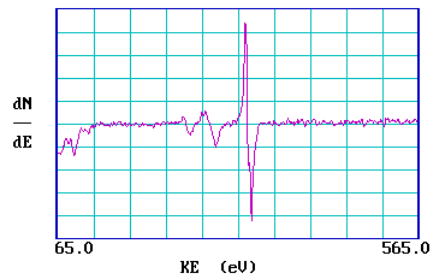
$K L_1 L_1$	$K L_1 L_{2,3}$	$K L_{2,3} L_{2,3}$
-------------	-----------------	---------------------

In general, since the initial ionization is non-selective and the initial hole may therefore be in various shells, there will be many possible Auger transitions for a given element - some weak, some strong in intensity. **AUGER SPECTROSCOPY is based upon the measurement of the kinetic energies of the emitted electrons.** Each element in a sample being studied will give rise to a characteristic spectrum of peaks at various kinetic energies.



This is an Auger spectrum of Pd metal - generated using a 2.5 keV electron beam to produce the initial core vacancies and hence to stimulate the Auger emission process. The main peaks for palladium occur between 220 & 340 eV. The peaks are situated on a high background which arises from the vast number of so-called *secondary electrons* generated by a multitude of inelastic scattering processes.

Auger spectra are also often shown in a differentiated form: the reasons for this are partly historical, partly because it is possible to actually measure spectra directly in this form and by doing so get a better sensitivity for detection. The plot below shows the same spectrum in such a differentiated form.



## Summary

Auger Electron Spectroscopy (AES) is a surface-sensitive spectroscopic technique used for elemental analysis of surfaces; it offers

- high sensitivity (typically ca. 1% monolayer) for all elements except H and He.
- a means of monitoring surface cleanliness of samples
- quantitative compositional analysis of the surface region of specimens, by comparison with standard samples of known composition.

In addition, the basic technique has also been adapted for use in:

1. [Auger Depth Profiling](#): providing quantitative compositional information as a function of depth below the surface
2. [Scanning Auger Microscopy \(SAM\)](#): providing spatially-resolved compositional information on heterogeneous samples

---

This page titled [5.2: Auger Electron Spectroscopy](#) is shared under a [CC BY-NC-SA 4.0](#) license and was authored, remixed, and/or curated by [Roger Nix](#).

## 5.3: Photoelectron Spectroscopy

Photoelectron spectroscopy utilizes photo-ionization and analysis of the kinetic energy distribution of the emitted photoelectrons to study the composition and electronic state of the surface region of a sample. Traditionally, when the technique has been used for surface studies it has been subdivided according to the source of exciting radiation into:

- **X-ray Photoelectron Spectroscopy (XPS):** using soft x-rays (with a photon energy of 200-2000 eV) to examine *core*-levels.
- **Ultraviolet Photoelectron Spectroscopy (UPS):** using vacuum UV radiation (with a photon energy of 10-45 eV) to examine *valence* levels.

The development of synchrotron radiation sources has enabled high resolution studies to be carried out with radiation spanning a much wider and more complete energy range ( 5 - 5000+ eV ) but such work remains a small minority of all photoelectron studies due to the expense, complexity and limited availability of such sources.

### Physical Principles

Photoelectron spectroscopy is based upon a single photon in/electron out process and from many viewpoints this underlying process is a much simpler phenomenon than the Auger process. The energy of a photon of all types of electromagnetic radiation is given by the Einstein relation:

$$E = h\nu \quad (5.3.1)$$

where  $h$  is Planck constant (  $6.62 \times 10^{-34}$  J s ) and  $\nu$  is the frequency (Hz) of the radiation.

Photoelectron spectroscopy uses monochromatic sources of radiation (i.e. photons of fixed energy). In XPS, the photon is absorbed by an atom in a molecule or solid, leading to ionization and the emission of a core (inner shell) electron. By contrast, in UPS the photon interacts with valence levels of the molecule or solid, leading to ionization by removal of one of these valence electrons. The kinetic energy distribution of the emitted photoelectrons (i.e. the number of emitted photoelectrons as a function of their kinetic energy) can be measured using any appropriate electron energy analyzer and a photoelectron spectrum can thus be recorded. The process of photoionization can be considered in several ways: one way is to look at the overall process as follows:



Conservation of energy then requires that:

$$E(A) + h\nu = E(A^+) + E(e^-) \quad (5.3.3)$$

Since the electron's energy is present solely as kinetic energy (KE) this can be rearranged to give the following expression for the KE of the photoelectron:

$$KE = h\nu - (E(A^+) - E(A)) \quad (5.3.4)$$

The final term in brackets, representing the difference in energy between the ionized and neutral atoms, is generally called the *binding energy* (BE) of the electron - this then leads to the following commonly quoted equation:

$$KE = h\nu - BE \quad (5.3.5)$$

An alternative approach is to consider a one-electron model along the lines of the following pictorial representation; this model of the process has the benefit of simplicity but it can be rather misleading.



The BE is now taken to be a direct measure of the energy required to just remove the electron concerned from its initial level to the vacuum level and the KE of the photoelectron is again given by:

$$KE = h\nu - BE \quad (5.3.6)$$

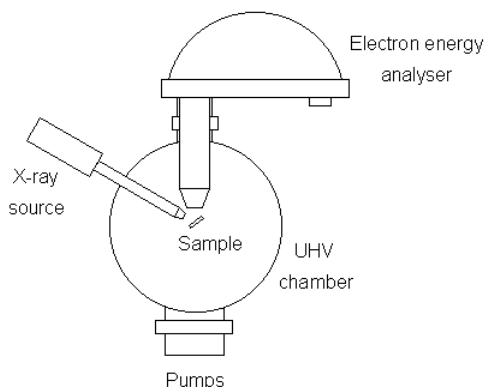
The binding energies (BE) of energy levels in solids are conventionally measured with respect to the Fermi level of the solid, rather than the vacuum level. This involves a small correction to Equation 5.3.6 to account for the *work function* ( $\varphi$ ) of the solid. For the purposes of the discussion below this correction will be neglected.

## Experimental Details

The basic requirements for a photoemission experiment (XPS or UPS) are:

1. a source of fixed-energy radiation (an x-ray source for XPS or, typically, a He discharge lamp for UPS)
2. an electron energy analyser (which can disperse the emitted electrons according to their kinetic energy, and thereby measure the flux of emitted electrons of a particular energy)
3. a high vacuum environment (to enable the emitted photoelectrons to be analyzed without interference from gas phase collisions)

Such a system is illustrated schematically below:



There are many different designs of electron energy analyzer but the preferred option for photoemission experiments is a concentric hemispherical analyser (CHA) which uses an electric field between two hemispherical surfaces to disperse the electrons according to their kinetic energy.

## X-ray Photoelectron Spectroscopy (XPS)

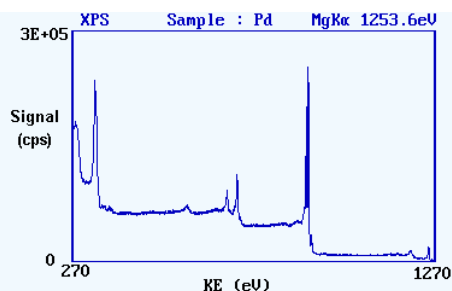
For each and every element, there will be a characteristic binding energy associated with each core atomic orbital i.e. each element will give rise to a characteristic set of peaks in the photoelectron spectrum at kinetic energies determined by the photon energy and the respective binding energies. The presence of peaks at particular energies therefore indicates the presence of a specific element in the sample under study - furthermore, the intensity of the peaks is related to the concentration of the element within the sampled region. Thus, the technique provides a *quantitative analysis of the surface composition* and is sometimes known by the alternative acronym, ESCA (Electron Spectroscopy for Chemical Analysis). The most commonly employed x-ray sources are those giving rise to:

- Mg  $K_{\alpha}$  radiation:  $h\nu = 1253.6$  eV
- Al  $K_{\alpha}$  radiation:  $h\nu = 1486.6$  eV

The emitted photoelectrons will therefore have kinetic energies in the range of ca. 0 - 1250 eV or 0 - 1480 eV. Since such electrons have very short IMFPs in solids (Section 5.1), the technique is necessarily surface sensitive.

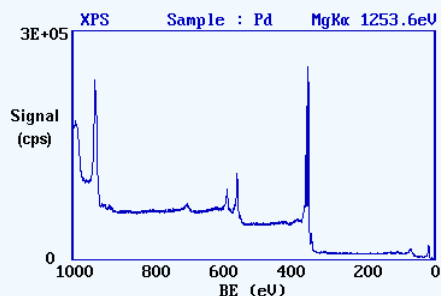
### ✓ Example 5.3.1: The XPS spectrum of Pd metal

The diagram below shows a real XPS spectrum obtained from a Pd metal sample using Mg  $K_{\alpha}$  radiation



- the main peaks occur at kinetic energies of ca. 330, 690, 720, 910 and 920 eV.

Since the photon energy of the radiation is always known it is a trivial matter to transform the spectrum so that it is plotted against BE as opposed to KE.

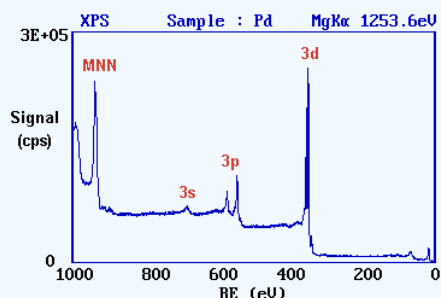


The most intense peak is now seen to occur at a binding energy of ca. 335 eV

Working downwards from the highest energy levels .....

1. the valence band ( $4d$ ,  $5s$ ) emission occurs at a binding energy of ca. 0 - 8 eV ( measured with respect to the Fermi level, or alternatively at ca. 4 - 12 eV if measured with respect to the vacuum level ).
2. the emission from the  $4p$  and  $4s$  levels gives rise to very weak peaks at 54 eV and 88 eV respectively
3. the most intense peak at ca. 335 eV is due to emission from the  $3d$  levels of the Pd atoms, whilst the  $3p$  and  $3s$  levels give rise to the peaks at ca. 534/561 eV and 673 eV respectively.
4. the remaining peak is not an XPS peak at all ! - it is an Auger peak arising from x-ray induced Auger emission. It occurs at a kinetic energy of ca. 330 eV (in this case it is really meaningless to refer to an associated binding energy).

These assignments are summarized below ...

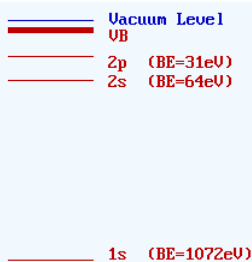


It may be further noted that

- there are significant differences in the natural widths of the various photoemission peaks
- the peak intensities are not simply related to the electron occupancy of the orbitals

### ? Exercise 5.3.1: The XPS Spectrum of NaCl

The diagram opposite shows an energy level diagram for sodium with approximate binding energies for the core levels.



If we are using Mg  $K_{\alpha}$  ( $h\nu = 1253.6 \text{ eV}$ ) radiation ...

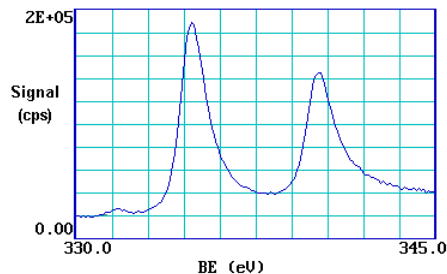
□... at what kinetic energy will the Na 1s photoelectron peak be observed ?

(the 1s peak is that resulting from photoionisation of the 1s level)

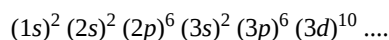
□... at what kinetic energy will the Na 2s and 2p photoelectron peaks be observed ?

## Spin-Orbit Splitting

Closer inspection of the spectrum shows that emission from some levels (most obviously 3p and 3d) does not give rise to a single photoemission peak, but a closely spaced doublet. We can see this more clearly if, for example, we expand the spectrum in the region of the 3d emission ...



The 3d photoemission is in fact split between two peaks, one at 334.9 eV BE and the other at 340.2 eV BE, with an intensity ratio of 3:2. This arises from spin-orbit coupling effects in the final state. The inner core electronic configuration of the initial state of the Pd is:



with all sub-shells completely full.

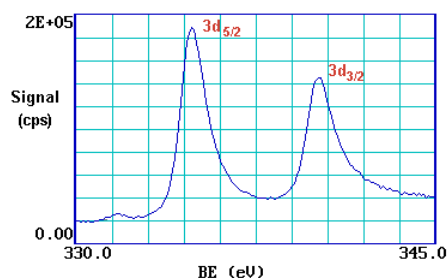
The removal of an electron from the 3d sub-shell by photo-ionization leads to a  $(3d)^9$  configuration for the final state - since the  $d$ -orbitals ( $l = 2$ ) have non-zero orbital angular momentum, there will be coupling between the unpaired spin and orbital angular momenta. Spin-orbit coupling is generally treated using one of two models which correspond to the two limiting ways in which the coupling can occur - these being the *LS* (or Russell-Saunders) coupling approximation and the *j-j* coupling approximation. If we consider the final ionised state of Pd within the [Russell-Saunders coupling](#) approximation, the  $(3d)^9$  configuration gives rise to two states (ignoring any coupling with valence levels) which differ slightly in energy and in their degeneracy ...

$2D_{5/2}$	$g_J = 2 \times \{5/2\} + 1 = 6$
$2D_{3/2}$	$g_J = 2 \times \{3/2\} + 1 = 4$

These two states arise from the coupling of the  $L = 2$  and  $S = 1/2$  vectors to give permitted  $J$  values of 3/2 and 5/2. The lowest energy final state is the one with maximum  $J$  (since the shell is more than half-full), i.e.  $J = 5/2$ , hence this gives rise to the "lower binding energy" peak. The relative intensities of the two peaks reflects the degeneracies of the final states ( $g_J = 2J + 1$ ), which in turn determines the probability of transition to such a state during photoionization.

The Russell-Saunders coupling approximation is best applied only to light atoms and this splitting can alternatively be described using individual electron *l-s* coupling. In this case the resultant angular momenta arise from the single hole in the  $d$ -shell; a  $d$ -shell electron (or hole) has  $l = 2$  and  $s = 1/2$ , which again gives permitted  $j$ -values of 3/2 and 5/2 with the latter being lower in energy.

The peaks themselves are conventionally annotated as indicated - note the use of lower case lettering



This spin-orbit splitting is of course not evident with  $s$ -levels ( $l = 0$ ), but is seen with  $p, d$  &  $f$  core-levels which all show characteristic spin-orbit doublets.

## Chemical Shifts

The exact binding energy of an electron depends not only upon the level from which photoemission is occurring, but also upon both the formal oxidation state of the atom and the local chemical and physical environment. Changes in either give rise to small shifts in the peak positions in the spectrum - so-called *chemical shifts*. Such shifts are readily observable and interpretable in XP spectra (unlike in Auger spectra) because the technique is of high intrinsic resolution (as core levels are discrete and generally of a well-defined energy) and is a one electron process (thus simplifying the interpretation).

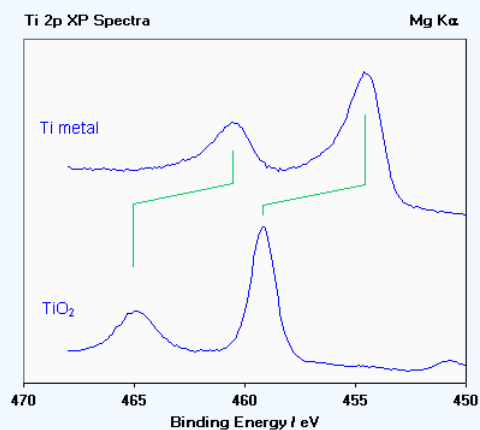
Atoms of a higher positive oxidation state exhibit a higher binding energy due to the extra coulombic interaction between the photo-emitted electron and the ion core. **This ability to discriminate between different oxidation states and chemical environments is one of the major strengths of the XPS technique.** In practice, the ability to resolve between atoms exhibiting slightly different chemical shifts is limited by the peak widths which are governed by a combination of factors; especially

- the intrinsic width of the initial level and the lifetime of the final state
- the line-width of the incident radiation - which for traditional x-ray sources can only be improved by using x-ray monochromators
- the resolving power of the electron-energy analyser

In most cases, the second factor is the major contribution to the overall line width.

### ✓ Example 5.3.2: Oxidation States of Titanium

Titanium exhibits very large chemical shifts between different oxidation states of the metal; in the diagram below a Ti 2p spectrum from the pure metal ( $Ti^0$ ) is compared with a spectrum of titanium dioxide ( $Ti^{4+}$ ).



Oxidation states of titanium [Ti 2p spectra].

#### Note

- the two spin orbit components exhibit the same chemical shift ( $\sim 4.6$  eV);
- metals are often characterised by an asymmetric line shape, with the peak tailing to higher binding energy' whilst insulating oxides give rise to a more symmetric peak profile;

iii. the weak peak at ca. 450.7 eV in the lower spectrum arises because typical x-ray sources also emit some x-rays of a slightly higher photon energy than the main Mg  $K_{\alpha}$  line; this *satellite peak* is a "ghost" of the main  $2p_{3/2}$  peak arising from ionisation by these additional x-rays.

### Angle Dependent Studies

As described [previously](#), the degree of surface sensitivity of an electron-based technique such as XPS may be varied by collecting photoelectrons emitted at different emission angles to the surface plane. This approach may be used to perform non-destructive analysis of the variation of surface composition with depth (with chemical state specificity).

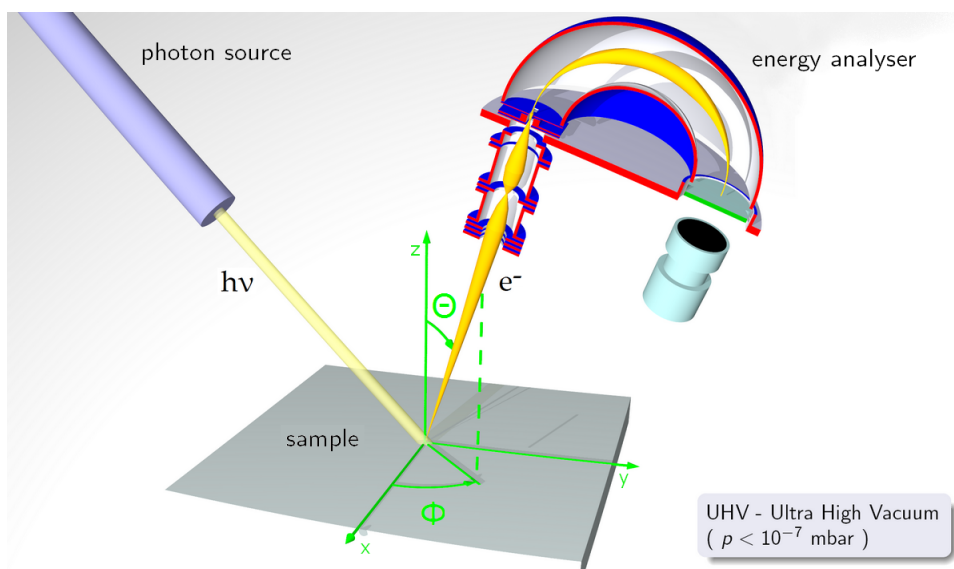
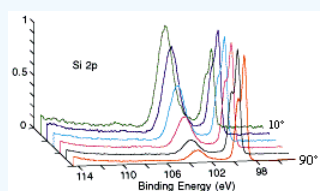


Figure 5.3.1: Principle of angle resolved photoelectron spectroscopy. (Public domain; [Saiht](#))

#### ✓ Angle-Dependent Analysis of a Silicon with a Oxide Surface Layer

A series of Si 2p photoelectron spectra recorded for emission angles of 10-90° to the surface plane. Note how the Si 2p peak of the oxide (BE ~ 103 eV) increases markedly in intensity at grazing emission angles whilst the peak from the underlying elemental silicon (BE ~ 99 eV) dominates the spectrum at near-normal emission angles.



(courtesy of [Physical Electronics, Inc. \(PHI\)](#))

**Note:** in this instance the emission angle is measured with respect to the surface plane (i.e. 90° corresponds to photoelectrons departing with a trajectory normal to the surface, whilst 10° corresponds to emission at a very grazing angle;

### Ultraviolet Photoelectron Spectroscopy (UPS)

In UPS the source of radiation is normally a noble gas discharge lamp; frequently a He-discharge lamp emitting He I radiation of energy 21.2 eV. Such radiation is only capable of ionizing electrons from the outermost levels of atoms - the valence levels. The advantage of using such UV radiation over x-rays is the very narrow line width of the radiation and the high flux of photons available from simple discharge sources. The main emphasis of work using UPS has been in studying:

1. the electronic structure of solids - detailed angle resolved studies permit the complete band structure to be mapped out in  $k$ -space.



2. the adsorption of relatively simple molecules on metals - by comparison of the molecular orbitals of the adsorbed species with those of both the isolated molecule and with calculations.

---

This page titled [5.3: Photoelectron Spectroscopy](#) is shared under a [CC BY-NC-SA 4.0](#) license and was authored, remixed, and/or curated by [Roger Nix](#).

## 5.4: Vibrational Spectroscopy

Vibrational spectroscopy provides the most definitive means of identifying the surface species generated upon molecular adsorption and the species generated by surface reactions. In principle, any technique that can be used to obtain vibrational data from solid state or gas phase samples (IR, Raman etc.) can be applied to the study of surfaces - in addition there are a number of techniques which have been specifically developed to study the vibrations of molecules at interfaces (EELS, SFG etc.).

There are, however, only two techniques that are routinely used for vibrational studies of molecules on surfaces - these are:

1. IR Spectroscopy (of various forms, e.g. RAIRS, MIR)
2. Electron Energy Loss Spectroscopy ( EELS )

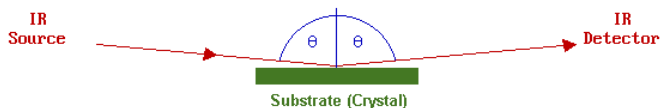
### IR Spectroscopy

There are a number of ways in which the IR technique may be implemented for the study of adsorbates on surfaces. For solid samples possessing a high surface area:

- **Transmission IR Spectroscopy**: employing the same basic experimental geometry as that used for liquid samples and mulls. This is often used for studies on supported metal catalysts where the large metallic surface area permits a high concentration of adsorbed species to be sampled. The solid sample must, of course, be IR transparent over an appreciable wavelength range.
- **Diffuse Reflectance IR Spectroscopy** ( DRIFTS ): in which the diffusely scattered IR radiation from a sample is collected, refocused and analysed. This modification of the IR technique can be employed with high surface area catalytic samples that are not sufficiently transparent to be studied in transmission.
- For studies on low surface area samples (e.g. single crystals):
- **Reflection-Absorption IR Spectroscopy** ( RAIRS ): where the IR beam is specularly reflected from the front face of a highly-reflective sample, such as a metal single crystal surface.
- **Multiple Internal Reflection Spectroscopy** ( MIR ): in which the IR beam is passed through a thin, IR transmitting sample in a manner such that it alternately undergoes total internal reflection from the front and rear faces of the sample. At each reflection, some of the IR radiation may be absorbed by species adsorbed on the solid surface - hence the alternative name of Attenuated Total Reflection (ATR).

### RAIRS - the Study of Adsorbates on Metallic Surfaces by Reflection IR Spectroscopy

It can be shown theoretically that the best sensitivity for IR measurements on metallic surfaces is obtained using a grazing-incidence reflection of the IR light.



Furthermore, since it is an optical (photon in/photon out) technique it is not necessary for such studies to be carried out in vacuum. The technique is not inherently surface-specific, but

- there is no bulk signal to worry about
- the surface signal is readily distinguishable from gas-phase absorptions using polarization effects.

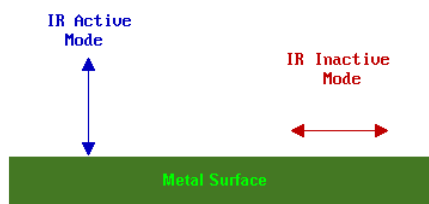
One major problem, is that of sensitivity (i.e. the signal is usually very weak owing to the small number of adsorbing molecules). Typically, the sampled area is ca.  $1 \text{ cm}^2$  with less than  $10^{15}$  adsorbed molecules (i.e. about 1 nanomole). With modern FTIR spectrometers, however, such small signals (0.01% - 2% absorption) can still be recorded at relatively high resolution (ca.  $1 \text{ cm}^{-1}$ ).

For a number of practical reasons, low frequency modes ( $< 600 \text{ cm}^{-1}$ ) are not generally observable - this means that it is not usually possible to see the vibration of the metal-adsorbate bond and attention is instead concentrated on the intrinsic vibrations of the adsorbate species in the range  $600 - 3600 \text{ cm}^{-1}$ .

### Selection Rules

The observation of vibrational modes of adsorbates on metallic substrates is subject to the *surface dipole selection rule*. This states that only those vibrational modes which give rise to an oscillating dipole perpendicular (normal) to the surface are IR active and

give rise to an observable absorption band.



Further information on the selection rules for surface IR spectroscopy can be found in the review by Sheppard & Erkelens [Appl. Spec. 38, 471 (1984)]. It also needs to be remembered that even if a transition is allowed it may still be very weak if the transition moment is small.

#### ✓ Example 5.4.1: Nitric Oxide (NO) adsorption on a Pt Surface

The sequence of spectra shown below demonstrate how IR spectroscopy can clearly reveal changes in the adsorption geometry of chemisorbed molecules. In this particular instance, all the bands are due to the stretching mode of the N-O bond in NO molecules adsorbed on a Pt surface, but the vibrational frequency is sensitive to changes in the coordination and molecular orientation of the adsorbed NO molecules.

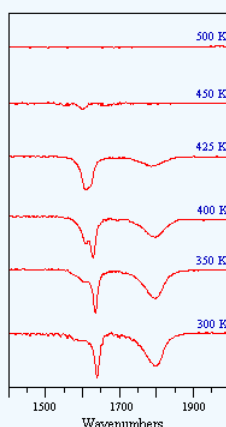
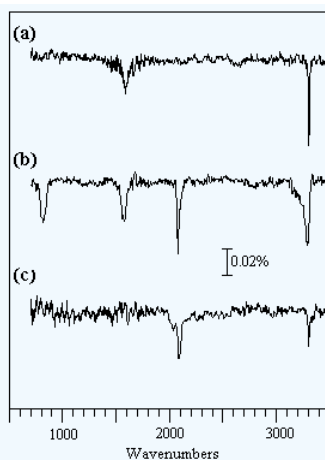


*Fig.  $\nu(\text{N-O})$  spectra obtained from a Pt surface subjected to a fixed exposure of NO at various temperatures*

Note - the surface coverage of adsorbed NO molecules decreases as the temperature is raised and little NO remains adsorbed at temperatures of 450 K and above.

#### ✓ Example 5.4.2: HCN adsorption on a Pt Surface

The RAIRS spectra shown below were observed during HCN adsorption on Pt at sub-ambient temperatures; the surface species which are generated give rise to much weaker absorptions than NO, and signal:noise considerations become much more important. These spectra also illustrate the effect of the surface normal selection rule for metallic surfaces.



(a) 0.15 L HCN at 100 K: The HCN molecules are weakly coordinated to the surface in a linear end-on fashion via the nitrogen; the  $\nu(\text{H-CN})$  mode is seen at  $3302\text{ cm}^{-1}$  but the  $\nu(\text{C-N})$  mode is too weak to be seen and the  $\delta(\text{HCN})$  mode expected at ca.  $850\text{ cm}^{-1}$  is forbidden by the surface selection rule. The overtone of the bending mode,  $2\delta(\text{HCN})$ , is however allowed and is evident at ca.  $1580\text{ cm}^{-1}$ .

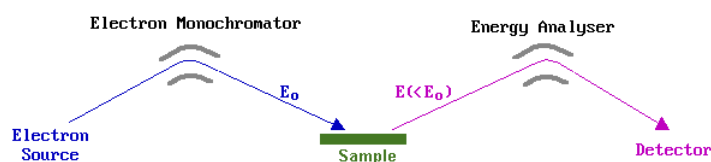
(b) 1.50 L HCN at 100 K: Higher exposures lead to the physisorption of HCN molecules into a second layer. These molecules are inclined to the surface normal and the HCN bending mode ( $\sim 820\text{ cm}^{-1}$ ) of these second layer molecules is no longer symmetry forbidden. Hydrogen bonding between molecules in the first and second layers also leads to a noticeable broadening of the  $\nu(\text{H-CN})$  band to lower wavenumbers.

(c) 30 L HCN at 200 K: At the higher temperature of 200 K only a small amount of molecular HCN remains bound in an end-on fashion to the surface. The relatively strong band at  $2084\text{ cm}^{-1}$  suggests that some dissociation has also occurred to give adsorbed CN groups, which give rise to a markedly more intense  $\nu(\text{C-N})$  band than the HCN molecule itself.

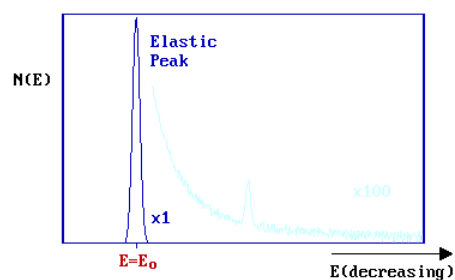
## Electron Energy Loss Spectroscopy (EELS)

This is a technique utilising the inelastic scattering of low energy electrons in order to measure vibrational spectra of surface species: superficially, it can be considered as the electron-analogue of Raman spectroscopy. To avoid confusion with other electron energy loss techniques it is sometimes referred to as HREELS - high resolution EELS or VELS - vibrational ELS. Since the technique employs low energy electrons, it is necessarily restricted to use in high vacuum (HV) and UHV environments - however, the use of such low energy electrons ensures that it is a surface specific technique and, arguably, it is the vibrational technique of choice for the study of most adsorbates on single crystal substrates.

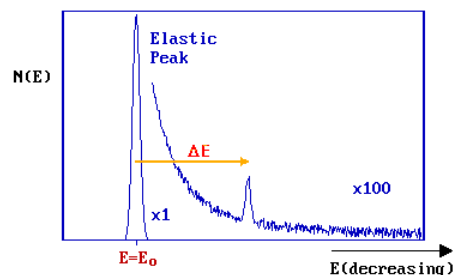
The basic experimental geometry is fairly simple as illustrated schematically below - it involves using an electron monochromator to give a well-defined beam of electrons of a fixed incident energy, and then analysing the scattered electrons using an appropriate electron energy analyser.



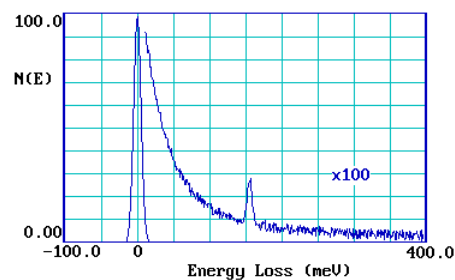
A substantial number of electrons are elastically scattered ( $E = E_0$ ) - this gives rise to a strong *elastic peak* in the spectrum.



On the low kinetic energy side of this main peak ( $E < E_0$ ), additional weak peaks are superimposed on a mildly sloping background. These peaks correspond to electrons which have undergone discrete energy losses during the scattering from the surface.

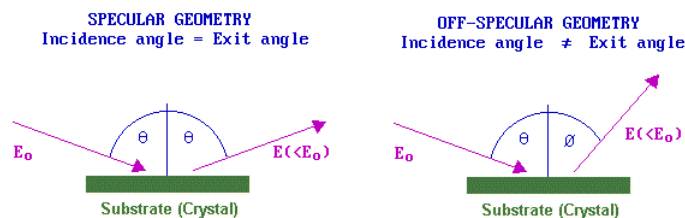


The magnitude of the energy loss,  $\Delta E = (E_0 - E)$ , is equal to the vibrational quantum (i.e. the energy) of the vibrational mode of the adsorbate excited in the inelastic scattering process. In practice, the incident energy ( $E_0$ ) is usually in the range 5-10 eV (although occasionally up to 200 eV) and the data is normally plotted against the energy loss (frequently measured in meV).



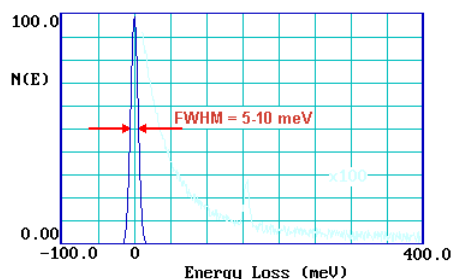
## Selection Rules

The selection rules that determine whether a vibrational band may be observed depend upon the nature of the substrate and also the experimental geometry: specifically the angles of the incident and (analysed) scattered beams with respect to the surface. For **metallic substrates** and a **specular** geometry, scattering is principally by a long-range dipole mechanism. In this case the loss features are relatively intense, but only those vibrations giving rise to a dipole change normal to the surface can be observed.



By contrast, in an **off-specular** geometry, electrons lose energy to surface species by a short-range impact scattering mechanism. In this case the loss features are relatively weak but all vibrations are allowed and may be observed. If spectra can be recorded in *both* specular and off-specular modes the selection rules for metallic substrates can be put to good use - helping the investigator to obtain more definitive identification of the nature and geometry of the adsorbate species. The resolution of the technique (despite

the HREELS acronym !) is generally rather poor;  $40\text{-}80\text{ cm}^{-1}$  is not untypical. A measure of the instrumental resolution is given by looking at the FWHM (full-width at half maximum) of the elastic peak.



This poor resolution can cause problems in distinguishing between closely similar surface species - however, recent improvements in instrumentation have opened up the possibility of much better spectral resolution ( $< 10\text{ cm}^{-1}$ ) and will undoubtedly enhance the utility of the technique.

In summary, there are both advantages and disadvantages in utilising EELS, as opposed to IR techniques, for the study of surface species. It offers the advantages of ...

- high sensitivity
- variable selection rules
- spectral acquisition to below  $400\text{ cm}^{-1}$

but suffers from the limitations of ...

- use of low energy electrons (requiring a HV environment and hence the need for low temperatures to study weakly-bound species, and also the use of magnetic shielding to reduce the magnetic field in the region of the sample)
- requirement for flat, preferably conducting, substrates
- lower resolution

### Applications of Vibrational Spectroscopy

One of the classic examples of an area in which vibrational spectroscopy has contributed significantly to the understanding of the surface chemistry of an adsorbate is that of:

#### *Molecular Adsorption of CO on Metallic Surfaces*

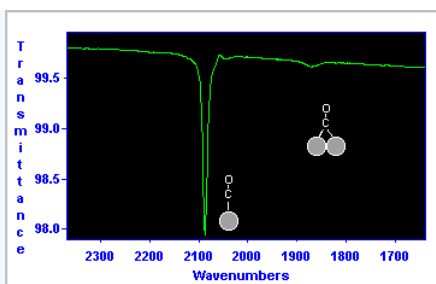
Adsorbed carbon monoxide usually gives rise to strong absorptions in both the IR and EELS spectra at the (C-O) stretching frequency. The metal-carbon stretching mode (ca.  $400\text{ cm}^{-1}$ ) is usually also accessible to EELS.

The interpretation of spectra of CO as an adsorbed surface species draws heavily upon IR spectra from related inorganic cluster and coordination complexes - the structure of such complexes usually being available from x-ray single crystal diffraction measurements. This comparison suggests that the CO stretching frequency can provide a good indication of the surface coordination of the molecule: as a rough guideline,

	$\nu(\text{C-O})$
CO ( gas phase )	$2143\text{ cm}^{-1}$
Terminal CO	$2100 - 1920\text{ cm}^{-1}$
Bridging ( 2f site )	$1920 - 1800\text{ cm}^{-1}$
Bridging ( 3f / 4f site )	$< 1800\text{ cm}^{-1}$

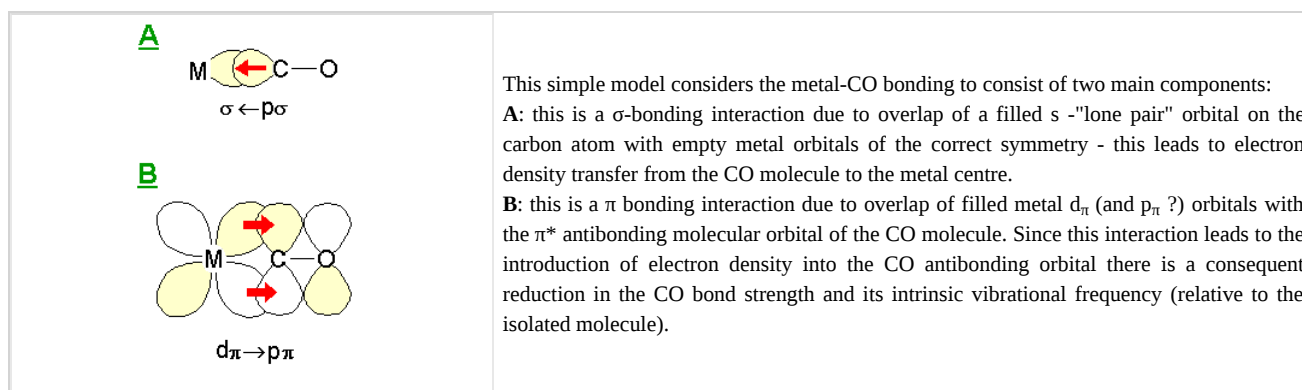
#### ✓ Example 5.4.3: CO chemisorbed on a clean Pt Surface

The RAIRS spectrum shown below was obtained for a saturation coverage of CO on a Pt surface at 300 K.



The data indicate that the majority of the CO molecules are bound in a terminal fashion to a single Pt surface atom ( $\nu_{\text{CO}} \sim 2090 \text{ cm}^{-1}$ ), whilst a smaller number of molecules are co-ordinated in a bridging site between two Pt atoms ( $\nu_{\text{CO}} \sim 1870 \text{ cm}^{-1}$ ).

The reduction in the stretching frequency of terminally-bound CO from the value observed for the gas phase molecule ( $2143 \text{ cm}^{-1}$ ) can be explained in terms of the Dewar-Chatt or *Blyholder model* for the bonding of CO to metals.



For a more detailed discussions on the bonding of CO to metals, you are recommended to refer to one of the following:

- " Advanced Inorganic Chemistry " by F.A. Cotton & G. Wilkinson (5th Edn.) pp. 58 - 62 .
- " Solids & Surfaces: a chemist's view of bonding in extended structures " by R. Hoffman pp. 71-74.

This page titled [5.4: Vibrational Spectroscopy](#) is shared under a [CC BY-NC-SA 4.0](#) license and was authored, remixed, and/or curated by [Roger Nix](#).

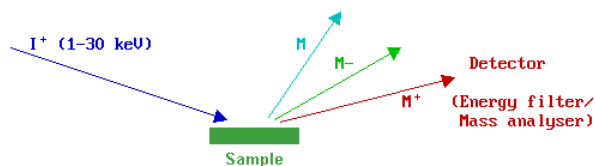
## 5.5: Secondary Ion Mass Spectrometry

The technique of Secondary Ion Mass Spectrometry (SIMS) is the most sensitive of all the commonly-employed surface analytical techniques - capable of detecting impurity elements present in a surface layer at  $< 1$  ppm concentration, and bulk concentrations of impurities of around 1 ppb (part-per-billion) in favorable cases. This is because of the inherent high sensitivity associated with mass spectrometric-based techniques.

There are a number of different variants of the technique:

- All of these variations on the technique are based on the same basic physical process and it is this process which is discussed here, together with a brief introduction to the field of static SIMS. Further notes on dynamic and imaging SIMS can be obtained in [Section 7.4 - SIMS Imaging and Depth Profiling](#).

In SIMS the surface of the sample is subjected to bombardment by high energy ions - this leads to the ejection (or *sputtering*) of both neutral and charged (+/-) species from the surface. The ejected species may include atoms, clusters of atoms and molecular fragments.



The mass analyzer may be a quadrupole mass analyzer (with unit mass resolution), but magnetic sector mass analyzers or time-of-flight (TOF) analyzers are also often used and these can provide substantially higher sensitivity and mass resolution, and a much greater mass range (albeit at a higher cost). In general, TOF analyzers are preferred for static SIMS, whilst quadrupole and magnetic sector analyzers are preferred for dynamic SIMS.

The most commonly employed incident ions (generically denoted by  $I^+$  in the above diagram) used for bombarding the sample are noble gas ions (e.g.  $Ar^+$ ) but other ions (e.g.  $Cs^+$ ,  $Ga^+$  or  $O_2^+$ ) are preferred for some applications. With TOF-SIMS the primary ion beam is pulsed to enable the ions to be dispersed over time from the instant of impact, and very short pulse durations are required to obtain high mass resolution.

This page titled [5.5: Secondary Ion Mass Spectrometry](#) is shared under a [CC BY-NC-SA 4.0](#) license and was authored, remixed, and/or curated by [Roger Nix](#).



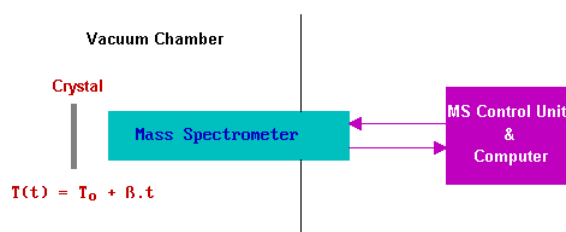
## 5.6: Temperature-Programmed Techniques

There are a range of techniques for studying surface reactions and molecular adsorption on surfaces which utilize temperature-programming to discriminate between processes with different activation parameters. Of these, the most useful for single crystal studies is: **Temperature Programmed Desorption (TPD)**. When the technique is applied to a system in which the adsorption process is, at least in part, irreversible and  $T$ -programming leads to surface reactions, then this technique is often known as: **Temperature Programmed Reaction Spectroscopy (TPRS)**

However, there is no substantive difference between TPRS and TPD. The basic experiment is very simple, involving

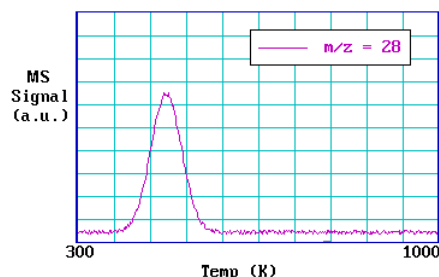
1. Adsorption of one or more molecular species onto the sample surface at low temperature (frequently 300 K, but sometimes sub-ambient).
2. Heating of the sample in a controlled manner (preferably so as to give a linear temperature ramp) whilst monitoring the evolution of species from the surface back into the gas phase.

In modern implementations of the technique the detector of choice is a small, quadrupole mass spectrometer (QMS) and the whole process is carried out under computer control with quasi-simultaneous monitoring of a large number of possible products.



The data obtained from such an experiment consists of the intensity variation of each recorded mass fragment as a function of time / temperature. In the case of a simple reversible adsorption process it may only be necessary to record one signal - that attributable to the molecular ion of the adsorbate concerned.

The graph below shows data from a TPD experiment following adsorption of CO onto a Pd(111) crystal at 300 K.



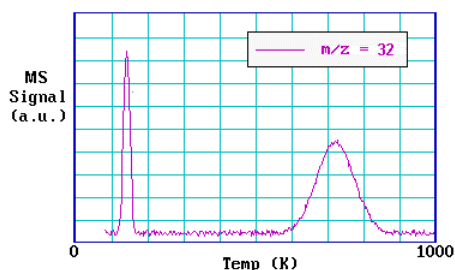
Since mass spectrometric detection is used the sensitivity of the technique is good with attainable detection limits below 0.1% of a monolayer of adsorbate.

The following points are worth noting:

1. The area under a peak is proportional to the amount originally adsorbed, i.e. proportional to the surface coverage.
2. The kinetics of desorption (obtained from the peak profile and the coverage dependence of the desorption characteristics) give information on the state of aggregation of the adsorbed species e.g. molecular v's dissociative.
3. The position of the peak (the *peak temperature*) is related to the enthalpy of adsorption, i.e. to the strength of binding to the surface.

One implication of the last point, is that if there is more than one binding state for a molecule on a surface (and these have significantly different adsorption enthalpies) then this will give rise to multiple peaks in the TPD spectrum.

The graph below shows data from a TPD experiment following adsorption of oxygen on Pt(111) at 80 K.



- Which peak corresponds to the state which is more weakly adsorbed ?

## Theory of TPD

As discussed in Section 2.6, the rate of desorption of a surface species will in general be given by an expression of the form:

$$R_{des} = \nu N^x \exp\left(\frac{-E_a^{des}}{RT}\right) \quad (5.6.1)$$

with

- $R_{des}$  - desorption rate ( $\nu (= -dN/dt)$ )
- $x$  - kinetic order of desorption (typically 0,1 or 2)
- $E_a^{des}$  - activation energy for desorption

In a temperature programmed desorption experiment in which the temperature is increased linearly with time from some initial temperature  $T_o$ , then:

$$T = T_o + \beta t \quad (5.6.2)$$

and

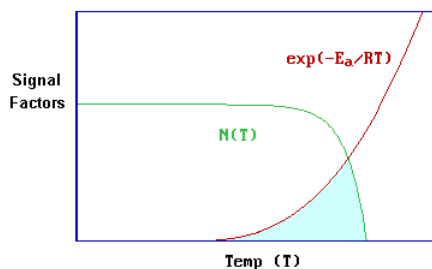
$$dT = \beta dt \quad (5.6.3)$$

The intensity of the desorption signal,  $I(T)$ , is proportional to the rate at which the surface concentration of adsorbed species is decreasing. This is obtained by combining [1] and [2] to give

$$I(T) \propto \frac{dN}{dT} = \frac{\nu N^x}{\beta} e^{-E_a^{des}/RT} \quad (5.6.4)$$

This problem may also be considered in a rather simplistic graphical way -the key to this is to recognize that the expression for the desorption signal given in the above equation is basically a product of a coverage term ( $N^x$  - where  $N$  depends on  $T$ ) and an exponential term (involving both  $E_a$  and  $T$ ).

Initially, at low temperatures  $E_a \gg RT$  and the exponential term is vanishing small. However, as the temperature is increased this term begins to increase very rapidly when the value of  $RT$  approaches that of the activation energy,  $E_a$ .



By contrast, the pre-exponential term is dependent upon the coverage,  $N(T)$ , at the temperature concerned - this term will remain at the initial value until the desorption rate becomes of significance as a result of the increasing exponential term. Thereafter, it will decrease ever more rapidly until the coverage is reduced to zero. The shaded area is an approximate representation of the product of these two functions, and hence also an approximate representation for the desorption signal itself - whilst this illustration may be overly simplistic it does clearly show why the desorption process gives rise to a well-defined desorption peak.

If you wish to see exactly how the various factors such as the kinetic order and initial coverage influence the desorption profile then try out the [Interactive Demonstration of Temperature Programmed Desorption](#) (note - this is based on the formulae given in Section 2.6); we will however continue to look at one particular case in a little more detail.

### CASE I (Molecular adsorption)

In this case the desorption kinetics will usually be first order (i.e.  $x = 1$ ). The maximum desorption signal in the  $I(T)$  trace will occur when  $(dI/dT) = 0$ , i.e. when

$$\frac{d}{dT} \left[ \frac{\nu N}{\beta} \exp\left(\frac{-E_a^{des}}{RT}\right) \right] = 0 \quad (5.6.5)$$

Hence, remembering that the surface coverage changes with temperature i.e.,  $N = N(T)$ ,

$$\left[ \frac{\nu N}{\beta} \exp\left(\frac{-E_a^{des}}{RT}\right) \right] = 0$$

where we have substituted  $E_a$  for  $E_a^{des}$  purely for clarity of presentation. Substituting for  $dN/dT$  from eq. 3 then gives

$$\left[ \frac{\nu}{\beta} \exp\left(\frac{-E_a}{RT_p}\right) \left( \frac{dN}{dT} + \frac{E_a N}{RT_p^2} \right) \right] = 0$$

The solution is given by setting the expression in square brackets to be equal to zero, i.e.,

$$\frac{E_a}{RT_p^2} = \frac{\nu}{\beta} \exp\left(\frac{-E_a}{RT_p}\right) \quad (5.6.6)$$

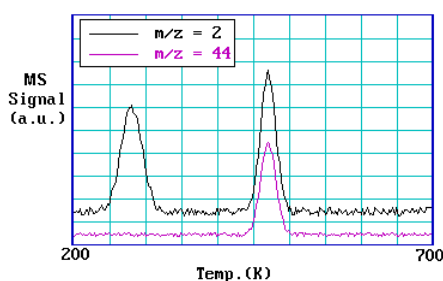
where we have now defined the temperature at which the desorption maximum occurs to be  $T = T_p$  (the *peak temperature*).

Unfortunately, this equation cannot be re-arranged to make  $T_p$  the subject (i.e. to give a simple expression of the form  $T_p = \dots$ ), but we can note that:

1. as  $E_a^{des}$  (the activation energy for desorption) increases, then so  $T_p$  (the peak temperature) increases.
2. the peak temperature is not dependent upon, and consequently does not change with, the initial coverage,  $N_t = 0$ .
3. the shape of the desorption peak will tend to be asymmetric, with the signal decreasing rapidly after the desorption maximum.


### Temperature Programmed Reaction Spectroscopy

In TPRS a number of desorption products will normally be detected in any one experiment - this is where mass spectrometric detection and multiple ion monitoring really becomes essential. A good example of TPRS results are those obtained from dosing formic acid ( $\text{HCOOH}$ ) onto a copper surface.



The spectra contain two regions of interest - the first at around room temperature where there is desorption of hydrogen  $\text{H}_2$  with  $m/z = 2$  alone, and the second between 400 K and 500 K, where there are coincident desorption peaks attributable to hydrogen and carbon dioxide  $\text{CO}_2$  with  $m/z = 44$ .

The lower temperature hydrogen peak is at about the same temperature at which hydrogen atoms recombine and desorb as molecular hydrogen from a hydrogen-dosed Cu(110) surface i.e. the kinetics of its evolution into the gas phase are those of the normal recombinative desorption process. By contrast, the higher temperature hydrogen peak is observed well above the normal hydrogen desorption temperature - its appearance must be governed by the kinetics of decomposition of another surface species. The carbon dioxide peak must also be *decomposition limited* since on clean Cu(110) carbon dioxide itself is only weakly physisorbed at very low temperatures.

 Note

More generally, coincident desorption of two species at temperatures well above their normal desorption temperatures is characteristic of the decomposition of a more complex surface species.

---

This page titled [5.6: Temperature-Programmed Techniques](#) is shared under a [CC BY-NC-SA 4.0](#) license and was authored, remixed, and/or curated by [Roger Nix](#).

## CHAPTER OVERVIEW

### 6: Overlayer Structures and Surface Diffraction

- 6.1: Classification of Overlayer Structures
- 6.2: Low Energy Electron Diffraction (LEED)
- 6.3: Reflection High Energy Electron Diffraction (RHEED)
- 6.4: Examples - Surface Structures

---

This page titled [6: Overlayer Structures and Surface Diffraction](#) is shared under a [CC BY-NC-SA 4.0](#) license and was authored, remixed, and/or curated by [Roger Nix](#).

## 6.1: Classification of Overlayer Structures

Adsorbed species on single crystal surfaces are frequently found to exhibit long-range ordering ; that is to say that the adsorbed species form a well-defined overlayer structure. Each particular structure may only exist over a limited coverage range of the adsorbate, and in some adsorbate/substrate systems a whole progression of adsorbate structures are formed as the surface coverage is gradually increased.

This section deals with the classification of such ordered structures - in most cases this involves describing the overlayer structure in terms of the underlying structure of the substrate.

There are two principal methods for specifying the structure:

1. Wood's notation
2. matrix notation.

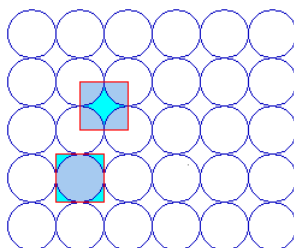
Before we start to discuss overlayer structures, however, we need to make sure that we can adequately describe the structure of the substrate !

### The Concept of the Surface Unit Cell

The primitive unit cell is the simplest periodically repeating unit which can be identified in an ordered array - the array in this instance being the ordered arrangement of surface atoms. By repeated translation of a unit cell, the whole array can be constructed. Let us consider the clean surface structures of the low index surface planes of fcc metals.

#### The fcc (100) surface

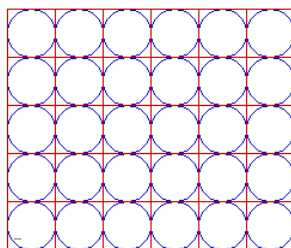
The *fcc*(100) surface has 4-fold rotational symmetry ("square symmetry") - perhaps it should not surprise us therefore to find that the primitive unit cell for this surface is square in shape !



**fcc(100) surface**

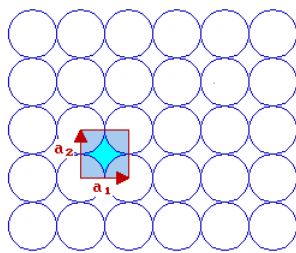
Two possible choices of unit cell are highlighted - it is clear that a unit cell of this size is indeed going to be the simplest possible repeating unit for this surface. The two alternatives drawn are in fact but two of an infinite number of possibilities; they have the same shape/symmetry, size and orientation, differing only in their translational position or "origin".

Whichever we choose then it is clear that we can indeed generate the whole surface structure by repeated translation of the unit cell; for example ....



In fact, I personally prefer the alternative choice of unit cell which has the corners of the unit cell coincident with the atomic centres.

We now need to think how to define the unit cell shape, size and symmetry - this is best done using two vectors which have a common origin and define two sides of the unit cell ...



For this  $fcc(100)$  surface the two vectors which define the unit cell, conventionally called  $\mathbf{a}_1$  &  $\mathbf{a}_2$ , are:

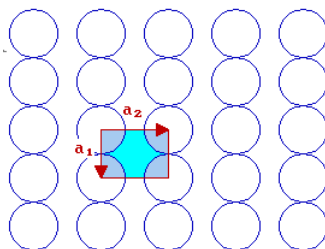
- the same length i.e.  $|\mathbf{a}_1| = |\mathbf{a}_2|$
- mutually perpendicular

By convention, one also selects the vectors such that you go anticlockwise from  $\mathbf{a}_1$  to get to  $\mathbf{a}_2$ .

The length of the vectors  $\mathbf{a}_1$  &  $\mathbf{a}_2$  is related to the bulk unit cell parameter,  $a$ , by  $|\mathbf{a}_1| = |\mathbf{a}_2| = a / \sqrt{2}$

### The $fcc(110)$ surface

In the case of the  $fcc(110)$  surface, which has 2-fold rotational symmetry, the unit cell is rectangular

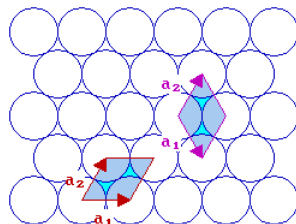


**$fcc(110)$  surface**

By convention,  $|\mathbf{a}_2| > |\mathbf{a}_1|$  - if we also recall the convention that one goes anticlockwise to get from  $\mathbf{a}_1$  to  $\mathbf{a}_2$ , then this leads to the choice of vectors shown.

### The $fcc(111)$ surface

With the  $fcc(111)$  surface we again have a situation where the length of the two vectors are the same i.e.  $|\mathbf{a}_1| = |\mathbf{a}_2|$ . We can either keep the angle between the vectors less than 90 degrees or let it be greater than 90 degrees. The normal convention is to choose the latter, i.e. the right hand cell of the two illustrated with an angle of 120 degrees between the two vectors.



**$fcc(111)$  surface**

## Overlayer Structures

If we have an ordered overlayer of adsorbed species (atoms or molecules), then we can use the same basic ideas as outlined in the previous section to define the structure. The adsorbate unit cell is usually defined by the two vectors  $\mathbf{b}_1$  and  $\mathbf{b}_2$ . To avoid ambiguities, it again helps if we stick to a set of conventions in choosing the unit cell vectors. In this case:

1.  $\mathbf{b}_2$  is again selected to be anticlockwise from  $\mathbf{b}_1$ .
2. if possible,  $\mathbf{b}_1$  is chosen to be parallel to  $\mathbf{a}_1$  and  $\mathbf{b}_2$  parallel to  $\mathbf{a}_2$ .

Once the unit cell vectors for substrate and adsorbate have been selected then it is a relatively simple matter to work out how to denote the structure.

### Wood's Notation

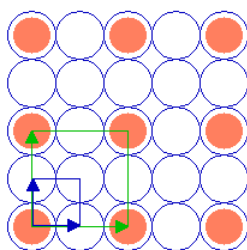
Wood's notation is the simplest and most frequently used method for describing a surface structure - it only works, however, if the two unit cells are of the same symmetry or closely-related symmetries (more specifically, the angle between  $\mathbf{b}_1$  &  $\mathbf{b}_2$  must be the same as that between  $\mathbf{a}_1$  &  $\mathbf{a}_2$ ).

In essence, Wood's notation first involves specifying the lengths of the two overlayer vectors,  $\mathbf{b}_1$  &  $\mathbf{b}_2$ , in terms of  $\mathbf{a}_1$  &  $\mathbf{a}_2$  respectively - this is then written in the format:

$$(|b_1|/|a_1| \times |b_2|/|a_2|) \quad (6.1.1)$$

i.e. a (2 x 2) structure has  $|b_1| = 2|a_1|$  and  $|b_2| = 2|a_2|$ .

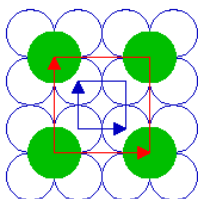
The following diagram shows a (2 x 2) adsorbate overlayer on an *fcc*(100) surface in which the adsorbate is bonded terminally on-top of individual atoms of the substrate.



**Substrate: *fcc*(100)**  
**Substrate unit cell**  
**Adsorbate unit cell**

The unit cells of the (100) substrate and the (2 x 2) overlayer are both highlighted.

The next diagram shows another (2 x 2) structure, but in this case the adsorbate species is bonded in the four-fold hollows of the substrate surface. Of course, only a very limited section of the structure can be shown here - in practice, the unit cell shown would repeat to give a complete overlayer structure extending across the substrate surface.

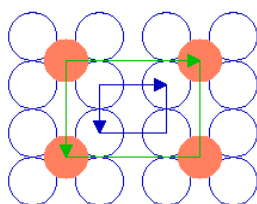


**Substrate: *fcc*(100)**  
**Substrate unit cell**  
**Adsorbate unit cell**

The highlighted unit cells of the adsorbate and substrate are identical in size, shape and orientation to those of the previously illustrated (2 x 2) structure. Both this and the previous structure are examples of *primitive* (2 x 2), or *p*(2 x 2), structures. That is to say that they are indeed the simplest unit cells that may be used to describe the overlayer structure, and contain only one "repeat unit". For the purposes of this tutorial I shall follow common practice and omit the preceding "p" - referring to such structures simply as (2 x 2) structures (in spoken language, "two by two" structures).

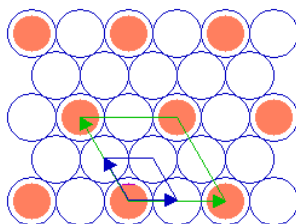
Such (2 x 2) structures are also found on other surfaces, but they may differ markedly in superficial appearance from the structure on the *fcc*(100) surface. The following diagram, for example, shows a (2 x 2) structure on a *fcc*(110) surface





**Substrate: fcc(110)**  
**Substrate unit cell**  
**Adsorbate unit cell**

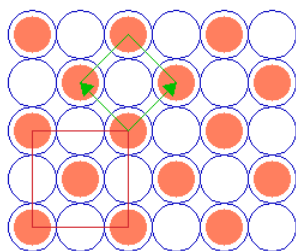
The adsorbate unit cell is again twice as large as that of the substrate in both dimensions - it retains the same aspect ratio as the rectangular substrate unit cell (1: 1.414) and does not exhibit any rotation with respect to the substrate cell. The following diagram shows yet another ( 2 x 2 ) structure, in this case on the fcc(111) surface ...



**Substrate: fcc(111)**  
**Substrate unit cell**  
**Adsorbate unit cell**

Again, the adsorbate unit cell is of the same symmetry as the substrate cell but is scaled up by a factor of two in its linear dimensions (and corresponds to a surface area four times as large as that of the substrate unit cell).

The next example is a surface structure which is closely related to the ( 2 x 2 ) structure: it differs in that there is an additional atom in the middle/centre of the ( 2 x 2 ) adsorbate unit cell. Since the middle atom is "crystallographically equivalent" to those at the corners (i.e. it is not distinguishable by means of different coordination to the underlying substrate or any other structural feature), then this is no longer a primitive ( 2 x 2 ) structure.



**Substrate: fcc(100)**  
**c( 2 x 2 )**  
**( 2 x 2 )R45**

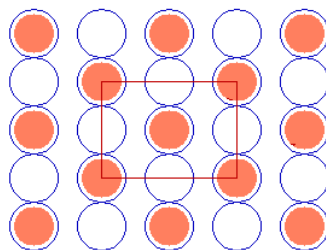
Instead it may be classified in one of two ways:

- i. As a *centered* ( 2 x 2 ) structure i.e. c( 2 x 2 ) [ where we are using a non-primitive unit cell containing 2 repeat units ]
- ii. As a " ( 2 x 2 )R45 " structure, where we are specifying the true primitive unit cell .

In using the latter Wood's notation we are stating that the adsorbate unit cell is a factor of 2 larger than the substrate unit cell in both directions and is also rotated by 45 degrees with respect to the substrate unit cell.

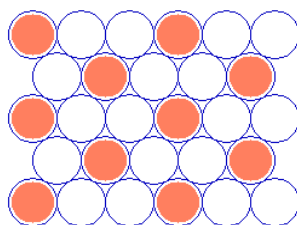
If the "central" atom is not completely crystallographically equivalent, then the structure formally remains a p(2x2) unit cell but now has a basis of two adsorbate atoms per unit cell.

In some instances it is possible to use a centred unit cell description for a structure for which the primitive unit cell cannot be described using Wood's notation - for example, the  $c(2 \times 2)$  structure on the  $fcc(110)$  surface shown below.



**Substrate:  $fcc(110)$   
 $c(2 \times 2)$**

As a final example, the next diagram illustrates a commonly-observed structure on  $fcc(111)$  surfaces which can be readily described using Wood's notation.



**Substrate:  $fcc(111)$  (  $3 \times 3$ )R30**

(You should confirm for yourself that the adsorbate unit cell is indeed scaled up from the substrate cell by the factor given and rotated by 30 degrees ! )

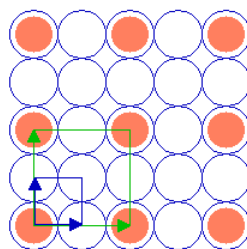
## Matrix Notation

This is a much more general system of describing surface structures which can be applied to all ordered overlayers: quite simply it relates the vectors  $\mathbf{b}_1$  &  $\mathbf{b}_2$  to the substrate vectors  $\mathbf{a}_1$  &  $\mathbf{a}_2$  using a simple matrix i.e.

$$\begin{pmatrix} \mathbf{b}_1 \\ \mathbf{b}_2 \end{pmatrix} = \begin{pmatrix} * & * \\ * & * \end{pmatrix} \begin{pmatrix} \mathbf{a}_1 \\ \mathbf{a}_2 \end{pmatrix}$$

**Matrix Notation:** remember  $\mathbf{a}_1$ ,  $\mathbf{a}_2$ ,  $\mathbf{b}_1$  and  $\mathbf{b}_2$  are vectors.

To illustrate the use of matrix notation we shall now consider two surface structures with which we are already familiar ...

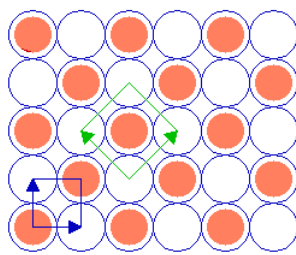


**Substrate:  $fcc(100)$   
 $(2 \times 2)$  overlayer**

For the  $(2 \times 2)$  structure we have:

$$\begin{aligned} \mathbf{b}_1 &= 2 \cdot \mathbf{a}_1 + 0 \cdot \mathbf{a}_2 \\ \mathbf{b}_2 &= 0 \cdot \mathbf{a}_1 + 2 \cdot \mathbf{a}_2 \end{aligned} \Rightarrow \mathbf{M} = \begin{bmatrix} 2 & 0 \\ 0 & 2 \end{bmatrix}$$

By contrast, for the  $c(2 \times 2)$  structure:



Substrate: fcc (100)  $c(2 \times 2)$  overlayer

we have

$$\begin{aligned} \mathbf{b}_1 &= 1 \cdot \mathbf{a}_1 + 1 \cdot \mathbf{a}_2 & \Rightarrow \quad \mathbf{M} &= \begin{bmatrix} 1 & 1 \\ -1 & 1 \end{bmatrix} \\ \mathbf{b}_2 &= -1 \cdot \mathbf{a}_1 + 1 \cdot \mathbf{a}_2 \end{aligned}$$

## Summary

Ordered surface structures may be described by defining the adsorbate unit cell in terms of that of the underlying substrate using:

1. **Wood's Notation:** in which the lengths of  $\mathbf{b}_1$  and  $\mathbf{b}_2$  are given as simple multiples of  $\mathbf{a}_1$  and  $\mathbf{a}_2$  respectively, and this is followed by the angle of rotation of  $\mathbf{b}_1$  from  $\mathbf{a}_1$  (if this is non-zero).
2. **Matrix Notation:** in which  $\mathbf{b}_1$  and  $\mathbf{b}_2$  are independently defined as linear combinations of  $\mathbf{a}_1$  and  $\mathbf{a}_2$  and these relationships are expressed in a matrix format.

---

This page titled [6.1: Classification of Overlayer Structures](#) is shared under a [CC BY-NC-SA 4.0](#) license and was authored, remixed, and/or curated by [Roger Nix](#).

## 6.2: Low Energy Electron Diffraction (LEED)

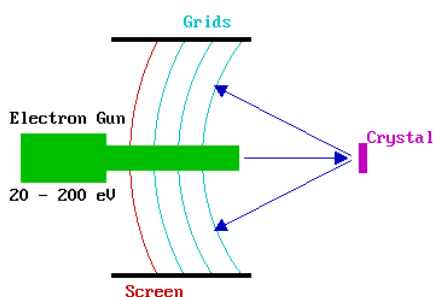
LEED is the principal technique for the determination of surface structures. It may be used in one of two ways:

1. Qualitatively: where the diffraction pattern is recorded and analysis of the **spot positions** yields information on the size, symmetry and rotational alignment of the adsorbate unit cell with respect to the substrate unit cell.
2. Quantitatively: where the **intensities** of the various diffracted beams are recorded as a function of the incident electron beam energy to generate so-called I-V curves which, by comparison with theoretical curves, may provide accurate information on atomic positions.

In this section, we will only consider the qualitative application of this experimental technique.

### Experimental Details

The LEED experiment uses a beam of electrons of a well-defined low energy (typically in the range 20 - 200 eV) incident normally on the sample. The sample itself must be a single crystal with a well-ordered surface structure in order to generate a back-scattered electron diffraction pattern. A typical experimental set-up is shown below.



Only the elastically-scattered electrons contribute to the diffraction pattern; the lower energy (secondary) electrons are removed by energy-filtering grids placed in front of the fluorescent screen that is employed to display the pattern.

### Basic Theory of LEED

By the principles of wave-particle duality, the beam of electrons may be equally regarded as a succession of electron waves incident normally on the sample. These waves will be scattered by regions of high localised electron density, i.e. the surface atoms, which can therefore be considered to act as point scatterers.

The wavelength of the electrons is given by the de Broglie relation:

$$\lambda = \frac{h}{p} \quad (6.2.1)$$

where  $\lambda$  is the electron wavelength and  $p$  is its momentum.

Now,

$$p = mv = \sqrt{2mE_k} = \sqrt{2meV} \quad (6.2.2)$$

where

- $m$  - mass of electron [ kg ]
- $v$  - velocity [ m s<sup>-1</sup> ]
- $E_k$  - kinetic energy
- $e$  - electronic charge
- $V$  - acceleration voltage ( = energy in eV )

⇒ Wavelength,

$$\lambda = \frac{h}{\sqrt{2meV}} \quad (6.2.3)$$

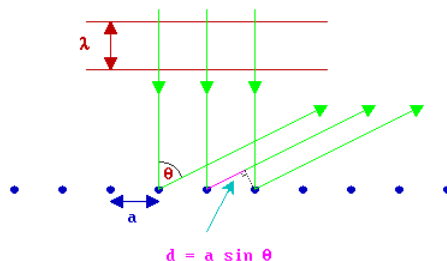
— What is the wavelength of electrons of energy 20 eV ?

— What is the wavelength of electrons of energy 200 eV ?

(Useful information:  $h = 6.62 \times 10^{-34}$  J s,  $e = 1.60 \times 10^{-19}$  C,  $m_e = 9.11 \times 10^{-31}$  kg ).

From the above examples the range of wavelengths of electrons employed in LEED experiments is seen to be comparable with atomic spacings, which is the necessary condition for diffraction effects associated with atomic structure to be observed.

Consider, first, a one dimensional (1-D) chain of atoms (with atomic separation  $a$  ) with the electron beam incident at right angles to the chain. This is the simplest possible model for the scattering of electrons by the atoms in the topmost layer of a solid; in which case the diagram below would be representing the solid in cross-section with the electron beam incident normal to the surface from the vacuum above.



If you consider the backscattering of a wavefront from two adjacent atoms at a well-defined angle,  $\theta$ , to the surface normal then it is clear that there is a "path difference" ( $d$ ) in the distance the radiation has to travel from the scattering centres to a distant detector (which is effectively at infinity) - this path difference is best illustrated by considering two "ray paths" such as the right-hand pair of green traces in the above diagram.

The size of this path difference is  $a \sin \theta$  and this must be equal to an integral number of wavelengths for constructive interference to occur when the scattered beams eventually meet and interfere at the detector i.e.

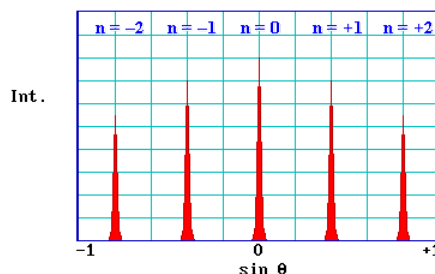
$$d = a \sin \theta = n \lambda \tag{6.2.4}$$

where:	$\lambda$ - wavelength $n$ - integer (..-1, 0, 1, 2,..)
--------	--

For two isolated scattering centres the diffracted intensity varies slowly between zero (complete destructive interference ;  $d = (n + \frac{1}{2}) \lambda$  ) and its maximum value (complete constructive interference ;  $d = n \lambda$  ) - with a large periodic array of scatterers, however, the diffracted intensity is **only** significant when the "Bragg condition"

$$a \sin \theta = n \lambda \tag{6.2.5}$$

is satisfied exactly. The diagram below shows a typical intensity profile for this case.

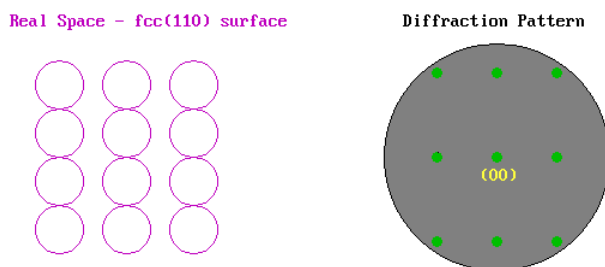


There are a number of points worth noting from this simple 1-D model

1. the pattern is symmetric about  $\theta = 0$  (or  $\sin \theta = 0$ )
2.  $\sin \theta$  is proportional to  $1 / V^{1/2}$  (since  $\lambda$  is proportional to  $1 / V^{1/2}$  )
3.  $\sin \theta$  is inversely proportional to the lattice parameter,  $a$

The aforementioned points are in fact much more general - all surface diffraction patterns show a symmetry reflecting that of the surface structure, are centrally symmetric, and of a scale showing an inverse relationship to both the square root of the electron energy and the size of the surface unit cell.

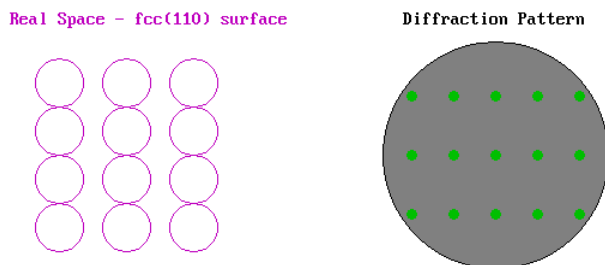
As an example we can look at the LEED pattern from an  $fcc(110)$  surface. In the diagram below the surface atomic structure is shown on the left in plan view, as if you are viewing it from the position of the electron gun in the LEED experiment (albeit greatly magnified). The primary electron beam would then be incident normally on this surface as if fired from your current viewpoint and the diffracted beams would be scattered from the surface back towards yourself. The diffraction pattern on the right illustrates how these diffracted beams would impact upon the fluorescent screen.




The pattern shows the same rectangular symmetry as the substrate surface but is "stretched" in the opposite sense to the real space structure due to the reciprocal dependence upon the lattice parameter. The pattern is also centrosymmetric about the (00) beam - this is the central spot in the diffraction pattern corresponding to the beam that is diffracted back exactly normal to the surface (i.e. the  $n = 0$  case in our 1-D model).

The above illustration of the diffraction pattern shows only the "first-order" beams i.e. it is representative of the diffraction pattern visible at low energies when only for  $n = 1$  is the angle of diffraction,  $\theta$ , sufficiently small for the diffracted beam to be incident on the display screen.

By contrast, the diagram below shows the diffraction pattern that might be expected if the energy of the incident electrons is doubled - some of the second order spots are now visible and the pattern as a whole has apparently contracted in towards the central (00) spot.



This is what the real diffraction patterns might look like ... 

In the case of such simple LEED patterns, it is possible to explain the diffraction pattern in terms of scattering from **rows** of atoms on the surface. For example, the rows of atoms running vertically on the screen would give rise to a set of diffracted beams in the horizontal plane, perpendicular to the rows, thus leading to the row of spots running in a line horizontally across the diffraction pattern through the (00) spot. The further the rows are apart, then the closer in are the diffracted beams to the central (00) beam. This is, however, a far from satisfactory method of explaining LEED patterns from surfaces.

A much better method of looking at LEED diffraction patterns involves using the concept of reciprocal space: more specifically, it can be readily shown that -

" The observed LEED pattern is a (scaled) representation of the reciprocal net of the pseudo-2D surface structure "

(No proof given !)

The *reciprocal net* is determined by (defined by) the reciprocal vectors:

$\mathbf{a}_1^*$  &  $\mathbf{a}_2^*$  (for the substrate) and  $\mathbf{b}_1^*$  &  $\mathbf{b}_2^*$  (for the adsorbate)

Initially we will consider just the substrate. The reciprocal vectors are related to the real space unit cell vectors by the scalar product relations:

$$\mathbf{a}_1 \cdot \mathbf{a}_2^* = \mathbf{a}_1^* \cdot \mathbf{a}_2 = 0$$

and

$$\mathbf{a}_1 \cdot \mathbf{a}_1^* = \mathbf{a}_2 \cdot \mathbf{a}_2^* = 1$$

For those not too keen on vector algebra these mean that:

- $\mathbf{a}_1$  is perpendicular to  $\mathbf{a}_2^*$ , and  $\mathbf{a}_2$  is perpendicular to  $\mathbf{a}_1^*$
- there is an inverse relationship between the lengths of  $\mathbf{a}_1$  and  $\mathbf{a}_1^*$  (and  $\mathbf{a}_2$  and  $\mathbf{a}_2^*$ ) of the form:

$$|\mathbf{a}_1| = 1 / (|\mathbf{a}_1^*| \cos A), \text{ where } A \text{ is the angle between the vectors } \mathbf{a}_1 \text{ and } \mathbf{a}_1^*.$$

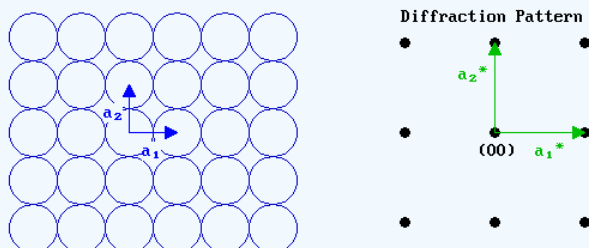
Note: when  $A = 0$  degrees ( $\cos A = 1$ ) this simplifies to a simple reciprocal relationship between the lengths  $\mathbf{a}_1$  and  $\mathbf{a}_1^*$ .

Exactly analogous relations hold for the real space and reciprocal vectors of the adsorbate overlayer structure:  $\mathbf{b}_1$ ,  $\mathbf{b}_1^*$ ,  $\mathbf{b}_2$  and  $\mathbf{b}_2^*$ .

To a first approximation, the LEED pattern for a given surface structure may be obtained by superimposing the reciprocal net of the adsorbate overlayer (generated from  $\mathbf{b}_1^*$  and  $\mathbf{b}_2^*$ ) on the reciprocal net of the substrate (generated from  $\mathbf{a}_1^*$  and  $\mathbf{a}_2^*$ )

### ✓ Example 6.2.1:

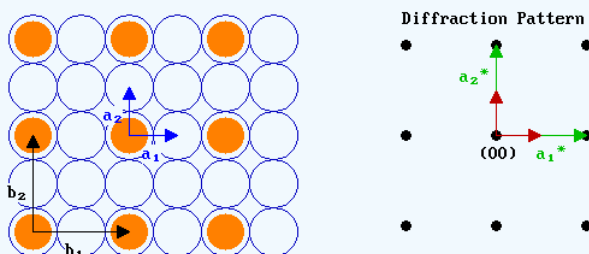
Let us now look at an example - the diagram below shows an *fcc*(100) surface (again in plan view) and its corresponding diffraction pattern (i.e. the reciprocal net).



We can demonstrate how these reciprocal vectors can be determined by working through the problem in a parallel fashion for the two vectors:

	$\mathbf{a}_1^*$ must be perpendicular to $\mathbf{a}_2$	$\mathbf{a}_2^*$ must be perpendicular to $\mathbf{a}_1$
⇒	$\mathbf{a}_1^*$ is parallel to $\mathbf{a}_1$	$\mathbf{a}_2^*$ is parallel to $\mathbf{a}_2$
⇒	The angle, A, between $\mathbf{a}_1$ & $\mathbf{a}_1^*$ is zero	The angle, A, between $\mathbf{a}_2$ & $\mathbf{a}_2^*$ is zero
⇒	Hence, $ \mathbf{a}_1^*  = 1 /  \mathbf{a}_1 $	Hence, $ \mathbf{a}_2^*  = 1 /  \mathbf{a}_2 $
⇒	If we let $ \mathbf{a}_1  = 1$ unit, then $ \mathbf{a}_1^*  = 1$ unit.	$ \mathbf{a}_2  =  \mathbf{a}_1  = 1$ unit, therefore $ \mathbf{a}_2^*  = 1$ unit.

Let us now add in an adsorbate overlayer - a primitive (2 x 2) structure with the adsorbed species shown bonded in on-top sites - and apply the same logic as just used above to determine the reciprocal vectors,  $\mathbf{b}_1^*$  and  $\mathbf{b}_2^*$ , for this overlayer.

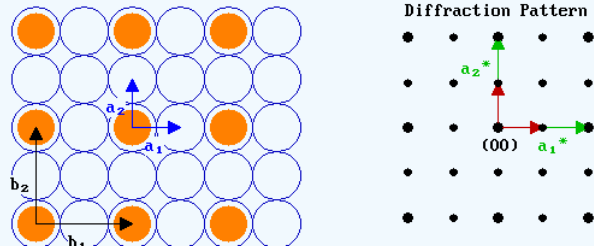


	$\mathbf{b}_1^*$ must be perpendicular to $\mathbf{b}_2$	$\mathbf{b}_2^*$ must be perpendicular to $\mathbf{b}_1$
⇒	$\mathbf{b}_1^*$ is parallel to $\mathbf{b}_1$	$\mathbf{b}_2^*$ is parallel to $\mathbf{b}_2$
⇒	The angle, B, between $\mathbf{b}_1$ & $\mathbf{b}_1^*$ is zero	The angle, B, between $\mathbf{b}_2$ & $\mathbf{b}_2^*$ is zero
⇒	Hence, $ \mathbf{b}_1^*  = 1 /  \mathbf{b}_1 $	Hence, $ \mathbf{b}_2^*  = 1 /  \mathbf{b}_2 $

$$\Rightarrow \quad |\mathbf{b}_1| = 2 \quad |\mathbf{a}_1| = 2 \text{ units}; \quad \therefore |\mathbf{b}_1^*| = \frac{1}{2} \text{ unit.}$$

$$|\mathbf{b}_2| = 2 \quad |\mathbf{a}_2| = 2 \text{ units}; \quad \therefore |\mathbf{b}_2^*| = \frac{1}{2} \text{ unit.}$$

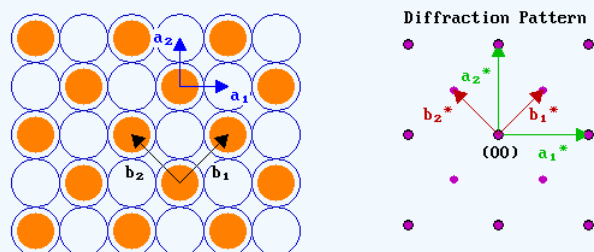
All we have to do now is to generate the reciprocal net for the adsorbate using  $\mathbf{b}_1^*$  and  $\mathbf{b}_2^*$  (shown in red).



That's all there is to it !

### ✓ Example 6.2.2:

For the second example, we will look at the  $c(2 \times 2)$  structure on the same  $fcc(100)$  surface. The diagram below shows both a real space  $c(2 \times 2)$  structure and the corresponding diffraction pattern:



In many respects the analysis is very similar to that for the  $p(2 \times 2)$  structure, except that:

1.  $|\mathbf{b}_1| = |\mathbf{b}_2| = \sqrt{2}$  units ; consequently  $|\mathbf{b}_1^*| = |\mathbf{b}_2^*| = 1/\sqrt{2}$  units.
2. the vectors for the adsorbate overlayer are rotated with respect to those of the substrate by  $45^\circ$ .

Note that the  $c(2 \times 2)$  diffraction pattern can also be obtained from the pattern for the primitive structure by "missing out every alternate adsorbate-derived diffraction spot". This is a common feature of diffraction patterns arising from centered structures.

This page titled [6.2: Low Energy Electron Diffraction \(LEED\)](#) is shared under a [CC BY-NC-SA 4.0](#) license and was authored, remixed, and/or curated by [Roger Nix](#).

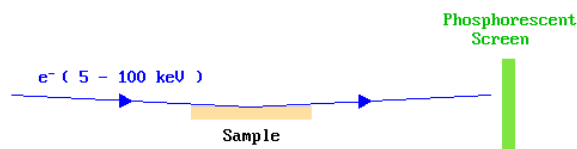


## 6.3: Reflection High Energy Electron Diffraction (RHEED)

Low Energy Electron Diffraction (LEED) utilizes the inherent surface sensitivity associated with low energy electrons in order to sample the surface structure. As the primary electron energy is increased not only does the surface specificity decrease but two other effects are particularly noticeable

1. forward scattering becomes much more important (as opposed to the backward scattering observed in LEED)
2. the scattering angle (measured from the incident beam direction) tends towards 180 degrees for back-scattering and 0 degrees for forward scattering.

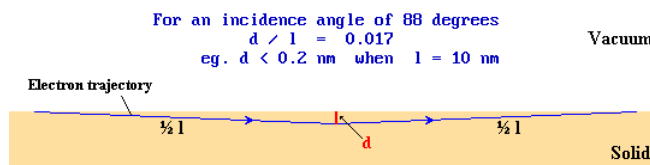
In order to extract surface structural information from the diffraction of high energy electrons, therefore, the technique has to be adapted and the easiest way of doing this is to use a reflection geometry in which the electron beam is incident at a very grazing angle - it is then known as **Reflection High Energy Electron Diffraction (RHEED)**.



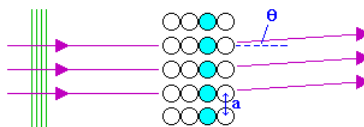
The diagram above shows the basic set-up for a RHEED experiment, with the sample viewed edge-on. In practice the display screen is usually a phosphor coating on the inside of a vacuum window (viewport) and the diffraction pattern can be viewed and recorded from the atmospheric side of the window. The small scattering angles involved are compensated for by using relatively large sample/screen distances.

The sample can be rotated about its normal axis so that the electron beam is incident along specific crystallographic directions on the surface.

In order to understand the diffraction process we need to consider how the electron beam can interact with the regular array of surface atoms in this experimental geometry. It is worth noting, however, that the use of glancing incidence ensures that, despite the high energy of the electrons, the component of the electron momentum perpendicular to the surface is small. Under these conditions an electron may travel a substantial distance through the solid (in accord with the much longer mean free path of such high energy electrons) without penetrating far into the solid. The technique, consequently, remains surface sensitive.



Now consider the **plan view** of a surface illustrated below in which we concentrate attention on just one row of atoms (shown shaded in pale blue) running in a direction perpendicular to the incident electron beam (incident from the left)



In addition to the change in momentum of the electron perpendicular to the surface, which leads to the apparent reflection, the diffraction process may also lead to a change in momentum parallel to the surface, which leads to the deflection by an angle  $\theta$  when looked at in plan view. Constructive interference occurs when the path difference between adjacent scattered "rays" ( $a \sin \theta$ ) is an integral number of wavelengths (i.e. the same basic condition as for LEED). This gives rise to a set of diffracted beams at various angles on either side of the straight through (specularly reflected) beam.

### 📌 What, if any, advantages does RHEED offer over LEED?

In terms of the quality of the diffraction pattern absolutely none ! - moreover, diffraction patterns have to be observed for at least two sample alignments with respect to the incident beam in order to determine the surface unit cell. However, ....

1. The geometry of the experiment allows much better access to the sample during observation of the diffraction pattern. This is particularly important if it is desired to make observations of the surface structure during growth of a surface film by evaporation from sources located normal to the sample surface or simultaneous with other measurements (e.g. AES, XPS).
2. Experiments have shown that it is possible to monitor the atomic layer-by-atomic layer growth of epitaxial films by monitoring oscillations in the intensity of the diffracted beams in the RHEED pattern.

By using RHEED it is therefore possible to measure, and hence also to control, atomic layer growth rates in **Molecular Beam Epitaxy** (MBE) growth of electronic device structures - this is by far and away the most important application of the technique.

---

This page titled [6.3: Reflection High Energy Electron Diffraction \(RHEED\)](#) is shared under a [CC BY-NC-SA 4.0](#) license and was authored, remixed, and/or curated by [Roger Nix](#).

## 6.4: Examples - Surface Structures

---

This section provides worked exercises in the classification of surface structures using both Wood's notation and matrix notation, and in the determination of surface coverages.

*Note - all surface coverages discussed in this section are defined in the conventional surface science manner, by reference to the number density of the underlying layer of surface atoms of the substrate*

---

### Structure #1



— How would this centred structure observed on fcc(100) surfaces be described using Wood's notation ?

— What is the coverage of adsorbate for this surface structure ?

---

### Structure #2



— How would this structure on the fcc(100) surface be described using Wood's notation ?

— What is the coverage of adsorbate for this surface structure ?

**Note** - in this instance the structure illustrated is but one of two equivalent domains - related by the symmetry of the substrate. The second domain is shown below.



It differs from the first only in that the closely-packed rows of the adsorbate now run at 90 degrees to their direction in the first domain. Patches of this domain structure would exist on the surface with statistically-equal probability to the other domain. It

obviously corresponds to the same adsorbate coverage and must possess identical properties (electronic, thermodynamic & reactivity).

---

### Structure #3



- ⇒ How would this adsorbate structure on the  $fcc(110)$  surface be described using Wood's notation ?
  - ⇒ What is the coverage of adsorbate for this surface structure ?
- 

### Structure #4



- ⇒ How might this adsorbate structure on the  $fcc(111)$  surface be described using Wood's notation ?
  - ⇒ What is the coverage of adsorbate for this surface structure ?
- 

### Structure #5



This shows an alloy surface layer on an  $fcc(111)$  substrate - such a layer might be formed by two metals which alloy if one is evaporated onto a  $(111)$  single crystal surface of the other.

- ⇒ How might this superstructure be described using Wood's notation ?
  - ⇒ What are the relative concentrations of the two elements in the surface layer ( specified as the ratio of A:B atoms ) ?
-

## Structure #6

The diagram below shows a "coadsorption" structure in which adsorption of two different species has led to the formation of an ordered surface layer containing both species - such structures ( albeit more complicated than the one shown ) are known for a number of pairs of adsorbates on a variety of surfaces e.g. benzene / CO - Rh(111)



The driving force for the formation of such structures may be an attractive dipole-dipole force between the two different adsorbed species (this might occur if, for example, one acts as an electron donor whereas the other acts as an electron acceptor on the substrate concerned).

— How would this structure be classified using Wood's notation ?

— What are the relative concentrations of the two species in the coadsorption structure ?

## Structure #7

The diagram below shows a molecular adsorption structure in which a diatomic molecule is bonded terminally to substrate atoms but is inclined to the surface normal. This particular structure has not been observed but similar structures involving a periodic tilting of the molecular axis have been discovered, e.g. CO / Pd(110) .



— How would this structure be classified using Wood's notation ?

## Summary

The structures of ordered adsorbate overlayers may be defined by specifying the adsorbate unit cell in terms of the ideal substrate unit cell - in many cases, such as the examples given, this can be done using the simple Wood's notation and this is the common practice. In more difficult cases it may be necessary to use matrix notation.

In all the examples studied :

1. the overlayers were simple structures in which the adsorbate unit cell dimensions corresponded to one of the atom-atom spacings in the underlying substrate structure ; this is generally the case for adsorbed overlayers of gaseous molecules. More complex "coincidence" and "incommensurate" structures are commonplace when the overlayer consists of one or more atomic layers of a distinct chemical compound e.g. oxide overlayers on metals.
2. it was assumed that the underlying substrate structure was undisturbed by the adsorption of species on the surface. Whilst such distortions may generally be small, this is far from always being the case and a number of examples involving adsorbate-induced reconstruction of the topmost layer of substrate atoms have now been well documented ( e.g. Ni(100) c(2x2)-C ).

This page titled [6.4: Examples - Surface Structures](#) is shared under a [CC BY-NC-SA 4.0](#) license and was authored, remixed, and/or curated by [Roger Nix](#).

## CHAPTER OVERVIEW

### 7: Surface Imaging and Depth Profiling

- 7.1: Basic concepts in surface imaging and localized spectroscopy
- 7.2: Electron Microscopy - SEM and SAM
- 7.3: Imaging XPS
- 7.4: SIMS - Imaging and Depth Profiling
- 7.5: Auger Depth Profiling
- 7.6: Scanning Probe Microscopy - STM and AFM

---

This page titled [7: Surface Imaging and Depth Profiling](#) is shared under a [CC BY-NC-SA 4.0](#) license and was authored, remixed, and/or curated by [Roger Nix](#).

## 7.1: Basic concepts in surface imaging and localized spectroscopy

---

Most surface spectroscopic techniques involve probing the surface by exposing it to a flux of "particles" ( $h\nu$ ,  $e^-$ ,  $A^+$  ...) and simultaneously monitoring the response to this stimulation by, for example, measuring the energy distribution of emitted electrons. In their most basic form, these techniques collect information from a relatively large area of surface ( $\sim \text{mm}^2$ ). In most cases, however, there are variations of these techniques which permit either,

1. The requirement in both cases is for **spatial localisation** of the spectroscopic technique. This may be achieved in one of two ways,

---

This page titled [7.1: Basic concepts in surface imaging and localized spectroscopy](#) is shared under a [CC BY-NC-SA 4.0](#) license and was authored, remixed, and/or curated by [Roger Nix](#).



## 7.2: Electron Microscopy - SEM and SAM

---

The two forms of electron microscopy which are commonly used to provide surface information are

### Secondary Electron Microscopy ( SEM )

- which provides a direct image of the topographical nature of the surface from all the emitted secondary electrons

### Scanning Auger Microscopy ( SAM )

- which provides compositional maps of a surface by forming an image from the Auger electrons emitted by a particular element.

Both techniques employ focusing of the probe beam (a beam of high energy electrons, typically 10 - 50 keV in energy) to obtain spatial localisation.

### A. Secondary Electron Microscopy ( SEM )

As the primary electron beam is scanned across the surface, electrons of a wide range of energies will be emitted from the surface in the region where the beam is incident. These electrons will include backscattered primary electrons and Auger electrons, but the vast majority will be *secondary electrons* formed in multiple inelastic scattering processes (these are the electrons that contribute to the background and are completely ignored in Auger spectroscopy). The secondary electron current reaching the detector is recorded and the microscope image consists of a "plot" of this current,  $I$ , against probe position on the surface. The contrast in the micrograph arises from several mechanisms, but first and foremost from variations in the surface topography. Consequently, the secondary electron micrograph is virtually a direct image of the real surface structure.



The attainable resolution of the technique is limited by the minimum spot size that can be obtained with the incident electron beam, and ultimately by the scattering of this beam as it interacts with the substrate. With modern instruments, a resolution of better than 5 nm is achievable. This is more than adequate for imaging semiconductor device structures, for example, but insufficient to enable many supported metal catalysts to be studied in any detail.

### B. Scanning Auger Microscopy ( SAM )

The incident primary electrons cause ionization of atoms within the region illuminated by the focused beam. Subsequent relaxation of the ionized atoms leads to the emission of Auger electrons characteristic of the elements present in this part of the sample surface (see the description of Auger spectroscopy in Section 5.2 for more details).



As with SEM, the attainable resolution is again ultimately limited by the incident beam characteristics. More significantly, however, the resolution is also limited by the need to acquire sufficient Auger signal to form a respectable image within a reasonable time period, and for this reason the instrumental resolution achievable is rarely better than about 15-20 nm.

---

This page titled [7.2: Electron Microscopy - SEM and SAM](#) is shared under a [CC BY-NC-SA 4.0](#) license and was authored, remixed, and/or curated by [Roger Nix](#).

## 7.3: Imaging XPS

The combination of the features of X-ray photoelectron spectroscopy (in particular, quantitative surface elemental analysis and chemical state information - see 5.3) together with spatial localization is a particularly desirable option in surface analysis. However, whilst much progress has been made in developing the technique of imaging XPS, there is still a considerable research effort being devoted to improving the available spatial resolution beyond that which is currently available.

Different manufacturers of imaging XPS systems have adopted different strategies for obtaining spatial localization - including all of those mentioned in Section 7.1 . Specifically, these include

1. Localization by selected (limited) area analysis.
2. Localization of the probe, by focusing the incident x-rays.
3. Use of array detectors, with associated imaging optics.

### 1. Limited Area Analysis

The simplest approach to localising an XPS analysis is to restrict the area of the sample surface from which photoelectrons are collected using a combination of lenses and apertures in the design of the electron energy analyser. The main problem with using this approach on its own is that as the sampled area is reduced, so is the collected signal - consequently, there is a direct trade-off between spatial resolution and data collection time.

The practically achievable spatial resolution is rarely better than 100  $\mu\text{m}$ . Imaging of the sample surface may then be achieved by either:

1. translating the sample position under the electron energy analyser, so that the analysed region is moved across the surface.
2. incorporating electrostatic deflection plates within the electron optics to move the region from which electrons are collected across the sample surface.

The advantage of this technique is its relative simplicity (and hence relatively low cost) - but this is reflected in the relatively poor performance!

### 2. Imaging XPS by X-ray Focussing

Until very recently this was not a popular option in commercial instruments, since x-rays are rather difficult to focus (compared to, for example, charged particles). Nevertheless, with recent improvements in technology, an x-ray spot size of better than 10  $\mu\text{m}$  has been achieved using this approach in commercially-available instruments, and significantly better resolution than this has been achieved in specialised research instruments (see state of the art" below). Images may then be obtained *either* by scanning the sample under the focused x-ray beam, *or* by scanning the microfocused x-ray beam.

Examples of spectrometers using this technology:

- PHI Quanterra XPS Microprobe

### 3. Array Detectors and Imaging Optics

There are a number of innovative designs for imaging spectrometers which combine array (i.e. multiple-segment) detectors with sophisticated imaging optics to obtain electron-energy resolved images at much faster acquisition rates. The spatial resolution achievable using this approach is also higher than that for either of the other techniques mentioned - state-of-the-art instruments give better than 5  $\mu\text{m}$  resolution

Examples of spectrometers using this technology:

- Omicron Nanotechnology "NanoESCA"


### State of the Art Imaging XPS Instrumentation

This is one area in which an ultra-high intensity x-ray source offers major advantages and the highest performance imaging XPS systems (scanning photoemission microscopes) are therefore those based at synchrotron sources. Using zone-plate technology to focus the x-rays (combined with multi-segment detectors to enhance data acquisition rates) it is possible on such systems to obtain XPS images with a resolution of better than 100 nm (see, for example, the ELETTRA ESCA microscopy web-pages).

## Summary

The spatial resolution currently achievable with commercial imaging XPS instruments limit the range of potential applications - nevertheless there are many areas of materials science where the information obtainable is incredibly useful and the relatively poor spatial resolution (compared, for example, with electron microscopic techniques such as SAM) is more than offset by the benefit of concurrent chemical state definition.

Selected examples of imaging XPS data:

	Imaging XPS data from Omicron NanoTechnology (Scroll-down the thumbnails in the right-hand frame, and click on each to see an enlarged image and a description of the measurement)
---	---

---

This page titled [7.3: Imaging XPS](#) is shared under a [CC BY-NC-SA 4.0](#) license and was authored, remixed, and/or curated by [Roger Nix](#).

## 7.4: SIMS - Imaging and Depth Profiling

The basic ideas behind the SIMS technique have already been discussed in the Section on [Secondary Ion Mass Spectrometry](#). Since the technique utilizes a beam of atomic ions (i.e. charged particles) as the probe, it is a relatively easy matter to focus the incident beam and then to scan it across the surface to give an imaging technique.

### Surface Imaging using SIMS

If the aim of the measurement is to obtain compositional images of the surface formed from the secondary ion spectrum with minimum possible damage to the surface, then the main problem is to ensure that sufficient signal is obtained at the desired spatial resolution whilst minimizing the ion flux incident on any part of the surface.

This is most easily achieved by switching from the traditional instrumental approach of using continuous-flux ion guns and quadrupole mass spectrometer detectors, to using pulsed ion sources and time-of-flight (TOF) mass spectrometers. The TOF mass spectrometers are a much more efficient way of acquiring spectral data, and also provide good resolution and sensitivity up to very high masses. Using such instruments, SIMS images with a spatial resolution of better than 50 nm are obtainable.

### SIMS Depth Profiling

The aim of depth profiling is to obtain information on the variation of composition with depth below the initial surface - such information is obviously particularly useful for the analysis of layered structures such as those produced in the semiconductor industry.

Since the SIMS technique itself relies upon the removal of atoms from the surface, it is by its very nature a destructive technique, but also, ideally suited for depth profiling applications. Thus a depth profile of a sample may be obtained simply by recording sequential SIMS spectra as the surface is gradually eroded away by the incident ion beam probe. A plot of the intensity of a given mass signal as a function of time, is a direct reflection of the variation of its abundance/concentration with depth below the surface.

One of the main advantages that SIMS offers over other depth profiling techniques (e.g. Auger depth profiling) is its sensitivity to very low (sub-ppm, or ppb) concentrations of elements - again this is particularly important in the semiconductor industry where dopants are often present at very low concentrations.

The *depth resolution* achievable (e.g. the ability to discriminate between atoms in adjacent thin layers) is dependent upon a number of factors which include:

1. the uniformity of etching by the incident ion beam
2. the absolute depth below the original surface to which etching has already been carried out
3. the nature of the ion beam utilized (i.e. the mass & energy of the ions )

as well as effects related to the physics of the sputtering process itself (e.g. ion-impact induced burial).

With TOF-SIMS instruments the best depth resolution is obtained using two separate beams; one beam is used to progressively etch a crater in the surface of the sample under study, whilst short-pulses of a second beam are used to analyze the floor of the crater. This has the advantage that one can be confident that the analysis is exclusively from the floor of the etch crater and not affected by sputtering from the crater-walls.

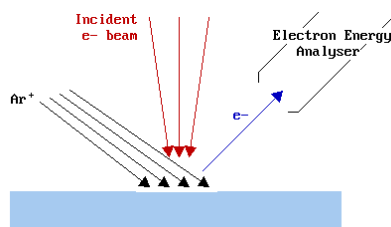
---

This page titled [7.4: SIMS - Imaging and Depth Profiling](#) is shared under a [CC BY-NC-SA 4.0](#) license and was authored, remixed, and/or curated by [Roger Nix](#).

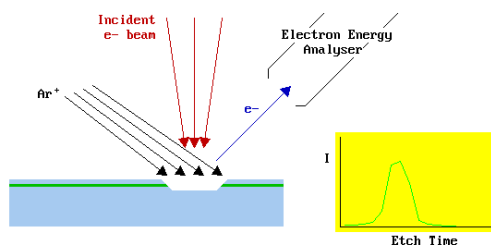
## 7.5: Auger Depth Profiling

As described in the Section on [Auger Spectroscopy](#) is a surface sensitive spectroscopic technique yielding compositional information. In its basic form it provides compositional information on a relatively large area ( $\sim 1 \text{ mm}^2$ ) of surface using a broad-focused electron beam probe. In this manner, sufficient signal can be readily obtained whilst keeping the incident electron flux low, and thus avoiding potential electron-induced modifications of the surface. As a consequence the technique is non-destructive when used in this manner.

To obtain information about the variation of composition with depth below the surface of a sample, it is necessary to gradually remove material from the surface region being analyzed, whilst continuing to monitor and record the Auger spectra. This controlled surface etching of the analyzed region can be accomplished by simultaneously exposing the surface to an ion flux which leads to sputtering (i.e. removal) of the surface atoms.



For example, suppose there is a buried layer of a different composition several nanometres below the sample surface. As the ion beam etches away material from the surface, the Auger signals corresponding to the elements present in this layer will rise and then decrease again.



The diagram above shows the variation of the Auger signal intensity one might expect from such a system for an element that is only present in the buried layer and not in the rest of the solid. In summary, by collecting Auger spectra as the sample is simultaneously subjected to etching by ion bombardment, it is possible to obtain information on the variation of composition with depth below the surface - this technique is known by the name of **Auger Depth Profiling**.

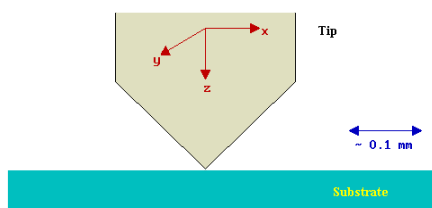
This page titled [7.5: Auger Depth Profiling](#) is shared under a [CC BY-NC-SA 4.0](#) license and was authored, remixed, and/or curated by [Roger Nix](#).

## 7.6: Scanning Probe Microscopy - STM and AFM

In the early 1980's two IBM scientists, Binnig & Rohrer, developed a new technique for studying surface structure - Scanning Tunneling Microscopy (STM). This invention was quickly followed by the development of a whole family of related techniques which, together with STM, may be classified in the general category of Scanning Probe Microscopy (SPM) techniques. Of these later techniques, the most important is Atomic Force Microscopy (AFM). The development of these techniques has without doubt been the most important event in the surface science field in recent times, and opened up many new areas of science and engineering at the atomic and molecular level.

### Basic Principles of SPM Techniques

All of the techniques are based upon scanning a probe (typically called the *tip* in STM, since it literally is a sharp metallic tip) just above a surface whilst monitoring some interaction between the probe and the surface.



The interaction that is monitored in:

- **STM** - is the *tunnelling current* between a metallic tip and a conducting substrate which are in very close proximity but **not** actually in physical contact.
- **AFM** - is the van der Waals force between the tip and the surface; this may be either the short range repulsive force (in contact-mode) or the longer range attractive force (in non-contact mode).

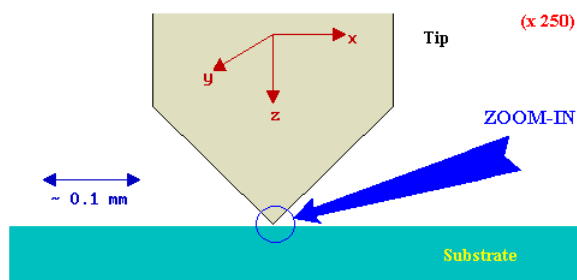
For the techniques to provide information on the surface structure at the atomic level (which is what they are capable of doing):

1. the position of the tip with respect to the surface must be very accurately controlled (to within about  $0.1 \text{ \AA}$ ) by moving either the surface or the tip.
2. the tip must be very sharp - ideally terminating in just a single atom at its closest point of approach to the surface.

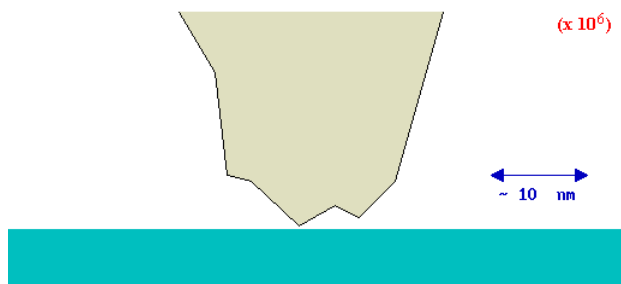
The attention paid to the first problem and the engineering solution to it is the difference between a good microscope and a not so good microscope - it need not worry us here, sufficient to say that it is possible to accurately control the relative positions of tip and surface by ensuring good vibrational isolation of the microscope and using sensitive piezoelectric positioning devices.

Tip preparation is a science in itself - having said that, it is largely serendipity which ensures that one atom on the tip is closer to the surface than all others.

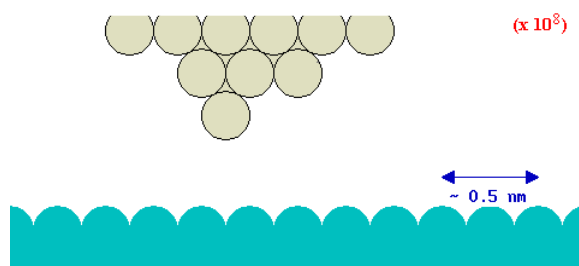
Let us look at the region where the tip approaches the surface in greater detail ....



... the end of the tip will almost invariably show a certain amount of structure, with a variety of crystal facets exposed ...



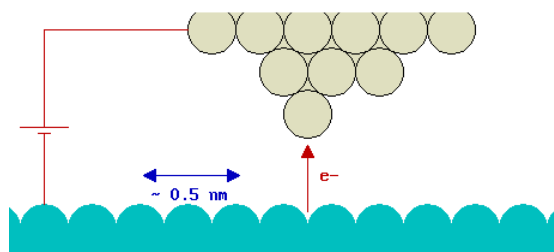
... and if we now go down to the atomic scale ....



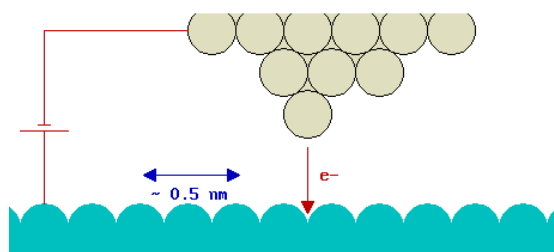
... there is a reasonable probability of ending up with a truly atomic tip.

If the tip is biased with respect to the surface by the application of a voltage between them then electrons can tunnel between the two, provided the separation of the tip and surface is sufficiently small - this gives rise to a *tunnelling current*.

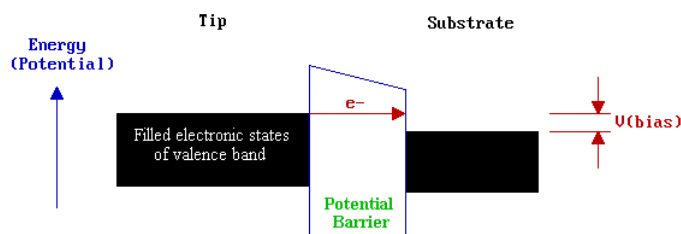
The direction of current flow is determined by the polarity of the bias.



If the sample is biased -ve with respect to the tip, then electrons will flow from the surface to the tip as shown above, whilst if the sample is biased +ve with respect to the tip, then electrons will flow from the tip to the surface as shown below.



The name of the technique arises from the quantum mechanical *tunnelling*-type mechanism by which the electrons can move between the tip and substrate. Quantum mechanical tunnelling permits particles to tunnel through a potential barrier which they could not surmount according to the classical laws of physics - in this case electrons are able to traverse the classically-forbidden region between the two solids as illustrated schematically on the energy diagram below.

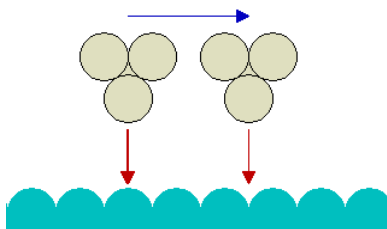


This is an over-simplistic model of the tunnelling that occurs in STM but it is a useful starting point for understanding how the technique works. In this model, the probability of tunnelling is exponentially-dependent upon the distance of separation between the tip and surface; the tunnelling current is therefore a very sensitive probe of this separation.

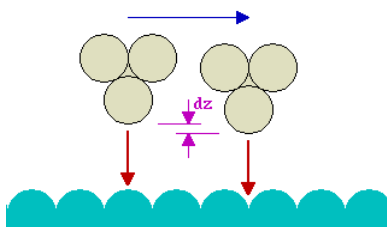
Imaging of the surface topology may then be carried out in one of two ways:

1. in constant height mode (in which the tunnelling current is monitored as the tip is scanned parallel to the surface)
2. in constant current mode (in which the tunnelling current is maintained constant as the tip is scanned across the surface)

If the tip is scanned at what is nominally a constant height above the surface, then there is actually a periodic variation in the separation distance between the tip and surface atoms. At one point the tip will be directly above a surface atom and the tunnelling current will be large whilst at other points the tip will be above hollow sites on the surface and the tunnelling current will be much smaller.



A plot of the tunnelling current v's tip position therefore shows a periodic variation which matches that of the surface structure - hence it provides a direct "image" of the surface (and by the time the data has been processed it may even look like a real picture of the surface !).



In practice, however, **the normal way of imaging the surface is to maintain the tunnelling current constant whilst the tip is scanned across the surface.** This is achieved by adjusting the tip's height above the surface so that the tunnelling current does not vary with the lateral tip position. In this mode the tip will move slightly upwards as it passes over a surface atom, and conversely, slightly in towards the surface as it passes over a hollow.

**The image is then formed by plotting the tip height (strictly, the voltage applied to the z-piezo) v's the lateral tip position.**

## Summary

In summary, the development of the various scanning probe microscopy techniques has revolutionized the study of surface structure - atomic resolution images have been obtained not only on single crystal substrates in UHV but also on samples at atmospheric pressure and even under solution. Many problems still remain, however, and the interpretation of SPM data is not always as straightforward as it might at first seem. There is still very much a place for the more traditional surface structural techniques such as LEED.



This introduction to STM has concentrated on the non-invasive imaging applications of the technique, yet there is increasing interest in using such techniques as a tool for the actual modification of surfaces. At the moment this is still at the "gimmicky" stage, but the longer term implications of being able to manipulate surface structure and molecules at the atomic level have yet to be fully appreciated: we can but await the future with interest !

---

This page titled [7.6: Scanning Probe Microscopy - STM and AFM](#) is shared under a [CC BY-NC-SA 4.0](#) license and was authored, remixed, and/or curated by [Roger Nix](#).

## Index

### A

#### Adsorption isotherms

- 3: The Langmuir Isotherm
- 3.2: Langmuir Isotherm - derivation from equilibrium considerations
- 3.3: Langmuir Isotherm from a Kinetics Consideration

#### Atomic Force Microscopy

- 7.6: Scanning Probe Microscopy - STM and AFM

#### Auger Depth Profiling

- 7.5: Auger Depth Profiling

#### Auger Electron Spectroscopy

- 5.2: Auger Electron Spectroscopy

#### Auger electrons

- 5.2: Auger Electron Spectroscopy

### B

#### binding energy

- 5.3: Photoelectron Spectroscopy

### D

#### desorption

- 2.6: The Desorption Process

### E

#### Electron Energy Loss Spectroscopy (EELS)

- 5.4: Vibrational Spectroscopy

#### ESCA (Electron Spectroscopy for Chemical Analysis)

- 5.3: Photoelectron Spectroscopy

### F

#### fcc structure

- 1.3: Surface Structures- fcc Metals

### I

#### imaging XPS

- 7.3: Imaging XPS

#### Inelastic Mean Free Path (IMFP)

- 5.1: Surface Sensitivity and Surface Specificity

### L

#### Langmuir isotherm

- 3: The Langmuir Isotherm
- 3.2: Langmuir Isotherm - derivation from equilibrium considerations
- 3.3: Langmuir Isotherm from a Kinetics Consideration
- 3.4: Variation of Surface Coverage with Temperature and Pressure

#### LEED

- 6.2: Low Energy Electron Diffraction (LEED)

#### Low Energy Electron Diffraction

- 6.2: Low Energy Electron Diffraction (LEED)

### M

#### Matrix Notation

- 6.1: Classification of Overlayer Structures

#### mean free path

- 4.2: Why is UHV required for surface studies ?

#### milller indices

- 1.2: Miller Indices (hkl)

#### MIR

- 5.4: Vibrational Spectroscopy

### P

#### Photoelectron Spectroscopy

- 5.3: Photoelectron Spectroscopy

#### physisorption

- 2.4: PE Curves and Energetics of Adsorption

### R

#### RAIRS

- 5.4: Vibrational Spectroscopy

#### Reflection High Energy Electron Diffraction

- 6.3: Reflection High Energy Electron Diffraction (RHEED)

#### RHEED

- 6.3: Reflection High Energy Electron Diffraction (RHEED)

### S

#### Scanning Auger Microscopy

- 7.2: Electron Microscopy - SEM and SAM

#### Scanning Tunneling Microscopy (STM)

- 7.6: Scanning Probe Microscopy - STM and AFM

#### Secondary Electron Microscopy

- 7.2: Electron Microscopy - SEM and SAM

#### Secondary Ion Mass Spectrometry

- 7.4: SIMS - Imaging and Depth Profiling

#### sticking coefficient

- 4.2: Why is UHV required for surface studies ?

#### surface residence time

- 2.6: The Desorption Process

#### Surface Unit Cell

- 6.1: Classification of Overlayer Structures

### T

#### Temperature Programmed Desorption (TPD)

- 5.6: Temperature-Programmed Techniques

#### Temperature Programmed Reaction Spectroscopy (TPRS)

- 5.6: Temperature-Programmed Techniques

#### tunnelling current

- 7.6: Scanning Probe Microscopy - STM and AFM

### U

#### Ultraviolet Photoelectron Spectroscopy (UPS)

- 5.3: Photoelectron Spectroscopy

### V

#### vicinal surfaces

- 1.9: Other Single Crystal Surfaces

### W

#### Wood's Notation

- 6.1: Classification of Overlayer Structures

# Index

---

## A

### Adsorption isotherms

- 3: The Langmuir Isotherm
- 3.2: Langmuir Isotherm - derivation from equilibrium considerations
- 3.3: Langmuir Isotherm from a Kinetics Consideration

### Atomic Force Microscopy

- 7.6: Scanning Probe Microscopy - STM and AFM

### Auger Depth Profiling

- 7.5: Auger Depth Profiling

### Auger Electron Spectroscopy

- 5.2: Auger Electron Spectroscopy

### Auger electrons

- 5.2: Auger Electron Spectroscopy

## B

### binding energy

- 5.3: Photoelectron Spectroscopy

## D

### desorption

- 2.6: The Desorption Process

## E

### Electron Energy Loss Spectroscopy (EELS)

- 5.4: Vibrational Spectroscopy

### ESCA (Electron Spectroscopy for Chemical Analysis)

- 5.3: Photoelectron Spectroscopy

## F

### fcc structure

- 1.3: Surface Structures- fcc Metals

## I

### imaging XPS

- 7.3: Imaging XPS

### Inelastic Mean Free Path (IMFP)

- 5.1: Surface Sensitivity and Surface Specificity

## L

### Langmuir isotherm

- 3: The Langmuir Isotherm
- 3.2: Langmuir Isotherm - derivation from equilibrium considerations
- 3.3: Langmuir Isotherm from a Kinetics Consideration
- 3.4: Variation of Surface Coverage with Temperature and Pressure

### LEED

- 6.2: Low Energy Electron Diffraction (LEED)

### Low Energy Electron Diffraction

- 6.2: Low Energy Electron Diffraction (LEED)

## M

### Matrix Notation

- 6.1: Classification of Overlayer Structures

### mean free path

- 4.2: Why is UHV required for surface studies ?

### milller indices

- 1.2: Miller Indices (hkl)

### MIR

- 5.4: Vibrational Spectroscopy

## P

### Photoelectron Spectroscopy

- 5.3: Photoelectron Spectroscopy

### physisorption

- 2.4: PE Curves and Energetics of Adsorption

## R

### RAIRS

- 5.4: Vibrational Spectroscopy

### Reflection High Energy Electron Diffraction

- 6.3: Reflection High Energy Electron Diffraction (RHEED)

### RHEED

- 6.3: Reflection High Energy Electron Diffraction (RHEED)

## S

### Scanning Auger Microscopy

- 7.2: Electron Microscopy - SEM and SAM

### Scanning Tunneling Microscopy (STM)

- 7.6: Scanning Probe Microscopy - STM and AFM

### Secondary Electron Microscopy

- 7.2: Electron Microscopy - SEM and SAM

### Secondary Ion Mass Spectrometry

- 7.4: SIMS - Imaging and Depth Profiling

### sticking coefficient

- 4.2: Why is UHV required for surface studies ?

### surface residence time

- 2.6: The Desorption Process

### Surface Unit Cell

- 6.1: Classification of Overlayer Structures

## T

### Temperature Programmed Desorption (TPD)

- 5.6: Temperature-Programmed Techniques

### Temperature Programmed Reaction Spectroscopy (TPRS)

- 5.6: Temperature-Programmed Techniques

### tunnelling current

- 7.6: Scanning Probe Microscopy - STM and AFM

## U

### Ultraviolet Photoelectron Spectroscopy (UPS)

- 5.3: Photoelectron Spectroscopy

## V

### vicinal surfaces

- 1.9: Other Single Crystal Surfaces

## W

### Wood's Notation

- 6.1: Classification of Overlayer Structures

## Detailed Licensing

---

### Overview

**Title:** Surface Science (Nix)

**Webpages:** 57

**Applicable Restrictions:** Noncommercial

#### All licenses found:

- [CC BY-NC-SA 4.0](#): 87.7% (50 pages)
- [Undeclared](#): 12.3% (7 pages)

### By Page

- [Surface Science \(Nix\) - CC BY-NC-SA 4.0](#)
  - [Front Matter - CC BY-NC-SA 4.0](#)
    - [TitlePage - CC BY-NC-SA 4.0](#)
    - [InfoPage - CC BY-NC-SA 4.0](#)
    - [Table of Contents - Undeclared](#)
    - [Licensing - Undeclared](#)
  - [1: Structure of Solid Surfaces - CC BY-NC-SA 4.0](#)
    - [1.1: Introduction - CC BY-NC-SA 4.0](#)
    - [1.2: Miller Indices \(hkl\) - CC BY-NC-SA 4.0](#)
    - [1.3: Surface Structures- fcc Metals - CC BY-NC-SA 4.0](#)
    - [1.4: Surface Structures- hcp Metals - CC BY-NC-SA 4.0](#)
    - [1.5: Surface Structures- bcc metals - CC BY-NC-SA 4.0](#)
    - [1.6: Energetics of Surfaces - CC BY-NC-SA 4.0](#)
    - [1.7: Relaxation and Reconstruction - CC BY-NC-SA 4.0](#)
    - [1.8: Particulate Metals - CC BY-NC-SA 4.0](#)
    - [1.9: Other Single Crystal Surfaces - CC BY-NC-SA 4.0](#)
  - [2: Adsorption of Molecules on Surfaces - CC BY-NC-SA 4.0](#)
    - [2.1: Introduction to Molecular Adsorption - CC BY-NC-SA 4.0](#)
    - [2.2: How do Molecules Bond to Surfaces? - Undeclared](#)
    - [2.3: Kinetics of Adsorption - CC BY-NC-SA 4.0](#)
    - [2.4: PE Curves and Energetics of Adsorption - CC BY-NC-SA 4.0](#)
    - [2.5: Adsorbate Geometries and Structures - CC BY-NC-SA 4.0](#)
    - [2.6: The Desorption Process - CC BY-NC-SA 4.0](#)
  - [3: The Langmuir Isotherm - CC BY-NC-SA 4.0](#)
    - [3.1: Introduction - CC BY-NC-SA 4.0](#)
    - [3.2: Langmuir Isotherm - derivation from equilibrium considerations - CC BY-NC-SA 4.0](#)
    - [3.3: Langmuir Isotherm from a Kinetics Consideration - CC BY-NC-SA 4.0](#)
    - [3.4: Variation of Surface Coverage with Temperature and Pressure - CC BY-NC-SA 4.0](#)
    - [3.5: Applications - Kinetics of Catalytic Reactions - CC BY-NC-SA 4.0](#)
  - [4: UHV and Effects of Gas Pressure - CC BY-NC-SA 4.0](#)
    - [4.1: What is UltraHigh Vacuum? - Undeclared](#)
    - [4.2: Why is UHV required for surface studies ? - Undeclared](#)
    - [4.E: UHV and Effects of Gas Pressure \(Exercises\) - CC BY-NC-SA 4.0](#)
  - [5: Surface Analytical Techniques - CC BY-NC-SA 4.0](#)
    - [5.1: Surface Sensitivity and Surface Specificity - CC BY-NC-SA 4.0](#)
    - [5.2: Auger Electron Spectroscopy - CC BY-NC-SA 4.0](#)
    - [5.3: Photoelectron Spectroscopy - CC BY-NC-SA 4.0](#)
    - [5.4: Vibrational Spectroscopy - CC BY-NC-SA 4.0](#)
    - [5.5: Secondary Ion Mass Spectrometry - CC BY-NC-SA 4.0](#)
    - [5.6: Temperature-Programmed Techniques - CC BY-NC-SA 4.0](#)
  - [6: Overlayer Structures and Surface Diffraction - CC BY-NC-SA 4.0](#)
    - [6.1: Classification of Overlayer Structures - CC BY-NC-SA 4.0](#)
    - [6.2: Low Energy Electron Diffraction \(LEED\) - CC BY-NC-SA 4.0](#)
    - [6.3: Reflection High Energy Electron Diffraction \(RHEED\) - CC BY-NC-SA 4.0](#)
    - [6.4: Examples - Surface Structures - CC BY-NC-SA 4.0](#)
  - [7: Surface Imaging and Depth Profiling - CC BY-NC-SA 4.0](#)
    - [7.1: Basic concepts in surface imaging and localized spectroscopy - CC BY-NC-SA 4.0](#)

- [7.2: Electron Microscopy - SEM and SAM - CC BY-NC-SA 4.0](#)
  - [7.3: Imaging XPS - CC BY-NC-SA 4.0](#)
  - [7.4: SIMS - Imaging and Depth Profiling - CC BY-NC-SA 4.0](#)
  - [7.5: Auger Depth Profiling - CC BY-NC-SA 4.0](#)
  - [7.6: Scanning Probe Microscopy - STM and AFM - CC BY-NC-SA 4.0](#)
- [Back Matter - CC BY-NC-SA 4.0](#)
    - [Index - CC BY-NC-SA 4.0](#)
    - [Index - Undeclared](#)
    - [Glossary - CC BY-NC-SA 4.0](#)
    - [Detailed Licensing - Undeclared](#)